

TOPICAL REVIEW

The development of topography in the visual cortex: a review of models

N V Swindale

Department of Ophthalmology, University of British Columbia, 2550 Willow Street, Vancouver, BC, Canada V5Z 3N9

Received 27 February 1996

Abstract. The repetitive stochastic patterns of eye dominance and orientation preference found in the mammalian visual cortex have attracted much attention from theoretical neurobiologists during the last two decades. Reasons for this include the visually intriguing nature of the patterns and the fact that many aspects of their development seem likely to be dependent upon both spontaneous and visually driven patterns of neural activity. Understanding these processes holds out the promise that general theories of learning and memory may be derived from those found to be applicable to the visual cortex. It has turned out, in fact, that remarkably simple models, based on Hebbian synaptic plasticity, intracortical interactions and competitive interactions between cells and growing axons, have been able to explain much of the phenomenology.

This article reviews the models of topographic organization in the visual cortex in a roughly historical sequence, beginning with von der Malsburg's paper 1973 paper in *Kybernetik* on self-organization of orientation selectivity. The principles on which each of the models is based are explained, and the plausibility of each model and the extent to which it is able to account for the relevant experimental data are evaluated. Attention is drawn to the underlying similarities and differences between the models and suggestions are made for future directions in research.

Contents

1	Introduction	163
2	Experimental background	163
2.1	Global retinotopy	163
2.2	Receptive field scatter and the cortical point image	166
2.3	Ocular dominance columns in adult animals	167
2.4	The development of ocular dominance columns	170
2.5	Orientation columns in adult animals	172
2.6	Singularities	174
2.7	Development of orientation columns	175
2.8	Genes versus the environment	175
2.9	Structural relationships between the different columnar systems	176
2.10	Analysis of experimental data	178
3	The models	179
3.1	A general overview	179
4	Von der Malsburg's model for self-organization of orientation selectivity	182
4.1	Extensions of von der Malsburg's model to retinotopy and ocular dominance column formation	184
5	Swindale's models for ocular dominance and orientation columns	186
5.1	Ocular dominance columns	186

5.2	Orientation columns	190
5.3	Conditions under which the models are valid	192
5.4	Empirical tests of the models	194
5.5	The origin of the postulated interactions	194
6	Linsker's model for orientation columns	195
7	Miller's models for ocular dominance and orientation	198
7.1	Ocular dominance columns	198
7.2	Orientation columns	199
7.3	Biological interpretation of Miller's models	200
8	Applications of Kohonen's self-organizing feature map (SOFM) algorithm	201
8.1	Goodhill's model for ocular dominance and retinotopy	201
8.2	Biological implications of Goodhill's model	204
8.3	Other high-dimensional competitive Hebbian models	206
9	Dimension-reduction models for cortical development	206
9.1	Elastic net models	208
9.2	Low-dimensional self-organizing feature map (SOFM) models	211
9.3	Strengths and weaknesses of the dimension-reduction approach	214
10	Other models	215
10.1	The tea-trade model	215
10.2	The diffusion-based model of Montague <i>et al</i>	216
10.3	Tanaka's thermodynamic approach	217
10.4	Band-pass filter models	218
10.5	The relationship between visual cortex shape and ocular dominance column morphology	219
10.6	Approaches based on information theory	222
11	Coverage, continuity and wirelength	223
11.1	Coverage	223
11.2	Continuity	224
11.3	Wirelength	226
12	Evaluation of assumptions common to most models	227
12.1	Patterned retinal activity	228
12.2	Hebb synapses	228
12.3	Radially symmetric, short-range excitatory and long-range inhibitory lateral cortical connections	228
12.4	Normalization of input strengths	229
13	Overall evaluation of the different models	229
13.1	Ocular dominance models	229
13.2	Orientation column models	230
13.3	Combined models of orientation, ocular dominance and retinotopy	231
13.4	Competitive Hebbian models versus linear Hebbian models	231
14	Comments on the field as a whole	232
14.1	How similar are the different models?	232
14.2	Complementarity and anticipation	233
15	Future directions	234
15.1	Questions for experimenters	234
15.2	Suggestions for modellers	235
16	General conclusions	236
	References	237

'The sciences do not try to explain, they hardly even try to interpret, they mainly make models. By a model is meant a mathematical construct which, with the addition of certain verbal interpretations, describes observed phenomena. The justification of such a mathematical construct is solely and precisely that it is expected to work.' John von Neumann

1. Introduction

The mammalian visual cortex is a highly ordered structure which, over the last two decades, has attracted much attention from theoretical neurobiologists. It is not hard to find reasons for this interest. The visual cortex is one of the most thoroughly studied brain regions and many aspects of its development have been shown to be dependent upon neural activity and visual experience. Understanding these processes holds out the promise that general theories of learning, memory and knowledge representation will be discovered that are applicable to the whole cortex. It has turned out, in fact, that remarkably simple models, based on competitive interactions and Hebbian synaptic plasticity, have been able to explain many of the intriguing features of visual cortex organization, in particular the presence of a retinotopic map and the repetitive, stochastic patterns of eye dominance and orientation preference which are overlaid on it.

In this article I shall review, in a roughly historical sequence, a number of these models. I shall attempt to explain the principles on which each model is based, to evaluate its plausibility and relations with other models, and the extent to which it is able to account for the relevant experimental data. For reasons of space, the review will be restricted to models which attempt to explain the formation of spatial topography in the cortex: models which only address the question of how individual receptive fields develop will be ignored.

Other reviews of this topic have recently appeared. Erwin *et al* (1995) evaluated some recent models of visual cortex topography in terms of the principles on which they were based and the similarity between their output and the experimental optical recording data; they paid less attention to the biological assumptions behind the different models and to agreement with other developmental data. Goodhill (1992) presented and analysed mathematically a number of different models but, unfortunately, this review is not widely available. Miller (see Miller and Stryker 1990, Miller 1990a, b, 1992a, 1995) has also provided detailed reviews and analyses of the role of correlation-based learning rules in the formation of receptive fields and spatial patterns in the cortex.

2. Experimental background

The aspects of visual cortical organization and development which have been of interest to theoreticians include:

- (i) retinotopy, i.e. the development of a continuous topographic mapping from the retina to the cortex;
- (ii) the development of eye dominance stripes;
- (iii) the development of orientation selectivity and orientation columns.

The recent discovery of a variety of structural relationships between these three parameters has also invited explanation.

2.1. Global retinotopy

The manner in which the retina projects onto the surface of the macaque monkey visual cortex is illustrated by the result (Tootell *et al* 1988b) shown in figure 1. In this experiment,

an anaesthetized monkey viewed a visual stimulus (shown on the left-hand side of the figure) with one eye, after intravenous injection of radioactively labelled 2-deoxyglucose. The resulting pattern of radioactivity in its visual cortex is shown on the right-hand side. It shows that lines of constant eccentricity, r (marked 1, 2 and 3 in figure 1), and lines of constant polar angle, θ (marked I, H and S in figure 1), in visual space, map, to a first approximation, onto straight lines which intersect approximately at right angles. This is consistent with the suggestion (Schwartz 1980) that the mapping can be described by a complex logarithmic function $w = a \log_e(z + b)$, where $w = (x + iy)$ is the position on the cortex in millimetres, and $z = re^{i\theta}$, where r is the visual field eccentricity in degrees of visual angle relative to the fovea, θ is the meridional angle in radians and a and b are constants which can be determined experimentally. This formula implies that angles are preserved, i.e. lines intersecting at right angles on the retina (as in figure 1) should project to lines that intersect at right angles on the cortex; in addition, it implies that the retinal magnification factor is locally isotropic, i.e. independent of whether it is measured along a horizontal or vertical direction in visual space. This magnification factor, in millimetres of cortex per degree of visual angle, is given by $a(x + b)/\{(x + b)^2 + y^2\}$, which at the fovea is equal to a/b (i.e. when $x = y = 0$).

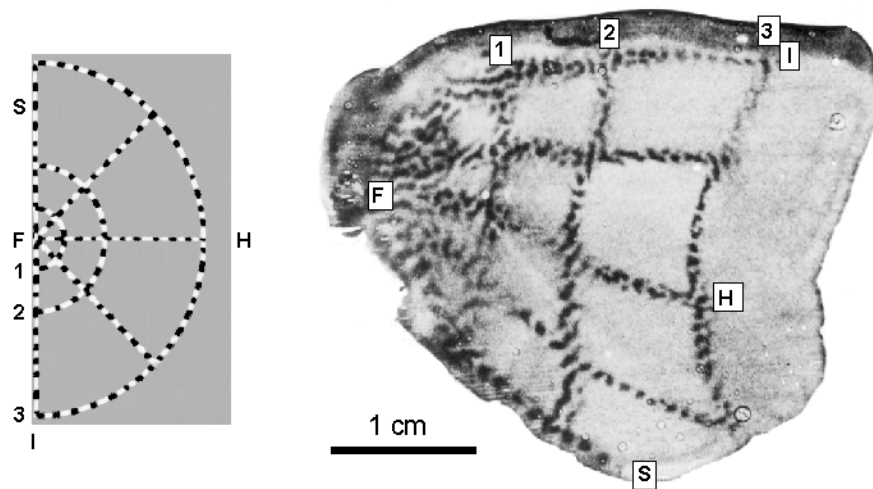


Figure 1. Deoxyglucose autoradiograph showing the distribution of activity (darkened regions) evoked in macaque monkey striate cortex by the visual stimulus shown on the left. The cortex was flattened before sectioning. The stimulus was viewed monocularly and ocular dominance columns are visible as periodic interruptions in the pattern of activity. Corresponding regions in the visual field and the visual cortex are indicated by letters and numbers: S = superior visual field; F = fovea; I = inferior visual field; H = horizontal meridian. The semicircles in the stimulus (1, 2, 3) are positioned at 1° , 2.3° and 5.4° eccentric to the fovea respectively. The black and white checks in the stimulus were contrast-reversed at 3 Hz during the period of stimulation. (Reproduced, with modifications, from Tootell *et al* (1988b).)

Experimental data obtained by Dow *et al* (1985) supported Schwartz's model, and led to an estimate of $a = 7.7$ and $b = 0.33$. This formula gives a good approximation for the variation in magnification factor with retinal position in many regions of cortex, although other authors (Van Essen *et al* 1984, LeVay *et al* 1985, Tootell *et al* 1988b) have found that the magnification factor is significantly anisotropic in many regions of the cortex and this is inconsistent with a simple complex logarithmic mapping. The anisotropy, however,

is usually less than a factor of two, being more marked along the representation of the vertical meridian than the horizontal, and shows significant inter-animal variability. With these qualifications, Van Essen *et al* (1984) suggest that magnification factors outside of the fovea can be described by the formulae $M_p = 12.0 E^{-1.11}$ and $M_e = 9.0 E^{-1.15}$ where E is visual field eccentricity in degrees radial to the fovea, and M_p and M_e are the cortical magnifications in mm per degree along iso-polar and iso-eccentricity lines in visual space, respectively.

The mechanisms responsible for the formation of the retinotopic map in mammalian visual cortex have received relatively little attention and are not well understood. In contrast, there is a large body of experimental data on the formation of topographic projections between the retina and the optic tectum of lower vertebrates, such as frogs and goldfish (Udin and Fawcett 1988). Work on this system, among others, has shown that the formation of connections between physically separate neural structures generally involves the following sequence (Easter *et al* 1994):

- (i) axonal outgrowth in a fibre bundle, towards the target structure;
- (ii) initial innervation of the target structure by axons which often branch profusely within it;
- (iii) selective removal of parts of the axonal tree; and possibly
- (iv) selective strengthening or weakening of connections within axonal arbors.

There are a number of ways in which topographic order may be maintained during these stages.

- Fibres within developing tracts tend to maintain order as the tract grows towards its target structure, so that a principle of 'neighbours in, neighbours out' applies (Horder and Martin 1978).
- A relationship exists between position on the retina and the time at which fibres leave the retina, enter the optic nerve and arrive at the tectum; this can be used to establish a topography if space is allocated in the tectum on a 'first come, first served' basis.
- Chemical markers label nerve cells according to their position of origin in the retina; another set of complementary labels exists in the tectum and determines a correct match between the two structures (Sperry 1944).
- Gradients of chemo-repellant and/or chemo-attractive molecules are present in the tectum which act selectively on cells from different regions of the retina causing their axons to avoid terminating in certain regions of the tectum (Gierer 1987, Sanes 1993, Baier and Bonhoeffer 1994).
- The neural impulse activity of nearby retinal ganglion cells tends to be more closely correlated than that in pairs further apart (Arnett 1978, Arnett and Spraker 1981, Mastrorade 1983); as will be explained in more detail later (section 4.1), this can be used to establish a topography if Hebbian rules apply to the formation of connections (Willshaw and von der Malsburg 1976).

From the point of view of the modeller, an important conclusion from the research which has been performed to disentangle the application of these hypotheses to the retino-tectal projection (reviewed by Udin and Fawcett (1988)) is that no one mechanism is sufficient to explain the establishment of order and few of the suggested mechanisms can be ruled out. For example, a roughly ordered projection can form in the complete absence of all electrical activity (Harris 1980). Thus, topographic ordering within the afferent pathway, maintained by selective adhesion and/or time of outgrowth cues, spatial gradients of chemo-attractive and chemo-repellant molecules within the target structure and activity-dependent

addition and removal of neural connections may all be important in the eventual formation of topographic projections. However, these different mechanisms seem likely to operate at different stages of development: initially, topography is probably established by time of outgrowth, selective adhesion, axonal guidance and chemical cues, while in the final stages, a neural-activity-dependent mechanism may lead to a further increase in topographic precision (see e.g. Schmidt and Edwards (1983), Cook (1987), Cook and Becker (1990), Constantine-Paton *et al* (1990)).

These same mechanisms may operate in the formation of the visual field map in the visual cortex (Molnár and Blakemore 1995). However, a curious difference between the cortex and the tectum is that incoming geniculate axons make their first synaptic contacts in the weeks before birth, not with cortical neurons but within a region known as the subplate (Rakic 1977, Shatz and Luskin 1986, Allendoerfer and Shatz 1994). This lies immediately beneath the embryonic visual cortex. During this period, the geniculate axons branch widely (Ghosh and Shatz 1992) and make functional synaptic contacts with subplate neurons (Chun and Shatz 1988, Friauf *et al* 1990). At the same time, the layers of the visual cortex are formed by cell division and migration (Rakic 1978, Shatz *et al* 1988, McConnell 1988). It is possible that a significant amount of topographic refinement occurs at this stage. A few days before birth, the geniculate axons leave the subplate and invade the cortex where they establish connections within layer IV. The subplate neurons die during this period and have mostly gone by the time segregation into ocular dominance columns is complete.

As yet, there is little direct evidence that visually driven, or spontaneous, neural activity plays a role in either the initial formation, or refinement, of retinal topography in the visual cortex. A reasonably accurate topography is presumably present at birth in the macaque monkey (Wiesel and Hubel 1974) and by the time of eye opening in the kitten (Hubel and Wiesel 1963) and this suggests that visually evoked neural activity does not play a major role. However, visual stimulation might help to refine topography, as well as other receptive field properties, postnatally. This seems especially likely to be the case in the visual cortex, given that the maps of the left and right retinas must match almost exactly in order for the binocular correspondences necessary for stereopsis to be established. The most feasible cue for matching with the required degree of precision is the detection of inter-ocular correlations in visually evoked retinal activity. This is also suggested by the observation that receptive field positions are malleable in adult animals (Chino *et al* 1992, Gilbert and Wiesel 1992).

2.2. Receptive field scatter and the cortical point image

Although the topography of the projection from the retina to the visual cortex is remarkably precise, on a cellular level it is not perfectly accurate. This is shown by the fact that neurons in the same vertical column† of cells have receptive fields scattered in slightly different retinal locations (Hubel and Wiesel 1974b, Albus 1975a). The size of the region over which receptive field centres are scattered is comparable with the size of the individual receptive fields within a column. This relationship holds for a range of visual field eccentricities and receptive field sizes. In the part of visual cortex which represents the fovea, receptive field sizes and the corresponding scatter are both small, while with increasing distance from the fovea both the degree of scatter and receptive field size increase by similar amounts. This

† A column can be defined as a set of cells which occupy a region whose boundaries are perpendicular to the surface of the cortex and which share some functional property. The size and shape of the region are variable, depending upon the property in question. The smallest cortical region which might usefully be considered to be a column of some kind is about 30 μm in diameter and contains about 100–200 neurons.

finding has the corollary that a single point in visual space will lie in the centre (more accurately within some defined small region in the centre) of the receptive fields of cells in a number of different, neighbouring, cortical columns. This distribution can be referred to as the cortical point image[†]. Its size, σ_C , can be estimated, assuming a locally uniform magnification factor, M mm per degree, from the relationship $\sigma_C = M\sigma_R$, where σ_R is the receptive field scatter, or aggregate receptive field size, measured at a single location in the cortex. Hubel and Wiesel (1974b) found that σ_R and M are inversely related and concluded that σ_C remained constant over the surface of the visual cortex. Other authors (Dow *et al* 1981, Van Essen *et al* 1984) have found that receptive field size does not decrease in the fovea as much as would be expected from the change in magnification factor. Consequently, the cortical point image is probably larger in the fovea than elsewhere.

Accurate measurements of point image size do not exist: in the monkey, estimates vary from about 2–3 mm (Hubel and Wiesel 1974b); 1–2 mm (Hubel and Wiesel 1977); 10 mm at the fovea and decreasing to 1 mm at 50° eccentricity (Dow *et al* 1981) and 0.5–0.75 mm with a minimum at 5° (Van Essen *et al* 1984). Point image size is different in different layers of the cortex (Tootell *et al* 1988b). For example, in layer IVc of primate visual cortex, receptive fields are concentric and very small, and there seems to be an extremely orderly mapping of receptive field position (Hubel *et al* 1974, Blasdel and Fitzpatrick 1984) which is described in more detail in subsection 2.9.1. In area 17 of the cat, Albus (1975a) estimated point image diameter to be about 2.7 mm; in area 18 of the same species, Cynader *et al* (1987) found that scatter in receptive field centre positions (measured as twice the standard deviation) was about 0.6 mm along the medio-lateral axis and 1.2 mm along the antero-posterior axis. This anisotropy was positively correlated with the magnification factor anisotropy found in the same cortical area. It is worth emphasizing that there is no necessary connection between point image shape and magnification factor anisotropy. However, a positive correlation between the two will have the effect of making the retinal point image (the locus of retinal receptive fields of a single point on the cortical surface) circular rather than elliptical.

2.3. Ocular dominance columns in adult animals

The physiological studies of Hubel and Wiesel (1963, 1968, 1977) showed that many cells in the visual cortex had binocular receptive fields and that the fields had the same position in visual space, whether plotted in the ipsilateral or contralateral eye. However, cells varied in their relative responsiveness to each eye, with some showing a greater response to stimulation through the contralateral eye, some preferring the ipsilateral eye and others being equally responsive to both eyes. In addition, some cells, particularly those located in layer IV of the cortex, where the inputs from the LGN terminate, were monocular and would respond only to one eye. These variations in ocular dominance were shown to obey the principle of columnar organization, i.e. cells in the same column tended to share a preference for stimuli presented to one eye or the other.

An anatomical explanation for the physiological variations in ocular dominance was first discovered by Hubel and Wiesel (1972) and, since then, a wide variety of anatomical techniques has been used to reveal the spatial pattern of ocular dominance columns (figure 2). These investigations have shown that in many, though not all, mammalian species, inputs

[†] The definition can be broadened to include all parts of the receptive field and not just the centre. The cortical point image would thus include cells, any part of whose receptive field overlapped the visual field location in question. The size of the image would be correspondingly larger. This definition is perhaps less satisfactory than the first, because it requires a definition of what constitutes the edge of a receptive field.

from the left and the right eyes are segregated within layer IV of the cortex into non-overlapping regions with a characteristic periodicity and morphology. In the macaque monkey (figure 2(a)) the regions are branching stripes with a fairly uniform width of around $400\ \mu\text{m}$ and an overall periodicity of about $800\ \mu\text{m}$ (Hubel *et al* 1977, LeVay *et al* 1985, Blasdel *et al* 1995). The stripes show a tendency to narrow at branch points and run orthogonally into the boundaries of area 17. Their resemblance to patterns found elsewhere in nature, e.g. on zebras, many species of frog and fish, and magnetic thin films, is striking, and has often been commented on (see e.g. Hubel *et al* (1977), Swindale (1980), Tanaka (1990a)) and has provided a stimulus for theoretical explanation in general terms.

In areas 17 and 18 of the cat (figure 2(b)) the pattern is less regular than in the macaque, although it is still periodic. There is also an asymmetry between the two eyes: about 40% of the surface area of cortex is devoted to inputs from the ipsilateral eye, which form a pattern of irregularly shaped blobs and elongated patches, while the remaining 60% is devoted to the contralateral eye. The overall periodicity in area 17 is between 0.8 and 1.2 mm (Löwel and Singer 1987, Swindale 1988, Diao *et al* 1990). In area 18 the periodicity is between 1.8 mm and 2.2 mm (Löwel and Singer 1987, Cynader *et al* 1987, Swindale 1988, Diao *et al* 1990). Ocular dominance columns are also present in chimpanzees (Tigges and Tigges 1979) and humans (Hitchcock and Hickey 1980, Horton and Hedley-White 1984, Horton *et al* 1990) where they have a periodicity of about 1.4 mm.

The phenomenology of ocular dominance column behaviour is rich and only some aspects of it will be covered here. The gamut of patterns found in adult animals ranges at one extreme from mostly parallel bands with relatively few branches in talapoin monkeys (Florence and Kaas 1992); the highly branched patterns found in macaque and New World *Ateles* (Florence *et al* 1986) and *Cebus* monkeys (Hess and Edwards 1987, Rosa *et al* 1988); less regular spots and patches in cats (Shatz *et al* 1977, Anderson *et al* 1988) and ferrets (Law *et al* 1988, Redies *et al* 1990), to nearly complete overlap in New World monkeys such as *Aotes* (Kaas *et al* 1976, Rowe *et al* 1978), and *Saimiri* (Tigges *et al* 1977, Hendrickson *et al* 1978). Ocular dominance columns are present transiently in young marmosets (*Callithrix jacchus*, a small New World primate) but disappear before the animal reaches maturity (Spatz 1979, 1989). Monocular deprivation causes the transient patches to remain permanent (DeBruyn and Casagrande 1981, Sengpiel *et al* 1996). Similarly, monocular deprivation, or alternating monocular deprivation, can cause eye dominance stripes to form in the owl visual cortex (Pettigrew 1982, Pettigrew and Gynther 1989) although they are not normally present in this species. In tree shrews, a vertical rather than a lateral pattern of segregation occurs, with ipsilateral eye inputs occupying the top and bottom of layer IV and contralateral eye inputs occupying the middle (Hubel 1975, Casagrande and Harting 1975, Conley *et al* 1984). As figure 2 illustrates, there can also be morphological variability within the cortex: in the macaque, the stripes show more parallel order peripheral to the blind spot; ipsilateral eye stripes break up into blobs close to the monocular segment, while overall periodicity in the extreme periphery is about half of that in the fovea (LeVay *et al* 1985). Needless to say, accommodating morphological variability within and between species is a challenge for any model.

From a functional point of view, ocular dominance columns remain an enigma. The possibility that they may not have a function at all should perhaps be taken seriously. Modelling results (described in more detail below, see e.g. von der Malsburg and Willshaw (1976), Goodhill (1993)) show that mechanisms whose main purpose is to ensure corresponding topographic mappings from two retinas onto a single sheet of cells, usually produce ocular dominance stripes. The fact that stripes can be made to develop in situations where they would not normally be present (e.g. in the marmoset, the owl, and the three-eyed

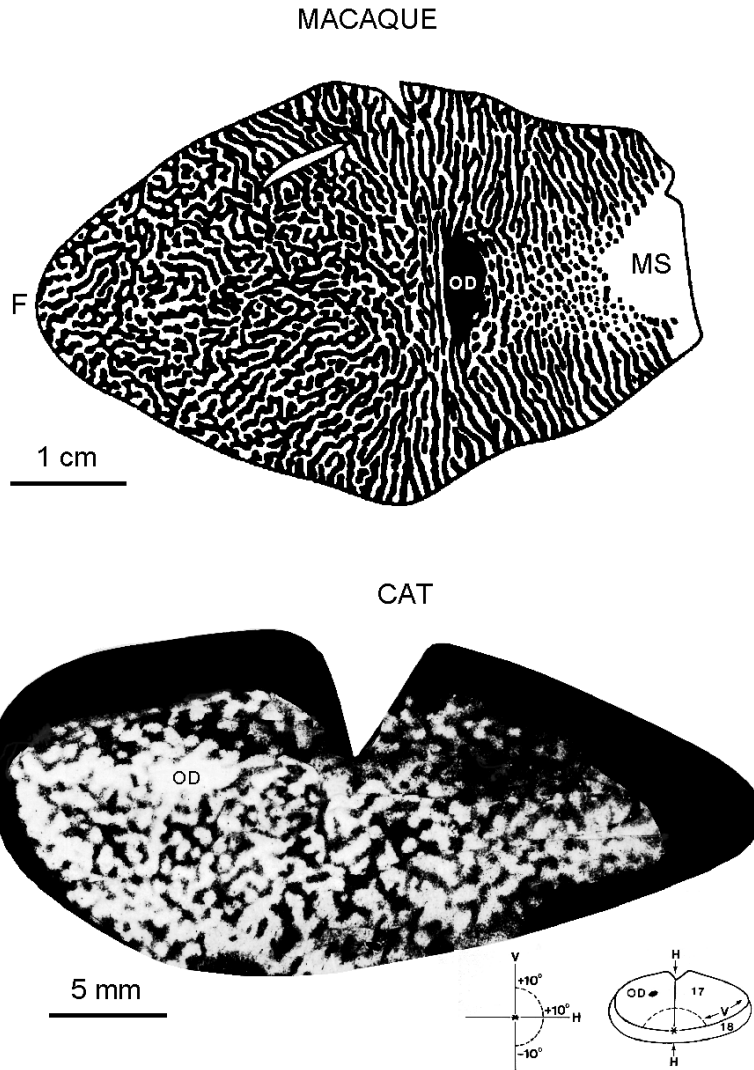


Figure 2. Ocular dominance columns in macaque monkey and cat. The upper panel shows the pattern over nearly the complete visual hemifield in a macaque monkey. The outer boundaries of the pattern correspond to the vertical midline of the visual field; F indicates the fovea; OD the optic disc, and MS the monocular segment. The pattern is a drawing made from a montage of sections stained for cytochrome oxidase in a monkey which had lost one eye over a year prior to sacrifice (from Florence and Kaas (1992)). The lower panel shows the distribution of radioactivity (bright regions) in a photomontage of sections of flattened cat striate cortex following injection of radioactive label into one eye. A sketch of the visual field and corresponding points in the visual cortex is shown below the figure. V = vertical midline; H = horizontal meridian; OD = optic disc; (from Anderson *et al* (1988), with modifications).

frog) also suggests that they might be an incidental outcome of development (Constantine-Paton 1983). And while an obvious candidate function for stripes is stereopsis, it has recently been reported that squirrel monkeys (*Saimiri*), which lack ocular dominance stripes, have a stereoacuity (as revealed by evoked potential methods) comparable with that of human

observers (Livingstone *et al* 1995). If this turns out to be true, it might be worth asking the opposite question: why do ocular dominance stripes not interfere with normal vision?

2.4. *The development of ocular dominance columns*

Ocular dominance columns emerge from an initially overlapping, unsegregated distribution of left- and right-eye inputs within layer IV. It was originally thought that, in macaque monkeys, this process begins shortly before birth and is not complete until four to six weeks of age (Rakic 1976, 1977, Hubel *et al* 1977, LeVay *et al* 1980). However, recent experiments by Horton and Hocking (1996), in which infant monkeys were delivered by Caesarean section one week before the normal time of birth and studied one week later, at around the time of normal birth, have suggested that a nearly adult-like pattern of stripes may normally be present at the time of birth. Because the infant monkeys studied by Horton and Hocking were kept in total darkness at all stages following delivery, the results also show that visual experience cannot have played a role in segregation. This confirms the earlier observation by LeVay *et al* (1980) of normal ocular dominance columns in a seven-week old dark-reared monkey.

In the cat, segregation begins at around three to four weeks postnatally, and ends at around six to eight weeks (LeVay *et al* 1978). The process is usually characterized as one in which spatially selective removal of parts of geniculate axonal arbors is dominant, but because overall synapse density in the visual cortex increases several-fold during the period of segregation (Cragg 1975, Rakic *et al* 1986), selective addition of connections might be more important than selective removal.

A variety of experimental manipulations affects the development of ocular dominance columns. Much of the data comes from cats, although there are some primate data. Almost all of the observations demonstrate that visually driven, as well as spontaneously occurring, patterns of neural activity determine the final outcome of segregation.

2.4.1. *Monocular deprivation.* If vision through one eye is prevented by suturing the eyelids shut for a period of a few days during, or shortly after, the period when segregation occurs, the stripes or patches formed by the deprived eye's inputs shrink, while those from the normal eye expand. This has been shown for both monkeys (Hubel *et al* 1977) and kittens (Shatz and Stryker 1978). These observations are among the strongest pieces of evidence that segregation is a competitive process in which the final outcome is determined, at least in part, by visually evoked neural activity.

2.4.2. *Dark rearing.* A normal pattern of ocular dominance stripes was found in a macaque monkey which had been reared in darkness after birth (LeVay *et al* 1980). Given this evidence, and the fact that Horton and Hocking (1996) carefully avoided exposing the infant monkeys in their study to visible light, it can be concluded that visually driven activity is not required for ocular dominance segregation to take place in the macaque. This does not seem to be true in cat area 17, where it has been found that depriving kittens of visual stimulation by rearing in darkness, or by binocular lid suture, leads to reduced or abnormal segregation of ocular dominance columns (Swindale 1981b, 1988, Kalil 1982, Mower *et al* 1985). A different result was obtained by Stryker and Harris (1986) who found that fluctuations in input density in dark-reared cats could be as large as those seen in normal cats. A possible explanation for the disagreement may come from the results of Fourier power spectral analysis (Swindale 1988) of the distribution of inputs revealed by trans-neuronal autoradiography in area 17. This showed an approximately $1/f$ spectrum, with

no evidence of the peak at a spatial wavelength of about 1 mm which is seen in normally reared animals. Intensity profiles giving rise to a $1/f$ spectrum will contain fluctuations which might be mistaken for normal segregation, but the important finding is the lack of any underlying periodicity. In contrast to area 17, segregation appears to proceed normally in area 18 of dark-reared cats (Swindale 1981b, 1988, Mower *et al* 1985).

2.4.3. Removal of all spontaneous retinal activity. If transmission of signals from the retina to the lateral geniculate nucleus (LGN) is abolished by intraocular injections of tetrodotoxin, segregation fails to occur in either area 17 or 18 of kittens (Stryker and Harris 1986). This suggests that normal segregation in area 17 of the cat requires both visually evoked and spontaneously occurring neural activity in the retina. Spontaneous activity in the LGN, if it occurs in the absence of retinal inputs, is not sufficient. In area 18 of the cat and in area 17 of the macaque, spontaneous retinal activity alone is sufficient.

2.4.4. Strabismus and anisometropia. Artificially induced strabismus (usually produced by cutting the lateral or medial rectus muscle) in the cat results in a more sharply segregated pattern of left- and right-eye inputs (i.e. less overlap at the boundaries (Shatz *et al* 1977)). It also significantly increases the size and spacing of the patches in area 17 (Löwel 1994). Preliminary reports also suggest that ocular dominance columns in rhesus monkeys made artificially anisometric (by rearing with a $-10D$ lens in front of one eye) might be more widely spaced and more irregularly organized than normal (Roe *et al* 1995). Taken together, these observations suggest that although ocular dominance segregation can occur prenatally, without visual experience, abnormal postnatal visual inputs can cause changes in subsequent columnar organization which go beyond the narrowing or widening of stripes produced by monocular deprivation. In particular, both results suggest that ocular dominance column spacing is not necessarily determined by intrinsic intracortical interactions. A comparable result, suggesting the possibility of postnatal reorganization of orientation columns has recently been reported (Blasdel *et al* 1995) and is described below (in section 2.6).

2.4.5. The role of the subplate. Destruction of subplate neurons in the cat during the first or third postnatal week (Ghosh and Shatz 1994) results in a failure of segregation of LGN inputs within layer IV of the cortex. This is a hard result to explain, but one clue is the probable presence of reciprocal connections between the subplate neurons and layer IV in the first few postnatal weeks (Friauf *et al* 1990, Callaway and Katz 1992). These pre-existing connections may serve as a physiological scaffolding to ensure that LGN axons reach their correct sites within layer IV, perhaps using correlated neural activity as a guide. In the absence of this scaffolding, the resulting lack of a normal topography might then cause segregation to fail. It has also been observed that destruction of subplate neurons leads to a loss of layer IV neurons (Ghosh and Shatz 1994) so perhaps it is the loss of their normal targets that prevents geniculate axons from segregating.

2.4.6. Interference with intracortical transmission. A number of experiments have shown that the effects of monocular deprivation in the kitten can be prevented by manipulations that are likely to interfere with normal synaptic function in the visual cortex. These include infusion of NMDA receptor antagonists (Kleinschmidt *et al* 1987, Bear *et al* 1990); muscarinic M_1 receptor antagonists (Gu and Singer 1993); combined removal of cholinergic and noradrenergic afferents to the cortex (Bear and Singer 1986) and combined blockage of serotonin $5-HT_1$ and $5-HT_2$ receptors (Gu and Singer 1995). Because these manipulations

appear to block the removal of relatively inactive geniculate synapses within the cortex, it is likely that they will interfere with the process of segregation as well, although this question has not been addressed experimentally. Infusion of the GABA agonist muscimol into the cortex of monocularly deprived kittens leads to a shift in the ocular dominance histogram in favour of the deprived eye (Reiter and Stryker 1988). This paradoxical result can be explained in Hebbian terms if it is supposed that:

- (i) inactive synapses are removed only when the postsynaptic membrane is depolarized; and/or
- (ii) increased levels of presynaptic activity cause a weakening of synaptic inputs when the postsynaptic membrane is simultaneously hyperpolarized.

The neurotrophins NT-4/5, and brain-derived neurotrophic factor (BDNF), both of which bind with a receptor known as TrkB, were found to block formation of ocular dominance columns when infused into kitten visual cortex (Cabelli *et al* 1995). Infusion of nerve growth factor (NGF) or NT-3 did not have the same effect. This result suggests that stimulation of the TrkB receptor overrides whatever signal causes axonal retraction during segregation.

2.5. Orientation columns in adult animals

Most neurons in mammalian visual cortex respond best to a bar or an edge moving at an appropriate orientation and velocity over the receptive field (Hubel and Wiesel 1962, 1968). A graph of response versus orientation allows one to estimate the cell's preferred orientation (the orientation giving the largest response) and the selectivity for orientation (e.g. the width of the curve at half height). Cells in the same column of tissue tend to have the same orientation preference (Hubel and Wiesel 1962, 1968, 1974a) although, in the cat, orientation preferences of neighbouring neurons can differ by as much as 30° (Lee *et al* 1977, Hetherington *et al* 1995). Whether orientation selectivity in the macaque visual cortex is more orderly than this has not been established. When a recording electrode is moved sideways past a series of columns, the preferred orientation rotates at nearly constant rates over distances of a millimetre or more (Hubel and Wiesel, 1974a) although the direction of rotation (clockwise or counter-clockwise) can change unpredictably. Occasionally, discontinuous jumps of up to 90° in preferred orientation are seen. Similar findings were made in the cat by Albus (1975b) and in the tree shrew by Humphrey and Norton (1980).

Despite the clear-cut one-dimensional evidence provided by recording electrodes, it proved hard to generalize to the probable two-dimensional layout of orientation preferences, and a number of different models were proposed (Hubel and Wiesel 1977, Braitenberg and Braitenberg 1979, Swindale 1982a, 1985, Dow and Bauer 1984). The issue was resolved by the development of the technique of optical recording, in which neural activity is detected with a sensitive camera, either after first applying a voltage-sensitive dye to the surface of the cortex, or by recording small changes in the reflectivity of neural tissue which occur in response to neural activity. Using the former of the two methods, Blasdel and Salama (1986) and Blasdel (1992a, b) recorded the activity evoked by stimuli of different orientations at different positions across the surface of the visual cortex in the macaque monkey. Figure 3 shows, in colour-coded form, the characteristic layout of orientation preferences revealed by this method. Some of the important features of the orientation topography (summarized in table 1) are:

- (i) *periodicity* (which can be measured from two-dimensional Fourier power spectra: see (Obermayer and Blasdel 1993, Blasdel *et al* 1995)) of about 680 μm , in agreement with earlier estimates based on electrode recording (Hubel and Wiesel 1974a);

- (ii) *linear zones*, i.e. regions in which the iso-orientation domains are approximately parallel slabs of uniform width;
- (iii) *saddle points*, i.e. regions which define a local peak in orientation value in one direction and a local valley in the orthogonal direction;
- (iv) half-rotation *singularities* where a single set of orientation domains meets at a point;
- (v) *fractures*, elongated regions characterized by a high orientation gradient, extending from the singularities.

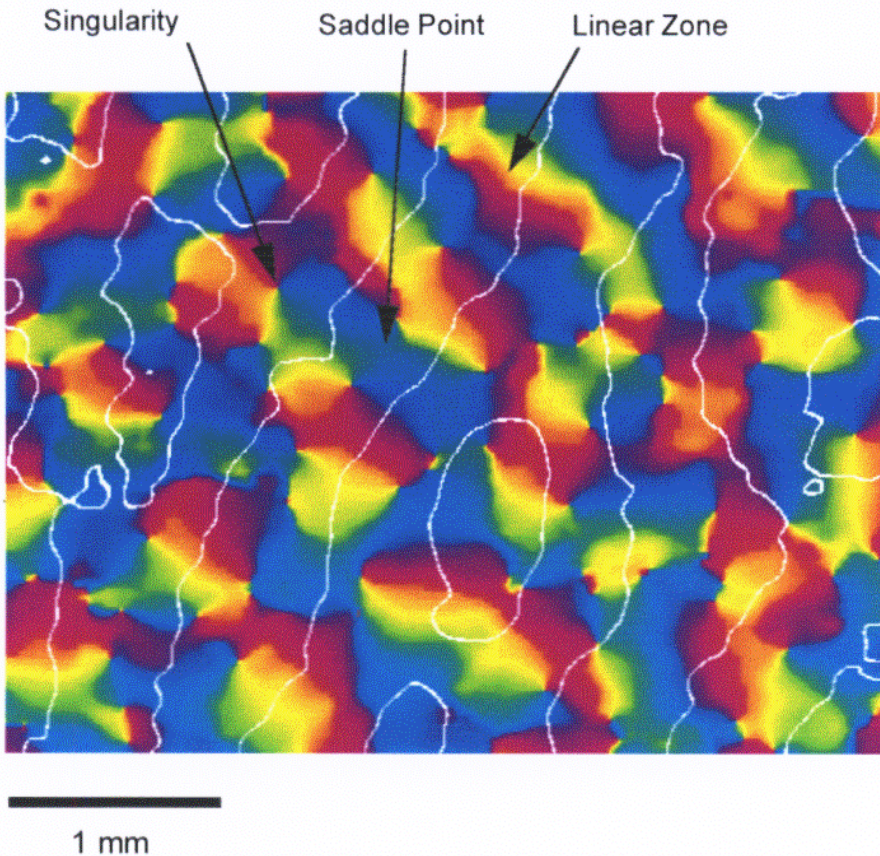


Figure 3. Composite figure showing the arrangement of orientation domains (a single colour represents a unique range of orientation preferences) and their relationship with ocular dominance column boundaries (white lines). The images were obtained by optical recording in macaque monkey striate cortex. Note that the iso-orientation domains tend to intersect ocular dominance column borders at right angles. (Figure supplied by K Obermayer, from data presented in Blasdel (1992b).)

Similar maps of orientation preference were found in areas 17 (Swindale *et al* 1990) and 18 (Swindale *et al* 1987) of the cat, by making multiple electrode penetrations and recording orientation preferences at numerous closely spaced sites in the upper layers of the cortex. More detailed maps were subsequently obtained by optical recording in area 18 (Bonhoeffer and Grinvald 1991) and show essentially similar features. The overall periodicity of the orientation columns in the cat is about 1.0–1.2 mm in area 17 (Albus 1979, Löwel *et al*

Table 1. Cardinal features of the retinotopic, orientation and ocular dominance maps in macaque striate cortex (modified from Obermayer *et al* 1992).

Number	Feature
1	The maps of orientation selectivity and ocular dominance have statistically similar properties across the cortex.
2	Orientation preference changes continuously as a function of cortical location except at singularities of index $\pm \frac{1}{2}$, which appear in approximately equal numbers.
3	There are line-like regions, across which orientation preferences change rapidly with distance ('fractures'), extending from the singularities.
4	There are linear zones, approximately $800 \times 800 \mu\text{m}^2$ in area, bounded by singularities, within which iso-orientation regions are organized as parallel slabs.
5	Correlations between the orientation vector and the orientation gradient vector are weak or absent.
6	The autocorrelation function for orientation preference is positive, with zero average orientation difference, for distances $< 200 \mu\text{m}$ and negative for intermediate distances of about $200\text{--}800 \mu\text{m}$. Correlations for distances $> 800 \mu\text{m}$ are weak or absent. Correspondingly, the Fourier power spectrum is approximately annular, with a peak spatial frequency of about $1.4\text{--}1.8$ cycles/mm.
7	The ocular dominance pattern in layer IVc is organized into sharp-edged stripes which sometimes branch and terminate. The Fourier power spectrum is annular or bi-lobed, with a peak spatial frequency of around 1.25 cycles/mm.
8	Iso-orientation slabs often cross the borders of ocular dominance bands at right angles.
9	Singularities tend to align with the centres of the ocular dominance stripes.
10	Regions of poor orientation selectivity are found in the upper layers of the cortex, above the centres of ocular dominance stripes.
11	Within layer IVc there is an orderly retinotopic map for each eye, which is divided between the stripes in such a way that the field positions represented at the edge of a stripe correspond retinotopically to the field positions mapped in the centres of adjacent stripes.

1987, Diao *et al* 1990) and about $1.2\text{--}1.4$ mm in area 18 (Löwel *et al* 1987 Cynader *et al* 1987). In the cat and in the tree shrew (Humphrey *et al* 1980), iso-orientation domains, for all orientations, show a tendency to be elongated in a direction perpendicular to the area 17/18 border. Little is known about the morphology of orientation columns in species other than the cat, tree shrew and monkey, although this information would be of interest.

2.6. Singularities

Singularities (often referred to somewhat less technically as pinwheels, see e.g. Bonhoeffer and Grinvald (1991)) can be classified into two kinds, positive and negative, depending upon whether the sequence of preferred orientation rotates clockwise for clockwise movement around the singularity, or anticlockwise. Obermayer and Blasdel (1996) analysed the distribution of singularities in maps obtained by optical recordings in squirrel and macaque monkeys. Histograms of the distances between nearest-neighbour singularities showed them to be more regularly spaced than a random distribution of points of the same overall density, although no consistent geometrical pattern was observed. Approximately 80% of nearest-neighbour singularities were of opposite sign: in other words, singularities of the same sign behave as though they repel each other, while unlike singularities are weakly attracted.

The overall density of singularities is best expressed relative to orientation column periodicity because, other structural factors being equal, the density can be expected to scale with the periodicity. In the macaque, the measured density (Swindale 1992a, Blasdel *et al* 1995, Obermayer and Blasdel 1996) appears to vary between about 3.0 and $4.5/\lambda_{\text{OR}}^2$, where λ_{OR} is the spatial wavelength of the orientation domains. This corresponds to a density of about 8 per mm^2 . The densities of positive and negative singularities are similar (Blasdel *et al* 1995, Obermayer and Blasdel 1996). In the cat (Diao *et al* 1990), singularity density appears to be lower than in the macaque: in areas 17 and 18 it is about $1.0/\lambda_{\text{OR}}^2$ (1.3 per mm^2 , $\lambda_{\text{OR}} = 1.14$ mm) although in the 17/18 border region a somewhat higher density of about $2.3/\lambda_{\text{OR}}^2$ (3.0 per mm^2) was measured. This difference may be a result of the greater tendency for iso-orientation domains to be locally parallel in the cat.

2.7. Development of orientation columns

In macaque monkeys (Blasdel *et al* 1995) optical recording experiments show that a normal pattern of iso-orientation domains is present by at least $3\frac{1}{2}$ weeks of age (younger monkeys have not so far been studied with this method). In kittens, optical recording shows that orientation columns are present, in rudimentary form, at 17 days of age (Kim and Bonhoeffer 1993). Between this time and 21 days a more orderly arrangement emerges. The eyes open at about 10 days, so it is possible that visual stimulation plays some role in column formation or refinement. However, both orientation selectivity and apparently normal columnar order are present in newborn macaque monkeys (Wiesel and Hubel 1974), and orientation selective cells can be found in visually inexperienced kittens (Blakemore and Van Sluyters 1975, Sherk and Stryker 1976, Albus and Wolf 1984). Thus, as with the formation of ocular dominance columns in the monkey, visual experience is not an essential component of the initial development of orientation selectivity or of its columnar organization.

2.8. Genes versus the environment

The question of whether or not the orientation preferences of cortical neurons are plastic in early development has aroused both interest and controversy. One view, inspired by the presence of orientation selectivity in newborn macaques (Wiesel and Hubel 1974) and visually inexperienced kittens (Hubel and Wiesel 1963, Sherk and Stryker 1976), is that orientation preferences are genetically determined and are therefore likely to be unmodifiable; another is that preferences result from oriented visual stimulation and can change when, for example, an animal is exposed to a visual environment in which lines of a narrow range of orientations predominate (Blakemore and Cooper 1970, Hirsh and Spinelli 1970).

The experimental evidence for and against these possibilities has been extensively debated (see e.g. Barlow (1975), Blakemore (1978), Movshon and Van Sluyters (1981), Swindale (1982b), Frégnac and Imbert (1984), Mitchell and Timney (1984), Rauschecker (1991)), with many, though not all, authors tending to favour the probability of postnatal modifiability. Recent observations made with the optical recording method add yet another interesting twist: Blasdel *et al* (1995) studied a series of infant monkeys of different ages and found that ocular dominance columns increase in size with age, at a slightly greater rate than do the orientation columns. Because the increase in size of the ocular dominance columns matched the growth of the cortex as a whole, Blasdel *et al* suggest that it is possible that the orientation map, and the preferences of individual neurons, might reorganize substantially during development. Therefore, while orientation columns may be present in very young

monkeys, and, like ocular dominance columns, may form without visual inputs, substantial reorganization might take place postnatally. The observations of Roe *et al* (1995) of the effects of early anisometropia in rhesus monkeys suggest that ocular dominance column morphology might also change postnatally, after an initial innately determined process of column formation (Horton and Hocking 1996).

Given these suggestions, and Löwel's (1994) discovery that strabismus changes the spacing of ocular dominance columns in the cat, it now seems possible that both sides in the debate may turn out to be correct: in the monkey (and to a lesser extent in the cat), both orientation and ocular dominance columns may be capable of forming in the absence of visually driven inputs, but structural reorganization may occur postnatally, especially when very abnormal forms of visual stimulation are present. Section 14.2 discusses some possible reasons for this.

2.9. Structural relationships between the different columnar systems

The maps of visual field position, ocular dominance and preferred orientation have a number of interesting structural relationships, which will be considered in turn.

2.9.1. Retinotopy and ocular dominance. In the macaque, within the central 5° of the visual field and in the fovea, ocular dominance stripes run in directions which have little relation to visual field coordinates (figure 2). More peripherally, the stripes run roughly circumferentially (LeVay *et al* 1985). The functional significance of this arrangement, if any, is unclear. Within layer IVc, where the geniculate afferents terminate and receptive fields are concentric, monocular and small, a very precise map of receptive field position is observed (Hubel *et al* 1974, Blasdel and Fitzpatrick 1984). As the recording electrode moves across layer IVc, perpendicular to ocular dominance stripes, receptive field positions shift at a constant rate in the direction predicted by the global retinotopic map. As the electrode crosses from one eye's ocular dominance stripe to the neighbouring one, receptive fields shift into the other eye, to a field location corresponding to the centre of the preceding stripe (figure 4). This arrangement is predicted by a number of the models of cortical map development discussed below.

2.9.2. Ocular dominance, orientation columns and cytochrome oxidase patches. Examination of orientation tuning curves obtained in long tangential penetrations through monkey visual cortex (Livingstone and Hubel 1984a) showed that there are regions in the upper layers of the cortex in which orientation selectivity is relatively poor or absent, with cells responding at all orientations of the stimulus. These regions, which are about 150–200 μm in diameter and about 400 μm apart, were found to coincide with patchy dark spots seen in histological stains (figure 5) for the cytochrome oxidase (CO) enzyme. Earlier experiments had shown that the CO patches were located in the centres of ocular dominance stripes (Horton and Hubel 1981, Hendrickson *et al* 1981, Horton 1984).

It is easy to demonstrate the CO patches histologically and it has been suggested (Livingstone and Hubel 1984a) that they are signposts for functionally and anatomically distinct channels in visual processing. As well as marking the centres of ocular dominance columns and having poor orientation tuning, cells within the patches and in columns which pass through them, have been reported to respond preferentially to low spatial frequencies (Tootell *et al* 1988a) and to be selective for coloured stimuli (Livingstone and Hubel 1984a, Ts'o and Gilbert 1988, Tootell *et al* 1988c). In addition, the patches have been shown (Livingstone and Hubel 1984a, Hubel and Livingstone 1987) to project to distinct regions

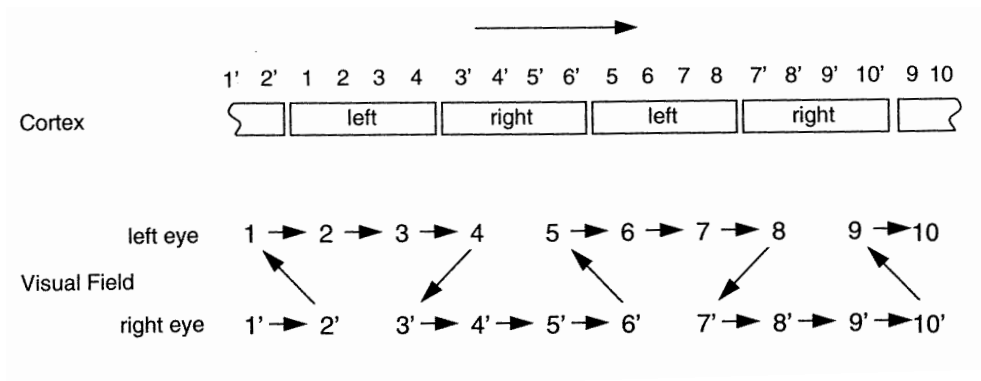


Figure 4. The probable fine-scale mapping of the visual field within single ocular dominance columns in layer IVc of the macaque monkey. In the bottom part of the figure, corresponding receptive field positions in the two eyes are represented by the numbers 1, 2, . . . , 10 in the left eye and 1', 2', . . . , 10' in the right eye. The upper part of the figure shows how these positions may be mapped within alternating left and right eye ocular dominance stripes in the cortex. A recording electrode moving sideways through the stripes would record the sequence of receptive field positions indicated by the arrows in the lower part of the figure.

(thin, darkly staining CO stripes) within area 18 (V2). Although it is highly plausible that the CO patches would contain cells with distinctive physiological properties, some recent studies have suggested that the chromatic tuning of cells within the patches (Lennie *et al* 1990, Leventhal *et al* 1993), their orientation tuning (Edwards and Kaplan 1992, Leventhal *et al* 1993) and their contrast sensitivity (O'Brien *et al* 1995) are no different from cells

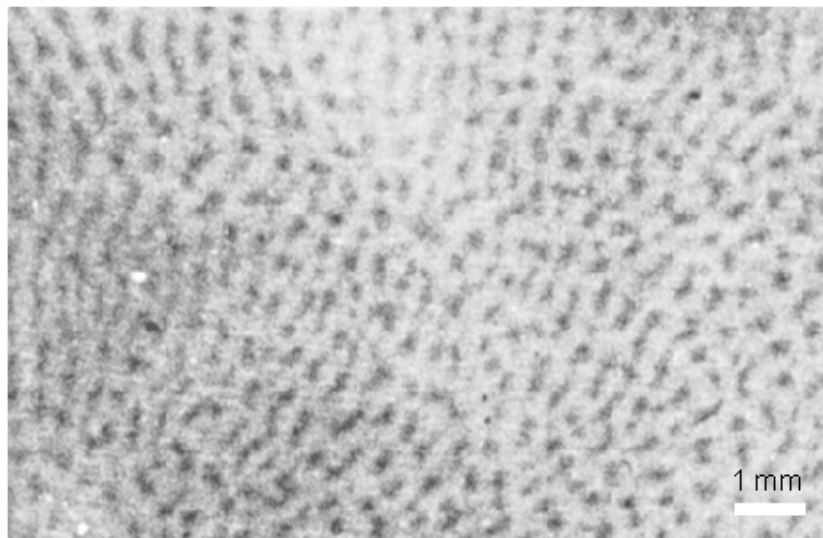


Figure 5. A cytochrome-oxidase stained section through the upper layers of the striate cortex of a macaque monkey. The overall elongation of the blobs in a roughly vertical direction probably indicates the direction of the associated ocular dominance stripes, which are not directly visible. (From Tootell *et al* 1988a.)

outside the patches. Although most of these contradictory findings have so far only appeared as abstracts (Lennie *et al* (1990) is the exception) the physiological distinctiveness of the CO patches should perhaps not yet be taken for granted.

Orientation singularities in the macaque have been shown to occur more frequently in the centres of ocular dominance stripes (Blasdel and Salama 1986, Swindale 1992a, Blasdel 1992b, Obermayer and Blasdel 1993). Although this suggests an association with CO patches, and, thereby, with regions of poor orientation selectivity, this is difficult to prove because the optical recording method averages the signals from many different neurons. Thus, a cortical region containing an orientation singularity may appear to have broad orientation tuning simply because signals from cells with a wide variety of orientation preferences are spatially averaged. One solution to this problem is to combine optical recording or CO staining with microelectrode recording[†] and measure the orientation selectivity of individual neurons, close to a singularity. Such evidence suggests that cells close to the centres of CO patches do not have unusually broad orientation tuning (Edwards and Kaplan 1992) but that local variability of preference is greater in these regions. This would be consistent with an association between singularities and CO patches.

Optical recording experiments (Blasdel 1992a, b, Obermayer and Blasdel 1993, Blasdel *et al* 1995) have shown a striking tendency for iso-orientation domains within the linear zones in the orientation maps to cross the borders of ocular dominance stripes at right angles (figure 3). To this extent, the arrangement is similar to Hubel and Wiesel's (1977) 'ice-cube' model of the visual cortex, although the presence of fractures, singularities and saddle zones in the orientation map means that this model cannot be true in a general sense. However, the reasons for the arrangement may well be those originally proposed by Hubel and Wiesel to justify the 'ice-cube' model, i.e. that it is a way of ensuring that all combinations of eye and orientation preference are represented within a volume of tissue no larger than the cortical point image (Hubel and Wiesel 1974b, 1977, Swindale 1991). Although it was not initially apparent (Löwel *et al* 1988), recent optical recording data from kitten visual cortex (Hübener *et al* 1995) suggest that a similar locally orthogonal relationship exists in the cat.

2.9.3. Orientation columns and retinotopy. Although some models predict a relationship between orientation gradient and local variations in magnification factor, there has been no direct test of this yet and there has been no indication so far of any relationship between the layout of orientation preference and receptive field topography in the monkey. In cat area 18, where magnification factor is anisotropic by a factor of 2–5 (Cynader *et al* 1987), iso-orientation domains show a strong tendency to run perpendicular to the direction in which magnification factor is largest. The cortical point image is also elongated in this direction, i.e. along the axis of greatest magnification factor. Similar relationships may exist in primates, but have not yet been noted. One reason for this may be that magnification factor anisotropies seem to be relatively small in these species and may not be present everywhere.

2.10. Analysis of experimental data

The experimental data are for the most part two-dimensional patterns which are essentially geometrical in nature. Comparison of a model with experimental data usually relies upon a visual impression of similarity between the experimental and computed images. While

[†] Even this method has its problems because, wittingly or unwittingly, microelectrode recordings can easily be multi-unit and, therefore, may also underestimate orientation tuning strength where there is significant local variability in preference.

this may be good enough for many purposes, it would be desirable to go further than this and find objective ways of quantifying and describing the various kinds of pattern that experimenters have come up with. Unfortunately, little work has been done in this area and most experimenters have been content to describe their visual impressions with vague terms, such as ‘banded’, ‘beaded’, ‘patchy’, ‘blobby’[†] etc. Simple techniques, such as calculating the two-dimensional autocorrelation function, or the power spectrum (see e.g. Swindale *et al* (1987), Diao *et al* (1990), Blasdel *et al* (1995)) are helpful in identifying periodicity and/or local order, but these measures do not manage to capture other pattern characteristics such as the extent to which the pattern is banded or patchy. So far, analytical techniques which would allow a quantification of these visual characteristics have either not been developed, or not used. Such measures which, ideally, should avoid the use of subjective estimates (e.g. of the centres of blobs, as in Anderson *et al* (1988)) would be very helpful in comparing results obtained in different areas and species and in assessing the realism of the outputs of different models. The recent quantitative comparison by Obermayer and Blasdel (1996) of singularity distributions in primate visual cortex and in a number of different models is a welcome development in this direction.

3. The models

Models necessarily simplify reality and make assumptions; if they did not, they would be of little use. Assumptions may be general principles (e.g. conservation laws), ideas about the behaviour of parts of the system (e.g. learning rules) or about the values of quantities for which reliable experimental data are lacking. Simplifying assumptions are often forced upon modellers by computational necessity, if not by conceptual elegance. For example, a synapse may be represented by a number, or a visual stimulus may be represented as a point in a stimulus space rather than as a luminance distribution in visual space. All kinds of assumption-making are fraught with difficulty for modellers in neurobiology. General principles which state that some measure is held constant, or minimized or maximized during development, may be very useful, but their application will be different in biology than in physics: there is no guarantee that biological mechanisms will adhere to them rigidly, or that the principles will generalize to other species or different developmental situations. Certain assumptions about biological mechanisms may be well supported by experimental observations, but incorporating them in a working model almost always forces the modeller to make other, less well tested, assumptions. While the aim of making a model detailed and testable throughout is laudable, the more detail that is put in, the more numerous are the possibilities for disproof. If the detail is not strictly necessary for the model to work, it may be unwise to include it.

Certain types of simplification can lead to powerful and elegant models and it will then be hard to interpret the behaviour of the model in biological terms. But, if we agree with von Neumann, if the model works, this should not worry us too much.

3.1. A general overview

Table 2 lists a number of different models of visual cortex organization. One class of model (see e.g. Hubel and Wiesel (1977), Braitenberg and Braitenberg (1979)) simply proposes an arrangement and does not suggest a computational or developmental process

[†] Use of these neutral adjectives is nevertheless preferable to the widely used term ‘module’, which is laden with undemonstrated functional implications and is not as descriptive anatomically (Swindale 1990).

that could give rise to the proposed pattern. A second class proposes some relatively simple computational procedure such as band-pass filtering (see e.g. Rojer and Schwartz (1990)) which will generate a possible set of structures, without necessarily suggesting that the algorithm mimics real development. A third class of model is loosely based on rather general developmental principles and simplifies the computational problem in some way, so that the structure of the model is somewhat abstract. Models based on lateral interactions whose origin is not specified (see e.g. Swindale (1980, 1982a)) and dimension-reduction models (see e.g. Durbin and Mitchison (1990), Obermayer *et al* (1992a, b)) can be placed into this class. Finally, many neural net models based explicitly upon Hebbian learning rules have been proposed. These fall into two main classes: linear and nonlinear models based on local Hebbian modification rules (see e.g. von der Malsburg (1973), Linsker (1986c), Miller *et al* (1989), Tanaka (1989)) and those based on Kohonen's (1982) competitive learning algorithm (see e.g. Obermayer *et al* (1990), Goodhill (1993)).

Nearly all the neural net models of visual cortical development proposed so far are based on a common set of postulates. These are:

- (i) Hebb synapses;
- (ii) correlated or spatially patterned activity in the afferents to cortical neurons;
- (iii) fixed connections between cortical neurons which are locally excitatory and inhibitory at slightly greater distances;
- (iv) normalization of synapse strength.

Normalization typically ensures that the sum of the synaptic weights converging on each postsynaptic neuron remains constant, or that the sum of the weights of each input cell remains the same, or some combination of the two. The constraints can be enforced by dividing or subtracting appropriate values from the weights.

Von der Malsburg (1973) was the first to show that these rules could lead to the emergence of spatial order in receptive field properties in a two-dimensional array of neurons. Subsequent papers by von der Malsburg and Willshaw (1976) and Willshaw and von der Malsburg (1976) showed how similar rules could lead to the emergence of topographic order and ocular dominance columns. More recently, Linsker (1986a, b, c) and Miller *et al* (1989) have extended the scope of these models by devising linear versions of the learning equations, by carrying out more extensive computations, and by making modified assumptions about the properties of the input correlations.

One class of successful model has been inspired by the idea that the visual cortex is a dimension-reducing map (Kohonen 1982, 1988, Mitchison and Durbin 1986, Durbin and Willshaw 1987, Durbin and Mitchison 1990). This follows, given that every point on the cortical surface can be assigned a list of stimulus values, for example, a receptive field position, an eye dominance value and a preferred orientation. This defines a point (or a region, if receptive field size and orientation tuning width are taken into account) in a high-dimensional space whose axes are the values of the stimuli in question. It is often helpful to think of the cortex as a sheet which is folded into this space in an orderly way determined by the values of eye dominance, retinal position and orientation at each point on its surface. Dimension-reduction models assume that this folding (or inverse mapping) attempts to satisfy two conflicting goals:

- (i) to keep the sheet locally smooth;
- (ii) to ensure that it passes through a representative selection of points in stimulus space.

Algorithms which achieve such projections have been devised (Kohonen 1982, Durbin and Willshaw 1987) and applied to the visual cortex (Durbin and Mitchison 1990, Goodhill

Table 2. Summary of models.

Author(s)	Retinal/LGN inputs	Cortical modification rule
<i>Retinotopy</i>		
Willshaw and von der Malsburg (1976)	neighbouring pairs of units	Hebbian
Willshaw and von der Malsburg (1979)	chemical markers	chemo-similarity
<i>Ocular dominance</i>		
von der Malsburg and Willshaw (1976)	neighbouring pairs of units	Hebbian
von der Malsburg (1979)	chemical markers	chemical markers
Swindale (1980)	n/a	lateral interactions
Miller <i>et al</i> (1989)	radially uniform correlations	Hebbian correlation
Goodhill and Willshaw (1990)	points in a stimulus space	dimension reduction (elastic net)
Tanaka (1990)	radially uniform correlations	Hebbian, thermodynamic
Roger and Schwartz (1990)	n/a	spatial filtering
Jones <i>et al</i> (1991)	n/a	n/a
Montague <i>et al</i> (1991)	travelling waves	Hebbian plus chemical diffusion
Goodhill (1993)	radially correlated noise	competitive Hebbian (Kohonen)
Elliott <i>et al</i> (1996a, b, c)	circular patches	competition for neurotrophins, simulated annealing
<i>Orientation</i>		
von der Malsburg (1973)	elongated patches	Hebbian
Braitenberg and Braitenberg (1979)	n/a	unspecified
von der Malsburg and Cowan (1982)	initially uncritical oriented stimulation	initial preferences, lateral interactions
Bienenstock <i>et al</i> (1982)	n/a	Hebbian
Swindale (1982)	n/a	lateral interactions
Linsker (1986)	uncorrelated noise	Hebbian, simulated annealing
Soodak (1987)	n/a	derived from the retinal mosaic
Barrow (1987)	natural images	competitive Hebbian (Kohonen)
Durbin and Mitchison (1990)	points in a stimulus space	elastic net
Obermayer <i>et al</i> (1990)	elongated patches	competitive Hebbian (Kohonen)
Tanaka (1990)	radially correlated noise	Hebbian, thermodynamic
Roger and Schwartz (1990)	n/a	gradient of filtered noise
Miller (1992, 1994)	radially uniform correlations, negative correlations between ON and OFF inputs	Hebbian
Miyashita and Tanaka (1992)	radially uniform correlations, negative correlations between ON and OFF inputs	Hebbian, thermodynamic
Niebur and Wörgötter (1993)	n/a	spatial filtering
<i>Orientation and ocular dominance</i>		
Hubel and Wiesel (1977)	n/a	n/a
Götz (1988)	n/a	neural activity gradient
Yuille <i>et al</i> (1991)	points in a stimulus space	dimension reduction
Obermayer <i>et al</i> (1992)	points in a stimulus space	low-dimensional Kohonen
Swindale (1992)	n/a	lateral interactions, competition between feature specificity
Grossberg and Olson (1994)	n/a	filtering in the frequency domain
Erwin <i>et al</i> (1995, figure 11)	points in a stimulus space	elastic net

and Willshaw 1990, Obermayer *et al* 1991, 1992a, b) and result in descriptively accurate patterns of retinotopy, ocular dominance and orientation preference. Although it is easiest to conceive of the behaviour of these models in abstract geometrical terms, as outlined below

(in section 9), their behaviour is closely analogous to that of a competitive Hebbian learning network in which modifications in connection strength are made to those cells which are maximally responsive to a given stimulus at any one time, with lesser modifications made to neighbouring cells.

For orientation and ocular dominance columns, simpler approaches than those used in neural network models can be adopted. It is possible to elaborate on the simple ideas of left–right eye competition proposed by Hubel *et al* (1977) to explain the formation of the characteristic striped pattern of ocular dominance (Swindale 1980). This model, which involves lateral inhibitory effects on the growth of synapses, is relatively simple to implement computationally and can be formulated mathematically as a single integro-differential equation. It is possible to show (Miller *et al* 1989) that the postulated lateral interactions can result from a Hebbian mechanism like that initially proposed by von der Malsburg (1973), although interpretation in terms of locally acting diffusible growth factors, or a combination of several different mechanisms is equally possible. Similar ideas can be used to describe the development of spatial pattern in the map of orientation selectivity in the cortex (Swindale 1982a) while the two models can be linked (Swindale 1992a, Erwin *et al* 1995) so as to reproduce the structural relationships between orientation and ocular dominance columns found experimentally in the monkey.

The following sections describe examples of specific models in more detail.

4. Von der Malsburg's model for self-organization of orientation selectivity

Von der Malsburg (1973) invented a simple model cortex, consisting of 169 E (excitatory) and an equal number of I (inhibitory) cells connected together in such a way that E cells excited neighbouring E cells and inhibited (via the I cells) E cells a slightly greater distance away. Each E cell received excitatory connections from a set of 19 retinal input neurons and each retinal neuron was connected with every E cell, initially with a random synaptic strength s_{ik} from retinal cell i to cortical cell k . The response, $H_k(t)$, of a cortical cell k to a stimulus pattern $A_i(t)$ was given by the following nonlinear differential equation†:

$$\frac{dH_k(t)}{dt} = -\alpha_k H_k(t) + \sum_{l=1}^N p_{lk} H_l^*(t) + \sum_{i=1}^M s_{ik} A_i^*(t) \quad k = 1, \dots, N \quad (1)$$

where α_k is a decay constant, p_{lk} is the connection strength from cell l to cell k and $H^*(t)$ and $A^*(t)$ are the values of $H(t)$ and $A(t)$, respectively, after the application of a threshold function. The first term on the right-hand side represents the natural tendency of a neural response to decay with time, the second term represents the combined excitation and inhibition produced via intracortical connections from other cortical neurons, while the third term represents the direct effect of the retinal inputs to the E cells in the network. The network was presented in turn with one of nine oriented patterns of activity in the set of retinal neurons (shown in figure 6(A)). In each pattern, only seven of the 19 inputs were active. Note that there is no topography in the retinal inputs, i.e. each retinal neuron is connected to every cortical neuron. For each stimulus, an approximate solution to (1) was obtained iteratively, following which the input synaptic strengths to the E cells were changed according to the rule:

$$\Delta s_{ik} \propto A_i^* H_k^* \quad (2)$$

† In presenting the equations for the different models I have used, for the most part, each author's own mathematical terminology. The meaning of a given symbol is therefore usually confined to the immediate context of the model under discussion.

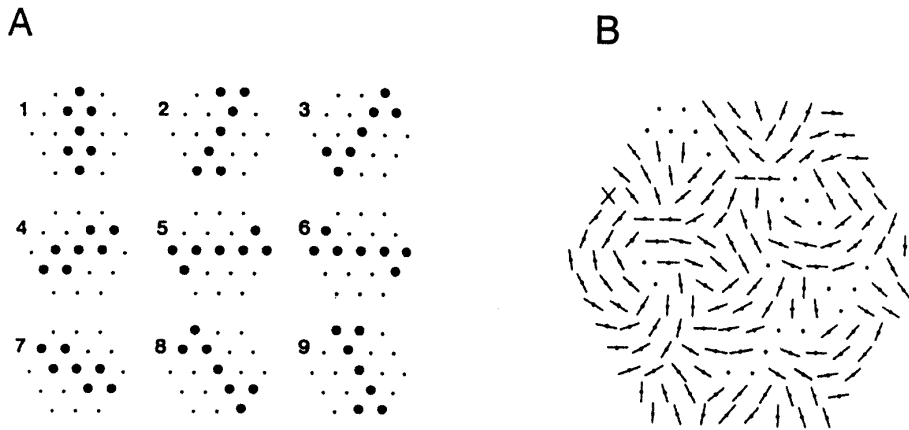


Figure 6. (A) The nine different stimuli used by von der Malsburg (1973). The large dots are active units. (B) The layout of orientation preference in the simulated cortex after 100 learning steps. The dots represent units which failed to learn to respond to any of the stimuli. (Reprinted by permission of Springer-Verlag from von der Malsburg (1973).)

After each learning step, the total of the synaptic strengths impinging on each cortical E cell was normalized by multiplying the s_{ik} by a factor proportional to $1/\sum_i s_{ik}$. As Δs_{ik} is always positive, normalization is the only way of decreasing synaptic strengths. After 100 iterations, in each of which a complete set of nine activity patterns was presented, most of the E cells in the network became selectively responsive to a small set of neighbouring stimulus orientations. Furthermore, the preferred orientation of neighbouring E cells was similar and changed systematically across the surface of the model cortex, much as had recently been found in cats (Hubel and Wiesel 1962) and monkeys (Hubel and Wiesel 1968). The pattern of orientation preferences produced in one of von der Malsburg's simulations is shown in figure 6(B).

Von der Malsburg's neural net model was one of the first to incorporate a local connectivity scheme based on short-range excitatory and longer-range inhibitory connections in a sheet of cells. It was also the first model to produce a spatial topography of orientation preference. Although the area of model cortex was small, the two-dimensional topography seems quite similar to that now known to exist: e.g. figure 6(B) shows regions of continuous change, evidence of an overall periodicity (of about five array units) and singularities. One minor problem with the model results from the application of a threshold function to the response of each cortical neuron: some E cells never responded to any of the standard stimuli used (despite subsequent changes in the responsiveness of nearby E cells) and so remained 'frozen' during development. Subsequent modellers have avoided the problem by using a mechanism (sometimes termed a 'conscience') which varies the probability of a cell's response according to how often it has responded in the past. A more important issue concerns the model's explicit dependence upon oriented patterns of stimulation during development. At the time the model was formulated, it seemed possible that the development of orientation selectivity in visual cortical neurons might be entirely a consequence of environmental visual stimulation (Blakemore and Cooper 1970, Hirsch and Spinelli 1970, Barlow and Pettigrew 1971), in which oriented patterns of activity on the retina would be common. However, when orientation selectivity was demonstrated in newborn animals

which had had, at the most, a few hours of visual experience (Wiesel and Hubel 1974, Sherk and Stryker 1976) it became clear that visually driven neural activity could not be the only initial determinant of orientation preferences. Although spontaneously occurring retinal activity did not seem likely to show other than radially symmetric correlations (which perhaps explains the dearth of neural net models of orientation specificity during the 1980s) it has since been found that spontaneously occurring waves of activity can traverse the developing prenatal retina (Galli and Maffei 1988, Meister *et al* 1991, Wong *et al* 1993). A model for this behaviour has been proposed (Burgi and Grzywacz 1994). It is possible that this stimulation might be enough to drive the initial formation of orientation preferences in cortical neurons, although Miller (1994) has argued that the waves are too slow and broad to be sufficient. An alternative strategy, taken by Linsker (1986a, b, c) and Miller (1992b, 1994), is to examine the possibility that local, circularly symmetric, patterns of correlation in retinal activity might drive the formation of orientation selective receptive fields. This is discussed in more detail in sections 6 and 7.2.

4.1. Extensions of von der Malsburg's model to retinotopy and ocular dominance column formation

The inputs to von der Malsburg's model cortex come from a retina whose projection to the cortex lacks any topography, i.e. each retinal neuron projects initially to each cortical neuron. An oriented pattern of retinal activity in this framework is a somewhat abstract concept because it is only defined as activity in a subset of neurons (in von der Malsburg's model, seven out of 19 inputs were active while the others were silent) and the selection of this subset is arbitrary, at least for the first pattern in the series. What is important is that

- (i) different stimulus patterns overlap,
- (ii) the pattern of overlap among members of the stimulus set implicitly defines a cyclic stimulus space[†]. (This is easily seen from inspection of the stimuli shown in figure 6(A)).

What von der Malsburg's network does (as do all neural nets) is to uncover structure in the input stimulus space (a space which has as many dimensions as there are input neurons) and, by virtue of the lateral connections, to make this structure explicit in the form of a map on the surface of the cortex.

Given these considerations, it is natural to ask what types of map would be formed if stimulus patterns other than the oriented set shown in figure 6 were presented to the network during learning. For example, would localized clusters of activity in the retinal neurons lead to the emergence of topographic order in the projection from the retina to cortex? What kind of projection would form if the model retina were divided into two separate subsets of neurons (i.e. left and right eyes) which were never (or rarely) simultaneously active? These questions were answered in two subsequent papers (von der Malsburg and Willshaw 1976, Willshaw and von der Malsburg 1976) which showed that localized clusters of activity in the retinal neurons did indeed lead to the emergence of a spatial topography in the projection from the retina to the cortex, provided that neighbouring clusters overlapped. During the process of map formation, the connections made by each retinal neuron, which were initially spread over the entire cortical surface, gradually contracted until each neuron made a dense

[†] One can define the similarity between two stimulus patterns most generally as the covariance between the patterns or, more simply (in the case of inputs which are either 1 or 0), as the number of points the two stimulus patterns have in common (the inverse of the Hamming distance between the patterns). For the stimulus patterns shown in figure 6, it is obvious that each pattern is most similar to the two patterns adjacent to it and can be mapped to a cyclic stimulus space of lower dimension 1, 2, ... 9, 1, 2 etc.

set of connections in a localized region of cortex. Correspondingly, the receptive fields of the cortical neurons, which were initially large, became smaller until they were similar in size to the activating clusters. As in the case of oriented inputs, synaptic normalization plays a large part in the process of receptive field refinement. Thus, as the inputs from one region of the retina to a cortical cell are strengthened, normalization ensures that the inputs from other regions are weakened.

Having shown how this model could explain the formation of retinotopy and orientation columns, von der Malsburg and Willshaw (1976) went on to show how it could explain ocular dominance stripe formation. Using essentially the same equations as those used previously (but with a modification, described in Willshaw and von der Malsburg (1976), which made them more stable), they examined the projection that was formed when two sets of retinal neurons were connected to the model cortex described above. As before, random weights were assigned to the connection strengths between these neurons and the cortex. Activity patterns were assumed to be locally correlated within each retina and anticorrelated between the two retinas. Although each retina was small and consisted of only five neurons, over time the projection from each retina to the cortex segregated into periodic stripes (figure 7).

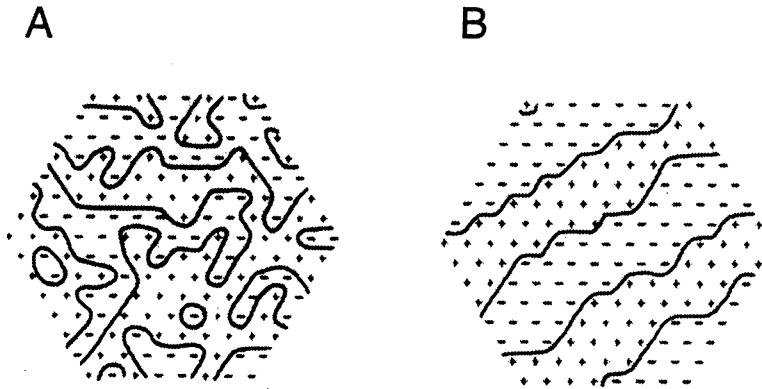


Figure 7. Formation of ocular dominance stripes in the model of von der Malsburg and Willshaw (1976). The layout of cortical units is the same as in figure 6(B). (A) The initial layout of eye dominance. (B) The final layout. (Reprinted by permission of Springer-Verlag from von der Malsburg and Willshaw (1976).)

Segregation in this model occurs for the following reason: clustered activity in one retina gives rise to one or more regions of activity in the cortex (determined by the pattern of lateral connections in the cortex). The strengthening of connections between these retinal inputs and the active ones in the cortex increases the probability that a second pattern of retinal activity, which partially overlaps with the first one, will activate a similarly overlapping pattern of cortical activity. In other words, strengthening the connections from one region of retina to one region of cortex increases the probability that the connections from nearby regions of retina to nearby regions of cortex will be increased. At the same time, the laterally inhibitory connections in the cortex restrict the size of the clusters of cortical activity and the distance over which the locally cooperative effects are exerted. Anticorrelations between the two eyes ensure that they are rarely active at the same time, so that when one eye's synapses are coactive with a cortical cell the less active synapses from the other eye onto

the same cell will not be strengthened. Finally, normalization ensures that whenever the inputs to a single cortical neuron from one eye are strengthened, inputs from the other eye are, on average, weakened.

It would be possible, in principle, to scale up von der Malsburg and Willshaw's network, to give it a much larger and more realistically structured retina and cortex and to present it with retinal activity patterns known to occur pre- or postnatally. In this form, the model might be capable of addressing the three problems studied separately: retinotopy, orientation selectivity and ocular dominance. However, at least until recently, it would have been beyond the capabilities of most computers to carry out the necessary computations in a feasibly short time. Partly for this reason, much of the work that followed that of von der Malsburg and Willshaw attempted to simplify the problem in various ways, allowing computational solutions to simpler (or more easily solved) sets of equations. The approaches of Swindale (1980, 1982a), Kohonen (1982, 1988), Linsker (1986a, b, c), Miller *et al* (1989), Durbin and Mitchison (1990), Goodhill (1993) and Obermayer *et al* (1990, 1991, 1992a, b) all fall into this category. The abstractions involved in making these simplifications will be considered in the following sections.

5. Swindale's models for ocular dominance and orientation columns

5.1. Ocular dominance columns

The models of von der Malsburg and Willshaw lead to the emergence of spatial order in the cortical map because of the existence of lateral interactions within the cortex that are excitatory at short range and inhibitory at slightly greater distances. Without these interactions, the weight values, and hence the receptive field properties of each cortical neuron, would develop independently of each other, and no spatial order would emerge. As described in the preceding section, the lateral interactions lead, in the case of ocular dominance, to distance-dependent effects of weight changes between pairs of synapses in the model. In the case of orientation preference, the net effect of the interactions is to cause nearby locations in the cortex to develop similar orientation preferences, while locations that are far enough apart to be reciprocally inhibitory will rarely respond to the same stimulus and might be expected to develop preferences for stimuli that are maximally dissimilar, i.e. orthogonally oriented.

This suggests that the description of how synaptic strengths change in the model, and in the real brain, might be simplified by specifying only the variables which are usually measured in experiments, namely the densities of left- and right-eye synapses, or an orientation preference, on the surface of the cortex, and by assuming that these values change interactively, with interactions that are cooperative over short distances and anticooperative over slightly greater distances. For ocular dominance, the following approach can be adopted: let the densities of left- and right-eye synapses at a point $\mathbf{r} = (x, y)$ on the cortical surface be described by the variables $n_L(\mathbf{r})$ and $n_R(\mathbf{r})$ and suppose that the effect of a small increase in the density of one type of synapse at a point \mathbf{r}_1 on the growth of other synapses at a point \mathbf{r}_2 can be described by the function $w(\mathbf{r}_2 - \mathbf{r}_1)$. Four types of interaction are possible: right-right, left-left, left-right and right-left, for which four corresponding interaction functions can be postulated: w_{RR} , w_{LL} , w_{LR} and w_{RL} . Assuming that the effects add linearly, the growth rates of right- and left-eye synapses can be given as:

$$\begin{aligned} \partial n_R / \partial t &= (n_R * w_{RR} + n_L * w_{LR}) f(n_R) \\ \partial n_L / \partial t &= (n_L * w_{LL} + n_R * w_{RL}) f(n_L) \end{aligned} \quad (3)$$

where the symbol $*$ denotes convolution, and the function $f(n)$ is used to terminate growth as the synapse density n reaches an upper or lower limit. Because synapse density cannot be negative, an appropriate form for $f(n)$ is the logistic function

$$f(n) = n(N - n) \quad (4)$$

where N is the maximum allowable synapse density: this ensures that $0 \leq n \leq N$. It is convenient, although not essential, to make w a difference of Gaussians,

$$w(x, y) = A \exp\{-(x^2 + \beta y^2)/2\sigma_E^2\} - B \exp\{-(x^2 + y^2)/2\sigma_I^2\} \quad (5)$$

where A and B are constants with the same sign; σ_E and σ_I are the space constants of the lateral interactions, with $\sigma_E < \sigma_I$, and β can be used (if $\neq 1$) to introduce a local anisotropy into the lateral interactions. For same-eye interactions (RR and LL) A and B will both be positive, while for opposite-eye interactions (RL and LR) they will be negative. Initially, n_R and n_L are assumed to be randomly distributed around some initial mean value (e.g. $N/2$) with a small variance.

Computer solutions to these equations result in the formation of striped patterns under a wide variety of choices of the parameters A , B , σ_E , and σ_I for each of the four w functions involved. Although the stability of the model to all possible choices has not been fully explored[†], there exist conditions in which both n_R and $n_L \rightarrow N$ everywhere, which may have some biological relevance, given that some animals lack ocular dominance stripes. (Other regimes of the model, in which one, or both n_R and $n_L \rightarrow 0$ are obviously of less biological interest). Although they are not a serious problem, these instabilities can be avoided and the model simplified, by assuming (as did von der Malsburg) a constant total density of left- and right-eye synapses, i.e. $n_R + n_L = N$ at each point in the cortex. It would be possible to implement this constraint as a separate computational step, but it is simpler (although not equivalent) to note that it implies that $\partial n_R/\partial t = -\partial n_L/\partial t$, which will be guaranteed if $w_{RR} = -w_{RL}$ and $w_{LL} = -w_{LR}$. Under these conditions, the model equations reduce to

$$\partial n/\partial t = (n * w + K)(1 - n^2) \quad (6)$$

where $n = (n_R - n_L)/N$, $w = N^2(w_{RR} + w_{LL}) = -N^2(w_{RL} + w_{LR})$ and $K = N^2 \int (w_{RR} - w_{LL}) d\mathbf{r}$. The latter term, K , is a constant whose value will be zero if the interaction between the eyes is symmetric. It will be non-zero when the interaction is asymmetric, as may be the case in monocular deprivation, or when the projection from one eye is stronger than the other, as in the cat. This equation leads to stable and spatially inhomogeneous values of $n = \pm 1$ everywhere, subject mainly to the constraints that $\int w(\mathbf{r}) d\mathbf{r} \leq 0$ and suitable initial values for n (e.g. random fluctuations around 0).

For small fluctuations of n around zero (i.e. $n_R \approx n_L$) and, denoting the Fourier transforms of $n(\mathbf{r})$ and $w(\mathbf{r})$ by $N(\boldsymbol{\nu})$ and $W(\boldsymbol{\nu})$, respectively, equation (6) gives[‡]

$$\partial N/\partial t \approx NW + K. \quad (7)$$

This has the solution

$$N(t) = N_0 \exp(Wt) + (K/W) \{\exp(Wt) - 1\} \quad (8)$$

where N_0 is the Fourier transform of N at time $t = 0$. If n is initially randomly distributed (as the biological data suggest) then its Fourier transform will contain energy distributed

[†] A linear stability analysis of the system may be less satisfactory than a computational exploration of it, given the nonlinear nature of (3) and (4).

[‡] Convolution becomes multiplication in the Fourier domain, and *vice versa*. A similar analysis can be carried out for (3), leading to somewhat more complicated expressions for $\partial N_R/\partial t$ and $\partial N_L/\partial t$.

over a wide range of spatial frequencies[†]. According to (8), energies at different frequencies will grow exponentially fast during the initial stages of development, with rates determined by W , i.e. the Fourier transform of the lateral interaction function w . It suggests that the dominant spatial frequency in the final pattern will be that for which $W(\nu)$ is a maximum[‡]. Calculations have suggested that this is actually the case. It also suggests that a sufficient condition for the formation of a periodic pattern is that $W(\nu)$ should have a clearly defined positive maximum. This is a requirement that will be satisfied by many different functional forms of $w(\mathbf{r})$.

Also of interest is the behaviour of $N(0)$, i.e. the DC component, or space-average value of n . Provided $W(0)(= \int w(\mathbf{r})d\mathbf{r}) < 0$, (8) has a stable equilibrium solution

$$N_{\infty}(0) = -K/W(0). \quad (9)$$

When $W(0) > 0$ there is a risk of non-periodic stable states forming, in which $n =$ either $+1$ or -1 everywhere, especially if $N(0)$ is not close to zero. This suggests that, in animals which have ocular dominance columns, $W(0) < 0$.

This system (as defined by (3), or the simplified version given by (6)) is capable of describing many of the observed phenomena of ocular dominance column segregation. These will be discussed in the following sections.

5.1.1. Stripe morphology. By an appropriate choice of parameters for w and K (6) the model can reproduce much of the inter-species variability in patterns, e.g. between cat and macaque monkey (Swindale 1981a). Most morphological features in the real patterns can also be found in the model patterns. These include Y- and H- type branches, a tendency for stripes to narrow at branch points, periodic variability in width along the length of the stripes and 'islands' (i.e. isolated spots or short patches and occasional small spine-like protrusions from one stripe into an adjacent one).

5.1.2. Long-range order. In talapoin monkeys (Florence and Kaas 1992) and in the peripheral visual field regions of the macaque (figure 2) ocular dominance stripes run in a uniform direction; in addition, the frequency of branching is reduced so that, overall, the pattern shows more long-range order. There are a number of possible reasons for this. Slight departures from circular symmetry in the laterally trophic and atrophic effects subsumed by $w(\mathbf{r})$ cause the stripes to orient themselves so as to maximize their intersection with the region within which w is positive, and to minimize their intersection with the region within which w is negative (Swindale 1980). Another factor that can impose long-range order is anisotropic expansion of the substrate in which the stripes are forming, without commensurate expansion of $w(\mathbf{r})$. This causes the stripes to run parallel to the direction of expansion (Swindale 1980). Both these factors might play a role in determining the global organization of ocular dominance stripes in the monkey: it has recently been suggested (Blasdel *et al* 1995) that growth of the visual cortex in the first few weeks of life is anisotropic, while tracer injections (Yoshioka *et al* 1996) show that lateral intrinsic connections extend further in a direction perpendicular to ocular dominance columns. If, as suggested by Tanaka (1991a), the growth equations are modified to include the continuous spontaneous creation and removal of a proportion of left- and right-eye connections during development, then the final pattern of stripes becomes more orderly, with a reduced number

[†] It should not be assumed that the spectrum will necessarily be flat: noise in biological systems is often $1/f$ rather than flat.

[‡] For (5) this frequency is given by: $\nu_{\max} = (1/\pi)[\log_e\{(\sigma_I/\sigma_E)2(B/A)^{1/2}\}/(\sigma_I^2 - \sigma_E^2)]^{1/2}$.

of bifurcations: eventually these may disappear entirely, although the process is very slow (Swindale, unpublished results).

5.1.3. Boundary effects. Ocular dominance stripes in most species show a tendency to run at right angles into the borders of the area in which they are present. This can be explained as a consequence of the truncation of $w(\mathbf{r})$ at the boundary: close to the boundary (across which both n_R and $n_L = 0$) the inhibitory surround is effectively elongated in a direction parallel to the border, which causes the stripes to run in an orthogonal direction (Swindale 1980). This is a relatively weak effect however, and it would not be surprising if the factors discussed in the preceding paragraph and/or others, played a more significant role.

5.1.4. Monocular and binocular deprivation. This can be expected to have many consequences, including a reduction in the overall firing rates of retinal ganglion cells, as well as changes in the spatio-temporal structure of their firing patterns. It is reasonable to assume that monocular deprivation will lead to a reduced ability of the deprived eye's synapses to interact locally with other synapses, whether from the same, or the other eye. One way of modelling this is to reduce the magnitude of the central, positive region of (for right-eye deprivation) the functions w_{RR} and w_{RL} (e.g. by reducing the value of A in (5)). This has the effect of making K (6) more negative, shifting the equilibrium mean value of n ($= N(0)$, equation (9)) to a negative value. The end result is to reduce the territory occupied by the deprived eye. If the simulated deprivation is initiated at the start of development, spots, rather than stripes, develop. If it is done for a short period in the middle of development, or when the stripes are forced to have a common orientation, narrow short stripes, rather than spots, are formed. This latter change corresponds with what has been observed in the monkey (Hubel *et al* 1977). Given that it now seems likely to be the case that ocular dominance stripes in the monkey are nearly fully formed at birth (Horton and Hocking 1996), monocular deprivation beginning at birth probably satisfies this requirement.

Binocular deprivation can be simulated by applying the changes assumed to occur with monocular deprivation to both eyes. Under these conditions, the model will still generate stripes. Because K remains unchanged by a symmetrical change to both eyes, any effects on the mean value of n will be relatively small; however, a consideration of the shape of the Fourier transform of $w(\mathbf{r})$, ($W(\nu)$: figure 8) shows that the amplitude of the frequency for which W is maximum (ν_{\max}) will be reduced. Since it is this that determines the overall rate of stripe formation, the rate at which stripes form should be reduced as a consequence of binocular deprivation. Although the experimental finding (discussed above, in section 2.4.2) of a permanently reduced degree of segregation in area 17 of binocularly deprived cats is somewhat at odds with the predictions of the model, it may be helpful to note that the effects of deprivation on the sizes of ocular dominance patches are mediated by a change in the value of $W(0)$, whereas the effects of deprivation on the segregation rate are dependent upon the values of $W(\nu_{\max})$. Therefore the two manipulations can, in principle, have independent effects.

5.1.5. Transient and deprivation-induced ocular dominance columns. As described in section 2.3, ocular dominance patches are present transiently in young marmosets but disappear in adulthood†. They can be induced to remain permanently by monocular or

† A suggested reason for this (Pettigrew, personal communication) is that the eyes of the marmoset are close together and, therefore, left and right retinal inputs are more highly correlated than in larger mammals.

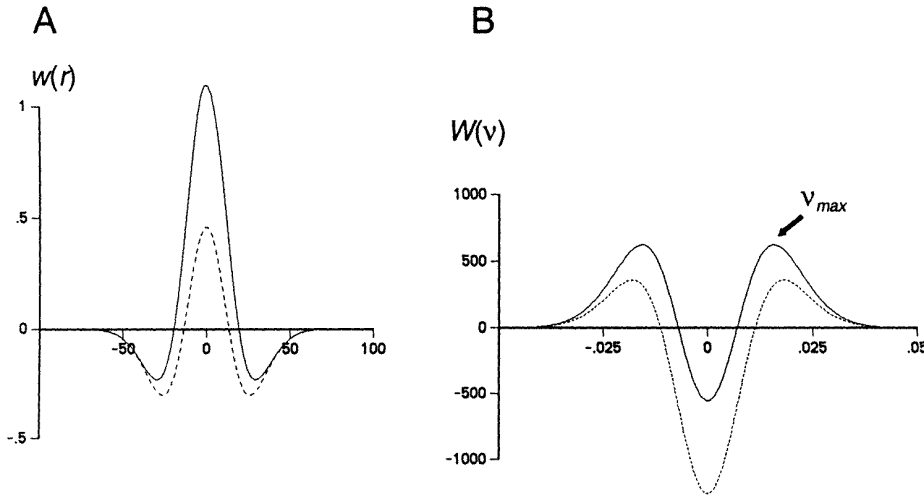


Figure 8. (A) Examples of difference-of-Gaussian lateral interaction functions, $w(r)$, used in the models of Swindale, and (B) their corresponding Fourier amplitude transforms, $W(v)$. The frequency for which $W(v)$ is a maximum, v_{max} , determines the periodicity of the stripes, while $W(v_{max})$ determines the rate at which stripes form. Simulated visual deprivation (dashed lines) causes a large decrease in $W(0)$, but has several other effects, including a reduction in the amplitude of $W(v_{max})$ and an increase in v_{max} .

binocular deprivation. Similarly, monocular deprivation causes stripes to form in the owl visual wulst, although they are not normally present. This apparently paradoxical behaviour is consistent with the behaviour of the system defined by (3) where one can choose parameters for w_{RR} , w_{LL} , w_{RL} , and w_{LR} such that both left- and right-eye synapses show a net increase in density and segregation fails as both eyes eventually reach their upper limiting density, N , everywhere. However, during this process the two eyes exhibit a transient reciprocal patchiness (figure 9). If one eye (or both) is ‘monocularly deprived’ (using the same change described above, i.e. a reduction in the magnitude of its local effects on growth) then the patchiness can persist as a stable state (figure 9).

5.2. Orientation columns

Extension of the above approach to orientation column formation is straightforward. Because orientation is a cyclic quantity, it is convenient to represent it as a complex number, $z = a + ib$. The orientation represented by z is then defined as

$$\theta = 0.5 \arctan(b/a) \quad (10)$$

where θ is cyclic over the range $0-\pi$. The modulus of z , $|z| = (a^2 + b^2)^{1/2}$, is assumed to bear some relation to the orientation tuning strength of the region in cortex in question. If response (e.g. as measured in an optical recording experiment) as a function of orientation is $R(\theta)$, then the components a and b might reasonably be defined as

$$a = \sum_i R(\theta_i) \cos(2\theta_i) \quad b = \sum_i R(\theta_i) \sin(2\theta_i) \quad (11)$$

DEPRIVATION-INDUCED OCULAR DOMINANCE COLUMNS

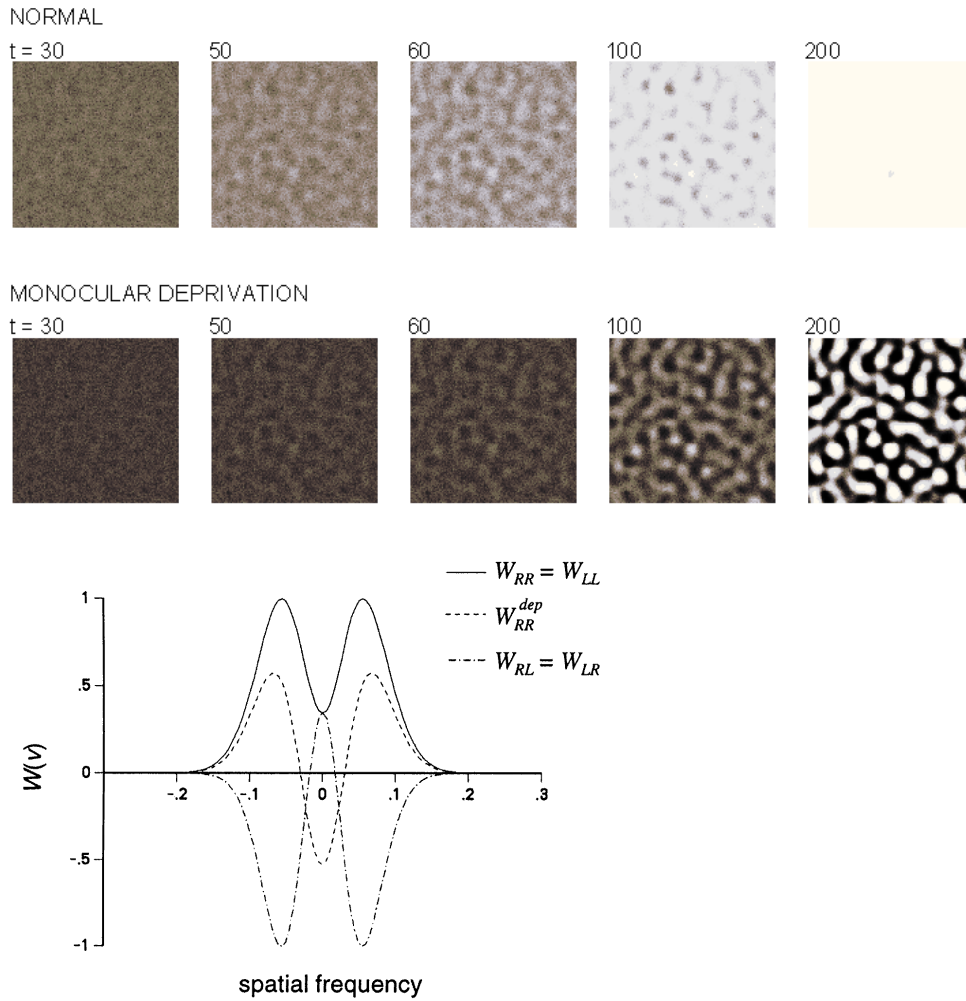


Figure 9. (TOP) Application of Swindale's (1980) model to transient and deprivation-induced ocular dominance segregation. Synaptic density is represented on a grey scale, with black indicating a low density of synapses, and white a high density. The model equations were as given in (3), (4) and (5), with $N = 1$ and synapse densities initially normally distributed with a mean of 0.25 and a standard deviation of 0.05. The array size was 128×128 . For the simulation shown in the upper set of panels, parameters for $w_{RR} = w_{LL}$ (equation (5)) were $A = 0.059$, $B = 0.027$, $\sigma_E = 3.12$, $\sigma_I = 4.41$; for $w_{RL} = w_{LR}$, $A = 0.054$, $B = 0.029$, $\sigma_E = 3.56$ and $\sigma_I = 5.03$. Between time steps $t = 50$ and $t = 100$ a periodic distribution of inputs is present, but this eventually disappears, with $n_i \approx n_1 \approx 1$ everywhere. To obtain the result shown in the lower set of panels, monocular deprivation was simulated by reducing the value of A in w_{RR} from 0.059 to 0.045. All other parameter values, including the initial synapse density values, were the same. The deprivation causes the transient patches to persist into the final pattern. The inputs from the deprived eye are shown. Inputs from the non-deprived eye have a more continuous distribution, with gaps corresponding to the centres of the patches of deprived eye inputs. (BOTTOM) The Fourier amplitude transforms of w_{RR} , w_{LL} etc, with horizontal axis values in cycles per array pixel. (From Swindale, unpublished results.)

where θ_i is a set of orientations uniformly spanning the range $0-\pi$. Note that if $R(\theta)$ is flat, or zero everywhere, then $|z| = 0$. This representation does not disambiguate a difference in the height of an orientation tuning curve from a difference in its width, but this limitation will be ignored for the present.

By analogy with the approach taken for ocular dominance column development, the orientation vectors z are assumed to be initially small in magnitude, with spatially random orientations over the range $0-\pi$. The change in orientation preference with time can then be described by the equation (Swindale 1982a)

$$\partial z / \partial t = z * w_z f(z) \quad (12)$$

where w_z is a (real) lateral interaction function which is positive for short distances and negative for longer ones, and $f(z)$ is used to set an upper limit on the value of $|z|$. For most purposes w_z can be defined as a difference of Gaussians (equation (5)) and $f(z) = (1 - |z|)$ will ensure that $0 \leq |z| \leq 1$. Solutions to (12) resemble the patterns of orientation preference found experimentally in the monkey and the cat. Most, if not all, of the features observed experimentally can be identified in the computed patterns (figure 10). These include point singularities of sign $\pm \frac{1}{2}$ with a somewhat irregular distribution and a density of about $3/\lambda_\theta^2$ where λ_θ is the period of the orientation columns, linear zones and saddle points, and periodic variations in the orientation gradient which resemble those found in the monkey (Swindale 1992a). The model additionally suggests that the orientation singularities should occur in, or close to (see Swindale 1982a, appendix 2), patchy regions of low orientation selectivity. As discussed above in section 2.9.2 there is circumstantial evidence in favour of this, because optical recording experiments show a higher density of orientation singularities in the centres of ocular dominance stripes, where, in the upper layers of the cortex, regions of poor orientation selectivity have been reported.

The latter observation—that regions of poor orientation selectivity occur in the centres of ocular dominance stripes—suggests that the development of orientation selectivity is linked in some way to the development of ocular dominance. Swindale (1992a) suggested that ocular dominance might interact with the development of orientation selectivity in the following way:

$$\partial z / \partial t = z * w_z (1 - |n * w_n|)^\alpha f(z) \quad (13)$$

where α is a positive constant which describes the strength of the coupling between the two systems, and w_n and n are as defined above in (5) and (6). This has the effect of reducing $\partial z / \partial t$ in the centres of developing ocular dominance columns, where $|n * w_n|$ is greatest. Although this formulation is not particularly elegant it has the desired effects: orientation singularities (and, as would be expected, regions of poor orientation selectivity) tend to lie in the centres of ocular dominance stripes, and (as pointed out by Erwin *et al* (1995)) iso-orientation domains tend to cross ocular dominance boundaries at right angles (figure 10), as observed experimentally. Biologically, an interaction of this kind might occur if orientation selectivity developed more slowly than ocular dominance and if plasticity was turned off first in the centres of the ocular dominance stripes.

5.3. Conditions under which the models are valid

The use of a convolution kernel to describe the emergence of functional properties in the cortex is valid only under certain conditions. These are:

- (i) *translational invariance*, i.e. the interactions taking place between two locations on the cortical surface depend only upon their lateral separation and not their absolute position;

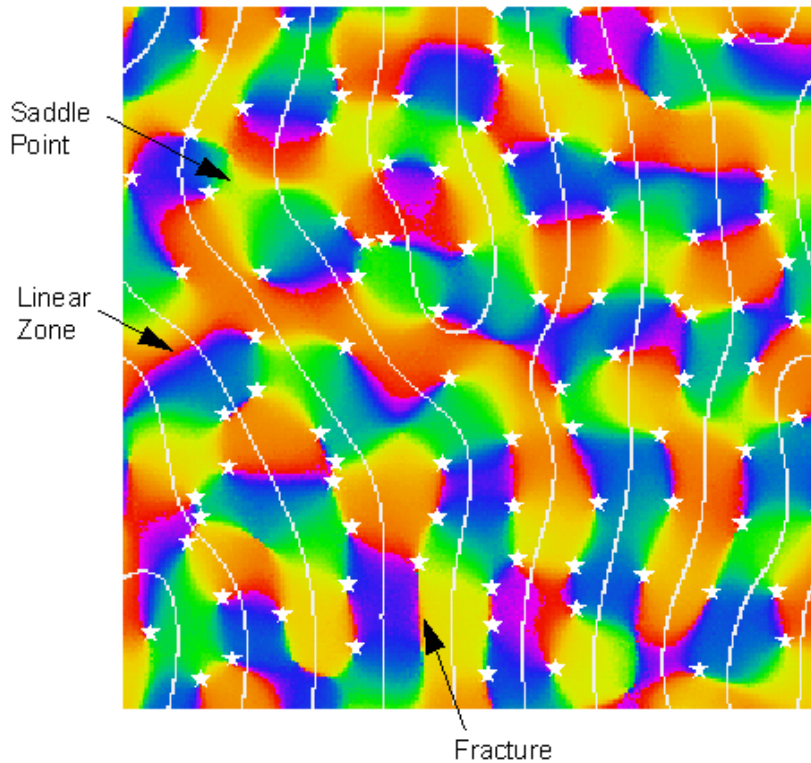


Figure 10. Simulation of combined orientation and ocular dominance column formation using Swindale's (1992) model. Ocular dominance borders are shown in white and a colour scheme similar to that used in figure 3 is used to represent orientation preference. Singularities are indicated by asterisks. Note that singularities tend to occur in the centres of ocular dominance stripes and iso-orientation domains intersect ocular dominance borders at right angles, as found experimentally (figure 3). The model equations were given in (5), (6), (10) and (13), with array size = 256×256 , $K = 0$, $\alpha = 20$; for w_n , $A = 2.64 \times 10^{-4}$, $B = 1.54 \times 10^{-4}$, $\sigma_E = 13.2$, $\sigma_I = 18.9$ and $\beta = 1.3$; for w_z , $A = 1.75 \times 10^{-4}$, $B = 1.06 \times 10^{-4}$, $\sigma_E = 10.1$, $\sigma_I = 14.3$ and $\beta = 1$.

- (ii) *linearity*, i.e. the combined effects of different locations on growth are the linear sum of the effects exerted by individual locations;
- (iii) *slowness*, i.e. growth must be slow compared with the time required to propagate the interactions through the cortical substrate.

It might be thought that translational invariance will be violated, because the effect of growth or removal of synapses in one location in a single geniculate arbor on the growth of those in another location in a second arbor is likely to depend not just upon the cortical distance between the two points in question, but upon the distance between the cell bodies in the geniculate nucleus (and their corresponding retinal receptive fields) as well. However, the model equations describe the aggregate effects of, and on, many different geniculate axons at each cortical location. When an average is taken across the many different axons present within each location the net effects on growth will tend to be invariant with position in the cortex and will be only a function of cortical separation. Integrative linearity can be loosely justified by the observation that many neurons in the visual cortex sum their

inputs approximately linearly (Movshon *et al* 1978). If diffusion of chemical signals is the substrate for the lateral interactions, linear additivity is also the simplest possibility. Finally, the slowness assumption is probably justified, given that ocular dominance and orientation columns take a few days, at least, to develop, while lateral interactions in the cortex are likely to be transmitted rapidly, e.g. neural effects with a time course of milliseconds and neurochemical ones (if present) with a diffusion time constant of a few seconds or less (Crick 1970).

5.4. Empirical tests of the models

The best formal test of the models is to see whether, during development, cortical orientation preferences, and/or ocular dominance values, change over time at rates predicted by the convolution relations described above. For this, patterns of ocular dominance n (or orientation z) would have to be measured at a series of times, e.g. t and $t + 1$, sufficiently close together for small, but reliably measurable, changes in the pattern to have occurred. Then, from (7) (assuming $K = 0$) a lateral interaction function w_t can be calculated by deconvolution

$$w_t = \mathcal{F} \{ \mathcal{F}(n_{t+1} - n_t) / \mathcal{F}(n_t) \} \quad (14)$$

where $\mathcal{F}(\cdot)$ denotes Fourier transformation. The equation determining w_z is similar. The test of the model would consist in showing that the calculated w_t resembled the postulated ‘Mexican hat’ function in some way, and that this shape remained similar during development. It is also possible to analyse the output from other types of model to see whether their behaviour can be approximated by this simpler equation[†].

5.5. The origin of the postulated interactions

Many possible mechanisms could give rise to the lateral interactions hypothesized above and, in fact, related models based on lateral inhibition have been proposed to account for periodic pattern formation in quite different systems (Meinhardt 1982, Young 1984). As suggested above, correlation-based mechanisms of the type proposed by von der Malsburg and Willshaw will give rise to distance-dependent cooperative and anticooperative behaviour, although a formal similarity between these models and Swindale’s has not been demonstrated. These types of mechanism are perhaps the best candidates at present, given the amount of direct and indirect evidence to support the existence of Hebbian plasticity in the developing visual cortex. From a broader biological perspective, however, it is likely that factors other than correlation-based Hebbian strengthening might need to be taken into account. For example, the strengthening of synapses on one part of an axonal arbor may result in an increased transport of materials (proteins required for transmitter synthesis etc) to that part of the arbor, resulting in a local facilitation of growth in that part of the arbor and a weakening or removal of connections further away. Conversely, removal of connections in one part of an arbor may result in an increased vigour of those further away (the ‘pruning hypothesis’: Pockett and Slack 1982, Sabel and Schneider 1988). The spatial scale of these interactions would be determined by the intracellular signalling mechanisms responsible for regulating axonal growth.

[†] I analysed the output from an implementation of the model of Miller *et al* (1989), using similar parameter values and applying divisive normalization of the inputs to cortical units, and recovered a close approximation to the lateral interaction function $I(x)$.

Other types of lateral interaction may be mediated by, for example, synaptically released neurotrophins (Russell 1995), which diffuse through tissue and may modulate synaptic growth and plasticity. Such an interaction is suggested by experimental data showing that when a connection between an afferent and a postsynaptic neuron was strengthened by the correlated stimulation of both cells, the connections from a nearby, but unstimulated, afferent were strengthened as well (Kossel *et al* 1990). It is possible that the difference between the two eyes is coded chemically in some way, although it has been shown that the inputs from two genetically identical eyes from the same half of the body can be induced to form eye dominance stripes within the frog tectum (Ide *et al* 1983). Although this does not rule out the possibility that a chemical cue is used to distinguish the eyes in mammalian visual cortex, it makes a neural activity based mechanism seem more likely. It seems similarly unlikely, although not impossible, that orientation preferences could be coded chemically, e.g. as a phase relation between two periodically distributed chemical signals. Such a model might need to be considered if it turns out (as suggested by Gödecke and Bonhoeffer (1996)) that patterned neural activity plays no role in setting up the initial distribution of orientation preferences in the cortex.

6. Linsker's model for orientation columns

In a series of three papers, Linsker (1986a, b, c) studied the behaviour of a multi-layer network, in which each point in any given layer projects connections approximating a Gaussian distribution centred on a corresponding point in the layer above it. In its complete form, the model has seven layers (although this is not an essential feature), with the first layer providing randomly structured inputs to the second layer which then projects to the third layer, and so on. Except in the seventh layer, assumed to correspond to a layer in the visual cortex, lateral connections between units are absent. Both inhibitory and excitatory connections occur and it is convenient to assume that a single connection can have a value that is bounded by positive and negative values (e.g. +0.5 and -0.5). Although this is biologically unrealistic, essentially similar results are obtained if separate excitatory and inhibitory connections are assumed. The output X^M of a unit in any layer M (which can also be positive or negative) is equal to the linear sum of its connection strengths w_i multiplied by the input values from the preceding layer L , plus a constant a_1 , i.e.

$$X^M = \sum_{i \in L} w_i X_i^L + a_1. \quad (15)$$

Connection strengths are changed according to a Hebbian learning rule

$$\Delta w_i = c_1(X^M - c_2)(X_i^L - c_3) + c_4 \quad (16)$$

where c_1 - c_4 are constants. This allows connection strengths to decrease as well as increase. Connection strengths can be changed following each presentation of an activity pattern in layer L to layer M , but, providing that constants are chosen so that the change in connection strengths is small following each presentation, it is possible to average over an ensemble of randomly varying presentations, and express Δw_i as a function of time-invariant statistical properties of the activity in layer L . This leads to the following equation for Δw_i

$$\Delta w_i = \sum_{j \in L} (Q_{ij}^L + k_2)w_j + k_1 \quad (17)$$

where k_1 and k_2 are constants and the quantity $Q_{ij}^L = \langle (X_i^L - x^L)(X_j^L - x^L) \rangle_t$ is the autocorrelation function (or covariance matrix) of points i and j in layer L and x^L is

the average of activity in L over the ensemble of presentations. Weight values are kept finite by clipping, so that $w_{\min} \leq w_i \leq w_{\max}$.

It is worth noting the main differences between Linsker's network and von der Malsburg's.

- (i) Each layer in the network sums its inputs linearly, i.e. there is no response thresholding.
- (ii) Because of (i) it is possible to average over the effects of many stimulus presentations, so that only the average spatial correlation functions of each input layer need to be used to determine weight changes in the following layer.
- (iii) There is no separate normalization process.

Linsker trained this network (naming the seven layers A–G) sequentially, first training the connections from A to B, using random, uncorrelated noise (for which Q_{ij}^A is the identity matrix) as the input from A to B. Once the connections to layer B had stabilized, the covariance function Q_{ij}^B was calculated and used to train the connections between layers B and C. This was repeated for subsequent layers. During this process, the receptive fields of units in the layers became progressively more complex, in ways which resembled the progression occurring in the visual pathways. Thus, the receptive fields in layers C to F typically had a radially symmetric centre-surround organization, like those found in retinal ganglion cells, LGN cells, and (in the monkey) cells in layer IVc α of the cortex. In the absence of lateral connections in layer G, a variety of non-circularly symmetric receptive field types developed, resembling orientation selective simple cells, with two or more alternating bands of excitation and inhibition (Linsker 1986b).

To increase the resemblance of layer G to the visual cortex, Linsker (1986c) added lateral connections between cells in the layer. To further simplify the calculations he suggested that rather than calculating weight values directly from the update equations (i.e. equation (17) modified to include lateral connections), a 'Hebb-optimal' configuration of orientation preferences could be calculated, by first assuming fully developed oriented receptive fields at each cortical location and by defining a lateral interaction function $Q^G(\theta_x, \theta_{x'}, \mathbf{x} - \mathbf{x}')$ where θ_x and $\theta_{x'}$ are the orientation preferences at locations \mathbf{x} and \mathbf{x}' . The 'Hebb-optimal' configuration was then found by minimizing an energy term E , defined as

$$E = - \sum_{\mathbf{x}} \sum_{\mathbf{x}'} \rho(|\mathbf{x} - \mathbf{x}'|) Q^G(\theta_x, \theta_{x'}, \mathbf{x} - \mathbf{x}') \quad (18)$$

where the summation is taken over the entire lattice of cortical points and $\rho(|\mathbf{x} - \mathbf{x}'|)$ is a decreasing function (e.g. a Gaussian) of the separation of each pair of points in the summation. Starting with an initially random assignment of orientation preferences to each lattice point, a configuration giving a minimum (not necessarily global) value of E was computed by simulated annealing. Linsker argued that configurations arrived at by this process would have similar characteristics to those produced by the more straightforward (but computationally more demanding) process of finding solutions to a modified equation (17). The resulting orientation maps had many of the properties of real orientation maps, including singularities and periodically spaced iso-orientation bands.

Linsker's lateral interaction function Q^G is comparable with Swindale's lateral interaction function, w_z , in its effects, but with an important difference: w_z is a function only of the separation between two interacting orientation columns, whereas Q^G is a more complex function which depends upon the absolute orientation of the two points in question, as well as their separation. This means that two orientations which point towards each

other on the cortex will interact differently from two orientations lying side by side. This is plausible, because given oriented patterns of activation, two orientation detectors a short distance apart which point towards each other will tend to be more highly correlated in their activity patterns than will two detectors which lie side by side. Because of this, iso-orientation domains for vertical orientations tend to be elongated in a vertical direction on the cortical surface while, conversely, iso-orientation domains for horizontal preferences tend to run in a horizontal direction. This interaction can be demonstrated quantitatively by computing a histogram, over all points on the cortical surface, of the difference between the orientation preference at each point, and the orientation of the associated orientation gradient vector[†]. When this is done (figure 15(d) in Erwin *et al* 1995) Linsker's orientation maps show, as expected, a strong bias towards orthogonal differences. Real orientation maps (Obermayer *et al* 1992, Obermayer and Blasdel 1993) show no such bias, the histogram being essentially flat (figure 15(a) in Erwin *et al* 1995). Data from the cat (Swindale *et al* 1987) and the tree shrew (Humphrey *et al* 1980) also suggest the lack of a strong interaction of this kind in these species.

This disagreement with experiment suggests that Linsker's Q^G may not be an accurate description of the types of lateral interactions that determine the spatial layout of orientation preference in the cortex. One reason for this may be that Linsker assumed an essentially perfect spatial topography in the projections between layers. The situation in the developing cortex is more complex since many receptive fields are present within each column of interacting orientations and these fields are not all in the same place[‡]. Because of this, neurons in columns that are less than 750 μm apart (the distances over which lateral interactions are likely to occur) and with similar orientation preferences, will often have receptive fields that lie side by side as well as others that are coaxially aligned. This suggests that a spatially averaged Q^G (Q^{iso} in Linsker (1986c)) may be the more correct interaction function (similar to Swindale's w_z). But the possibility remains that Q (or w_z) may not be exactly isotropic and it will be of interest to continue to examine experimental orientation data carefully for even a hint of a correlation between orientation and orientation gradient angles.

Although his model is unrealistic in some respects, Linsker (1986a) pointed out that it is not meant to be a literally accurate description of the visual pathways. With respect to the issues associated with visual cortical development, it is valuable in showing that Hebbian mechanisms can, under certain conditions, lead to the development of oriented receptive fields, in the absence of oriented patterns of retinal input. This may be an important clue to explaining how orientation selectivity can develop in the absence of visually evoked activity in the retina, if spontaneously occurring retinal activity lacks appropriately oriented structure. Another advantage is that the model is simple enough to allow an elegant mathematical analysis in which it can be shown that the receptive fields which develop in the different layers (primarily the third layer was analysed) are eigenfunctions of the covariance matrix (the Q functions) of the preceding layer (MacKay and Miller 1990a, b). For the third layer, conditions exist in which these eigenfunctions are the 1s, 2p and 2s operators of quantum mechanics.

[†] The orientation gradient is a vector which is orthogonal to the direction of elongation of the iso-orientation domains (defined in the limiting case of a small range of orientations centred on the point in question). The vector has zero magnitude at saddle points, is infinite in singularities and finite elsewhere.

[‡] Two contributions to this are receptive field scatter and the probability that the arrangements of ON and OFF subunits (sometimes referred to as the spatial phase) in the receptive fields of simple cells in neighbouring columns may differ.

7. Miller's models for ocular dominance and orientation

7.1. Ocular dominance columns

Miller *et al* (1989) formulated a model describing how spatially correlated neural activity in the two layers of the LGN might lead, in the presence of Hebbian synaptic modification rules, to the segregation of inputs in the cortex into periodically alternating ocular dominance stripes. As in Linsker's model, a pre-existing spatial topography was assumed to exist between the input layers and the cortex. Inputs from a location α in the LGN were assumed to make contact with cortical neurons centred on a location x in the cortex, and spread over a surrounding region, described by a fixed arborization function $A(x - \alpha)$. (For notational convenience it was assumed that any position α in the LGN maps directly to an equal position x in the cortex, so that LGN and cortical coordinates are interchangeable). The arborization function was usually 1 over a small square region and zero elsewhere, although in subsequent analyses (Miller and Stryker 1990, Miller 1990a) this restriction was relaxed. Like Linsker, Miller *et al* simplified the calculations by assuming that synaptic weight changes were slow compared with the rate of presentation of input patterns to the network, so that the time-averaged statistics of the patterns would be the primary determinants of weight changes. The statistical structure of these inputs was described by four radially symmetric functions, C^{LL} , C^{RR} , C^{LR} and C^{RL} (similar to Linsker's Q functions) specifying how the correlation in neural firing rates varies with lateral separation in the LGN. The strength of the connection from the two eyes, from a position α in the LGN, to a position x in the cortex at time t was given by two functions, $S^L(x, \alpha, t)$ and $S^R(x, \alpha, t)$. Lateral interactions in the cortex were described by a function $I(x)$ analogous to that used by von der Malsburg. The contribution of a synapse $S(x', \alpha')$ to the correlation value associated with a second synapse $S(x, \alpha)$ was assumed to be proportional to the product of the correlation value associated with the separation between the cells of origin in the LGN, i.e. $C(\alpha - \alpha')$, the strength of the synapse itself, i.e. $S(x', \alpha')$, and the value of the lateral interaction function for separation of the synapses in the cortex, i.e. $I(x - x')$. This led to the following equation for the change of synaptic strength with time:

$$\begin{aligned} dS^L(x, \alpha, t)/dt = \lambda A(x - \alpha) \sum_{\gamma, \beta} I(x - \gamma) [C^{LL}(\alpha - \beta) S^L(\gamma, \beta, t) \\ + C^{LR}(\alpha - \beta) S^R(\gamma, \beta, t)] \end{aligned} \quad (19)$$

with a corresponding equation for $dS^R(x, \alpha, t)/dt$ obtained by interchanging L and R. A multistep normalization procedure was also used, in which the sum of synaptic strengths at each cortical location was kept constant. This was done by subtracting from the weights, rather than dividing them (the method used by von der Malsburg). This difference is important because it has been shown that, if divisive normalization is used instead, segregation will not occur in the presence of positive correlations between the two eyes (Miller *et al* 1989, Miller 1990a, b, Miller and Mackay 1994, Goodhill and Barrow 1994). The total synaptic strength of each geniculate afferent was usually kept constant[†], although it was found that this constraint was only necessary if the cortical interaction function was purely excitatory (i.e. no intermediate-range inhibition). The reasons for this are discussed in Miller (1990a, b). In addition, separate limits were put on the maximum and minimum synaptic strengths possible in the network.

[†] The reason for doing this (in addition to normalizing the sum of the inputs to each cortical neuron) is to prevent some axons from disappearing entirely during development (i.e. all the weights go to zero). While such behaviour may seem undesirable, it may not be unrealistic as cell death is a frequent occurrence in the pre- and postnatal development of the visual system.

Miller examined the behaviour of this system by mathematical analysis and computer simulation. For the most part, the within-eye correlations C^{LL} and C^{RR} were assumed to be positive Gaussian functions, while the between-eye correlations C^{LR} and C^{RL} were assumed to be either zero or negative. The cortical interaction function was usually assumed to be a difference of Gaussians. Under these conditions, two separate processes occurred:

- (i) cortical receptive fields, which were initially binocular and equal in size to the arbor function, gradually became smaller and monocular;
- (ii) individual afferent arbors also became smaller and frequently broke up into patches, confined to neighbouring ocular dominance stripes.

As a result of these two changes, a striped, periodic pattern of ocular dominance developed on the cortical surface.

The simulations and analysis (Miller *et al* 1989 Miller and Stryker 1990, Miller 1990a, 1992a, 1995) allowed study of the effect of different arbor widths, different correlation functions and different cortical interaction functions. When the cortical interaction function contained both short-range excitatory and long-range inhibitory components, the spacing of the ocular dominance stripes (and of the patches within individual geniculate arbors) was determined by the shape of the cortical interaction function $I(x)$, i.e. by the position of the peak in its Fourier transform (analogous to the way in which periodicity can be predicted from w_n in Swindale's model) and not by the input correlations. Changing the widths of the input correlations mainly affected the receptive field sizes and the monocularity of the cortex: a narrower within-eye correlation function resulted in a less monocular cortex (i.e. more binocular cells at the borders of the stripes) and smaller receptive field sizes. When the intracortical interaction function was purely excitatory, then segregation occurred, provided that a constraint maintaining the total strength of individual axonal arbors was applied. In this case, the width of the individual ocular dominance stripes was about equal to the arbor size. It is easy to see that a constraint on total arbor strength is very similar to the within-eye lateral inhibitory effects postulated in Swindale's model because increasing the strength of synapses in one location in an arbor will necessarily lead to a decrease in the strengths of synapses further away and *vice versa*. However, in Swindale's model this is implemented as a tendency, rather than a rigid constraint.

7.2. Orientation columns

Most neural net models assume the presence of spatial correlations in the simplest possible model retina, in which only one type of input is present at each retinal location. However, it is well known that the retina has two major subdivisions: cells which respond to light increments, or positive contrasts (ON cells) and cells which respond to light decrements, or negative contrasts (OFF cells). It is also known that one cause of orientation selectivity in simple cells in the visual cortex is a receptive field organization in which one or more regions of ON responsiveness alternate with regions of OFF responsiveness (Hubel and Wiesel 1962). The preferred orientation of the cell can be predicted from the orientation of the line (or lines), which best separates the regions. The alternation of ON and OFF regions is reminiscent of ocular dominance segregation (although it is on a much smaller scale and occurs within the receptive field rather than in the projection pattern of the LGN afferents). Miller (1992b, 1994) therefore examined the possibility that his model for ocular dominance segregation might be able to explain the development of orientation selectivity and its accompanying cortical topography, as the result of competitive interactions between ON and OFF inputs. In this case, what the model has to produce is an alternation of inputs

within individual receptive fields, rather than receptive fields which are entirely ON or OFF dominated (as in the analogous case of the ocular dominance model). Miller showed that this can happen, provided that the input correlation functions change sign within a distance smaller than the arbor function. For his simulations of orientation column development, therefore, Miller used his ocular dominance column equation (19), replacing L and R with ON and OFF respectively. Instead of Gaussian correlation functions, a difference of Gaussians was used, an upright function (positive near the origin and negative further away) for ON–ON and OFF–OFF correlations and an inverted function (negative near the origin and positive further away) for ON–OFF and OFF–ON interactions. A slightly different arbor function (circular, rather than square) was also used. Normalization and other procedures used in the computations were similar to those used for the ocular dominance model.

This model performs well in many respects: individual receptive fields resemble those of simple cells, inasmuch as they are divided into two (or occasionally more) regions of ON and OFF responsiveness. From these, an orientation preference, a preferred spatial frequency, and a spatial phase, which reflects the relative positions of ON and OFF regions within the overall receptive field, can be calculated. Orientation preferences change continuously over the surface of the cortex, singularities are present and individual iso-orientation domains are elongated and morphologically similar to those observed in the monkey and cat (cf figure 15 in Miller (1994) and figure 14 in Erwin *et al* (1995)). In addition, the model predicts a continuous variation in spatial phase of the receptive field across the surface of the cortex and, for some parameter regimes, variations in the overall magnitude of ON versus OFF responses within receptive fields. There is a small amount of experimental evidence for the latter prediction: variations in ON and OFF responsiveness have been found in the mink (McConnell and LeVay 1984) and the ferret (Zahs and Stryker 1988) although not so far in cats or monkeys. Evidence for continuous variations in the spatial phase of simple cells is so far lacking; there is some evidence that adjacent pairs of simple cells are often in antiphase or quadrature (90°) phase (Liu *et al* 1992), although this does not rule out an additional continuous variation.

Miller's orientation columns are unrealistic in one important respect: although the model produces a well-developed ON–OFF periodicity within receptive fields and periodic variations in ON versus OFF responsiveness across the surface of the cortex, periodicity of orientation preference is essentially absent. This is shown by the fact that power spectra of the orientation maps (figure 15 in Miller (1994)) have low-pass rather than band-pass characteristics. Periodicity in real orientation maps is such a prominent characteristic that this would seem to invalidate the model's application to spatial organization in the cortex without further modification. In some, though not all, parameter regimes, the model, like Linsker's, produces a correlation between orientation and orientation gradient vectors. When this happens, the orientations tend to point in the same direction as the gradient vector (figure 15(c) in Erwin *et al* (1995)) rather than orthogonally as in Linsker's model.

Erwin and Miller (1995) have recently extended Miller's equations to include both ocular dominance and ON–OFF interactions (i.e. four separate types of synapse and associated correlation functions). Parameter values were found which permitted joint development of ocular dominance and orientation maps, although the orientation map was still aperiodic.

7.3. Biological interpretation of Miller's models

Miller intended to make his models 'biologically realistic' by specifying only parameters corresponding to measurable entities. Thus, the retinal correlation functions and the cortical interaction function are all, in principle, measurable, while other ingredients—the Hebb

synapses and the processes underlying the normalization of arbor strengths and input strengths—might be demonstrated experimentally to correspond with those used in the model. Other details seem less realistic: for example, the models assume a precise and fixed retinal topography on the cortical surface, whereas it seems probable that, at this stage, topography is not fixed and might be rather imprecise. The arbor function also seems somewhat unbiological, since it simply constrains axons not to grow further than a certain distance from a predefined and fixed retinotopic position on the cortex. It would be more natural if this constraint, or something like it, emerged from activity-dependent interactions producing and maintaining retinotopy, as well as some form of non-rigid constraint on the total number of synapses in the arbor. One reason for not applying a fixed constraint of this kind is that the density of synapses on geniculate axons probably increases substantially during the early stages of visual cortex development. Another is that monocular deprivation reduces the number of synapses on deprived arbors and so it can only be simulated by relaxing the constraint on total arbor strength. This comes uncomfortably close to assuming what one is trying to prove.

In his model of ocular dominance, Miller assumed zero or negative correlations between the eyes, although, in cats, positive correlations between the eyes are more likely to be present than not since ocular dominance columns develop while the eyes are open. Segregation in Miller's model can be disrupted by the presence of such correlations (Dayan and Goodhill 1992, Goodhill 1992), although this is less likely when subtractive normalization procedures are used. Finally, the periodicity of the columns in Miller's model is determined by fixed parameters such as the lateral interaction function and the arbor size; therefore, the period of the columns should be unaffected by changes in the visual input. This is inconsistent with evidence showing that strabismus in the cat (Löwel 1994) and monocular deprivation produced by severely defocusing one eye in infant monkeys (Roe *et al* 1995) both cause an increase in the spacing of ocular dominance patches. These results imply that ocular dominance column periodicity is not determined solely by fixed intracortical interactions, but by parameters which depend upon the correlation structure of retinal activity. The models discussed in the following sections are able to accommodate such findings.

8. Applications of Kohonen's self-organizing feature map (SOFM) algorithm

8.1. Goodhill's model for ocular dominance and retinotopy

The preceding discussion has suggested that it would be of interest to model the simultaneous development of retinotopy and ocular dominance segregation. Much experimental evidence (see e.g. Constantine-Paton and Law (1978), Udin and Fawcett (1988)) also suggests that ocular dominance stripe formation is simply a consequence of other mechanisms whose primary function is to refine the retinotopic map. Clearly, a Hebbian mechanism ought to be capable of coping with both problems and, in a recent paper, Goodhill (1993) has shown how a competitive Hebbian learning rule, first proposed by Kohonen (1982, 1988), may do this.

In Goodhill's implementation, two retinas project to a single layer of cortical units. Retinal inputs were modelled as random dot patterns with short-range spatial correlations introduced by convolution with a Gaussian blurring function with a standard deviation of σ_r . In this respect, the inputs are the same as those postulated by Miller and those present in Linsker's *B* layer. Goodhill also introduced positive between-eye correlations, since these are likely to be present whenever ocular dominance stripes form while the two eyes are

open (and strabismus is absent). This was done by replacing a proportion h of each retina's activity with the same proportion of the activity in the other retina. Thus, if $h = 0$ the inputs are uncorrelated (a possible model for strabismus) and if $h = 0.5$ the inputs are identical (which presumably never happens). Each point in both retinas projected to the whole of the cortex, i.e. no arbor function was specified, but connection strengths were biased to simulate a rough initial topography. This was done by calculating the initial weight values so that the connections between points in cortex and retina had strengths chosen from a range whose centre value decreased linearly with the topographic distance between the two points. (Initial receptive fields, and afferent arbors, are thus noisy cones truncated by the edges of the arrays.) Each cortical unit c had an output χ_c , given by the linear sum of its inputs times the weight values

$$\chi_c = \sum_r w_{cr} a_r \quad (20)$$

where the summation is over r , i.e. all the inputs from left and right retinas, to point c in the cortex. Following calculation of χ_c for all points in the cortex, the single cortical location g , for which χ_c was largest was found and the weight values for this point and surrounding ones were changed according to the following rule

$$\Delta w_{cr} = \alpha a_r s(c, g) \quad (21)$$

where α determines the rate of development, and $s(c, g)$ is a Gaussian function of the distance between points c and g on the cortical surface, often referred to as the cortical

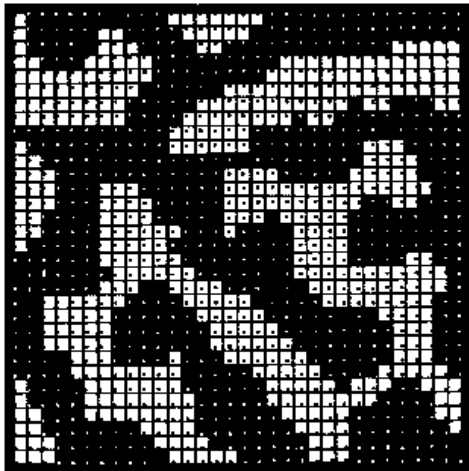


Figure 11. Combined formation of a retinotopic map and ocular dominance columns produced by the high-dimensional Kohonen learning rule (Goodhill 1993). Inputs to the network come from two 16×16 arrays of units, corresponding to the two eyes. These have locally positive within-eye correlations in activity, together with smaller positive correlations between the two eyes. The diagram shows a 32×32 array of cortical units: each unit is represented by a box which is white if most of the inputs come from one eye, and black if most of the inputs come from the other eye. Within each box is a small black or white dot: the position of the dot within the box indicates the position of the receptive field of that cortical unit. The existence of an overall retinal topography is shown by the fact that the position of the dot within each box corresponds with the position of the box within the cortex. Although they are not visually detectable, discontinuous changes in retinal position occur at the boundaries of the ocular dominance stripes, as illustrated in figure 4. (Reprinted by permission of Springer-Verlag from Goodhill (1993).)

neighbourhood function. This learning rule, which is the essence of Kohonen's (1982, 1988) original proposal, will make unit g even more responsive to the stimulus in question than it already is; in addition, points in the neighbourhood of g will tend to become responsive to similar stimuli, i.e. their weight vectors will tend to move in the same direction (in weight space) as g 's weight vector. One problem with this rule is that some units in the cortex may be initially unresponsive to stimuli (as an accidental result of the initial, random, assignment of weight values) and may never win out over other units. To avoid this problem, the response of each unit is divided by the number of times it has 'won' the competition, a technique which is sometimes referred to as a 'conscience' mechanism, but which can also be regarded as a form of stimulus adaptation.

Following each learning step (i.e. the presentation of a stimulus pattern and updating of the weight values) synaptic strengths were subjected to a subtractive normalizing process, similar to that used by Miller *et al* (1989). The goal of this is to ensure that the sum of the inputs to each cortical unit equals a constant value, N_c . It involves the following set of calculations: for each cortical unit c , calculate $t_c = (\sum_r w_{cr} - N_c)/n_c$, i.e. the difference between the mean value of the non-zero inputs to the unit (n_c in number) and the desired sum, N_c ; next, subtract t_c from each weight value w_{cr} , truncating the weight values at zero if $w_{cr} - t_c$ is negative. If truncation has occurred the sum is still not equal to N_c , therefore a further divisive normalization is applied by multiplying each w_{cr} value by $N_c / \sum_r w_{cr}$. Once these steps had been completed, the sum of the weights for each retinal unit was normalized by multiplying each w_{cr} value by $N_r / \sum_c w_{cr}$ where N_r is the desired net retinal weight. (Note that this final procedure means that the normalization of input weights to each cortical unit is no longer exact). Once normalization has been completed, another stimulus pattern is presented to the network and learning continues, typically for 100 000–350 000 iterations[†], when a stable set of receptive fields has emerged.

Development in this model can be followed by calculating, for each cortical unit, an ocular dominance value (i.e. the relative net strength of left- and right-eye inputs) and the 'centre-of-gravity' of each cortical unit's weight values in retinal coordinates, i.e. its receptive field location. At the start of development, ocular dominance values are binocular (with small random variations in ocularity), receptive fields are large and topography is imprecise. During development, receptive fields become increasingly monocular and a striped pattern of ocular dominance emerges (figure 11). At the same time, receptive fields become smaller, and topography becomes more regular. Correspondingly, the retinal arbors refine and occupy smaller regions of cortex (although Goodhill did not examine the shape of these explicitly).

It is of interest to examine the final pattern of retinal topography, once the cortex has divided itself up into stripes connected with either the left or the right eye. Each eye now innervates only half of the surface of the cortex: if each set of stripes contains a complete map of the visual field, how is this map split up, and what is the relation between the two interdigitating maps? As one moves across a stripe, receptive field positions move smoothly across a corresponding region in the retina connected to that stripe. As one crosses to the adjacent stripe, field positions (now in the other eye) shift backward to a position corresponding to the field positions seen in the centre of the first stripe. This is similar to

[†] As a practical point it should be noted that competitive Hebbian models generally require very large numbers of iterations (i.e. stimulus presentations) before converging to a stable state. In contrast, the models of von der Malsburg, Swindale, Linsker and Miller usually converge acceptably in a few hundred iterations. As discussed later, this difference (practical considerations aside) is probably a non-trivial consequence of the postulated developmental mechanisms. It may also be of interest to note that, if ocular dominance columns develop over a period of about 200 hours (Swindale 1988) the rate of stimulus presentation in Goodhill's model is about one every two seconds.

the shifts in field positions at ocular dominance borders observed experimentally (figure 4) in layer IVc of the macaque monkey. It is possible to visualize this arrangement by ‘back-projecting’ the cortex into retinal coordinates, representing the retinas as parallel sheets (or, if only one retinal dimension is considered, lines). The cortex can then be visualized as ‘zig-zagging’ back and forth between the two sheets, efficiently connecting up all points in both retinas (figure 13). This image will be helpful in understanding the behaviour of the elastic net and dimension-reduction models discussed in the following sections.

In exploring the effect of different parameter values on the behaviour of the model, Goodhill noted that decreasing the correlation between the two eyes (i.e. setting the value of his parameter h to zero), as would be caused by a strabismus, caused an increase in the spacing of the ocular dominance stripes. This prediction, which is one of only a few made in advance of experimental findings in this field, has been confirmed (Löwel 1994, Goodhill and Löwel 1995). The experimental observation is important because it confirms the general notion underlying most of the models discussed here, that the cortex is a self-organizing system in which the exact details of column shape and spacing are determined dynamically during development rather than by hard-wired and genetically determined mechanisms. The apparent increase in the spacing of ocular dominance stripes in monkeys made amblyopic by severe anisometropia (Roe *et al* 1995) may have a related explanation: for this, the effect of making one of the two eyes’ correlation functions very broad (i.e. increasing its σ_r) ought to be explored.

8.2. Biological implications of Goodhill’s model

The significant ingredients of Goodhill’s model are

- (i) its use of Kohonen’s competitive learning rule;
- (ii) the assumption of positive correlations between the two eyes;
- (iii) the use of a subtractive normalization rule.

With these it is able to explain the simultaneous development of retinotopy and ocular dominance segregation under the influence of correlated patterns of retinal activity, as a considerable amount of experimental evidence would now seem to require. It appears to describe the formation of retinal topography within ocular dominance stripes correctly and it can account for the effects of strabismus on stripe width. It may be possible to accommodate other phenomena within the scope of the model, although this has not yet been explored†. But how plausible are the three ingredients which lead to these successes?

Earlier models (see e.g. von der Malsburg and Willshaw (1976), Miller *et al* (1989)) usually assumed zero or negative correlations between the two eyes. Yet positive correlations seem certain to exist, given that strabismus would be unlikely to have any effect on ocular dominance column development, were it not that correlations are normally caused by the correct alignment of the two eyes. Goodhill’s model shows that segregation can occur in the presence of such correlations, but he reports that the model only works if subtractive, rather than divisive, normalization is used as a mechanism for regulating the sum of synaptic inputs to each cortical neuron. Although theoretical analyses of different kinds of normalization rule (Miller and MacKay 1994, Goodhill and Barrow 1994) provide insights into why this is so, very little is known about what cellular mechanisms might give rise to either type of mechanism. More experimental data about how cells regulate their inputs are needed; in addition, further clues might be obtained by modelling the process of synaptic regulation at

† As in Miller’s model, explaining monocular deprivation requires relaxation of the constraint keeping the total weight of each retinal input constant.

a subcellular level, to see if there are different types of biochemical regulatory mechanisms which produce subtractive, divisive or other types of regulation.

The learning rule used by Goodhill differs from those used in the Hebbian models described so far (i.e. von der Malsburg, Miller, Linsker) in which the rate of change at all synapses is proportional to the product of the pre- and postsynaptic activities. Here, the rate of change is proportional to the level of presynaptic activity a_r , but is conditional on the synapse in question being close to that region of cortex which is responding most strongly to the stimulus. This is usually referred to as *competitive Hebbian learning*[†], or sometimes as a 'winner take all' (WTA) mechanism and is a technique first introduced by Kohonen (1982). In this context, the term 'competitive' refers to the (hypothetical) process by which the most responsive region of cortex is selected from among those responding less strongly. Its use should be distinguished from other uses of the term 'competitive', e.g. to describe interactions where strengthening one group of synapses leads to a weakening of others.

The process of choosing the most responsive region and modifying connections only in its vicinity is, of course, highly nonlinear, and does not lend itself easily to mathematical analysis. Furthermore, although competitive Hebbian learning works well in a variety of neural net applications, it does not at first sight seem to be something that is likely to occur naturally in real brains. Why would connections in the cortex not be capable of being modified simultaneously in many different places? In fact, there are reasons why the cortex might behave in this way. First, if von der Malsburg's Mexican hat connectivity scheme is present in the cortex (i.e. short-range excitatory and mid-to-long-range inhibitory connections) activity will tend to occur in localized small patches (Kohonen 1982). Second, learning might be very rapid and contingent on the occurrence of strongly excitatory stimuli, whose simultaneous occurrence would be less likely if the timescale on which modifications occur is short. This type of development might be characterized as quantal, with each event consisting of the brief modification of connections within a small region of tissue a few hundred microns in diameter, contingent on activity within the region crossing some threshold level. Competitive Hebbian learning can therefore be distinguished from the type of learning which occurs in Linsker's and Miller's models. In the latter case synaptic modifications are continuous and slow, are governed in a linear fashion by the time-averaged statistics of the neural inputs, and direct interactions between synapses only occur when they are on the same cell or belong to the same axon.

Some physiological evidence appears to point towards mechanisms similar to those postulated by competitive Hebbian models. For example, in infant rat visual cortex it has been observed that when a connection between an afferent and a postsynaptic neuron is strengthened by the correlated stimulation of both cells, the connections from a nearby, but unstimulated afferent become strengthened as well (Kossel *et al* 1990). A similar spatial spread of synaptic strengthening has been observed in the hippocampus (Bonhoeffer *et al* 1989). This suggests that synaptic potentiation is accompanied by a signal which travels through tissue and potentiates nearby synapses. Possible mechanisms for the spread include glial depolarization, release of nitric oxide, arachidonic acid, carbon monoxide or hydrogen peroxide (Gally *et al* 1990, Dawson and Snyder 1994, Montague and Sejnowski 1994, Schuman and Madison 1994, Dawson and Dawson 1995) or the diffusion of molecules between intercellularly coupled neurons (Peinado *et al* 1993). Other good candidates include members of the neurotrophin family, which are known to be released from dendrites in response to neural activity and to play a role in regulating developmental plasticity (Thoenen

[†] Strictly speaking this type of learning is non-Hebbian because, for at least some of the synapses involved, the strengthening that occurs is independent of the response of the postsynaptic neuron

1995, Cabelli *et al* 1995). To be consistent with a Kohonen-type mechanism, release of this substance (or substances) would have to be an all-or-none event, with a relatively high threshold. It would not be surprising if other substances which depressed synaptic modifiability were released as well: these would be expected to act more slowly and diffuse over longer distances. Kohonen (1993) has also proposed a physiological interpretation of competitive Hebbian learning in terms of the release of diffusible chemical agents.

8.3. Other high-dimensional competitive Hebbian models

Obermayer *et al* (1990) applied Kohonen's SOFM algorithm to the simultaneous formation of retinotopy and orientation columns, and subsequently to the simultaneous formation of retinotopy, ocular dominance and orientation preference (Obermayer *et al* 1992b). With the exception of the competitive aspect of the Hebbian learning rule used and the use of a larger retina (allowing the addition of retinal position to the input stimulus space), the model was also similar to that of von der Malsburg (1973). A single, two-dimensional layer of randomly positioned input units projected to a two-dimensional cortex. Oriented patterns of stimulus activity in the input layer were defined by Gaussian ellipses with specific positions and orientations in the input array chosen from a uniform probability distribution. Connection strengths between the two layers were changed according to (20) and (21), with the difference that Obermayer *et al* normalized the sum of the squares of the weight values to each cortical unit multiplicatively. The size of the cortical neighbourhood function was also reduced over time by a factor of about 100 as stimulus specificity increased. The resulting pattern of orientation preference was similar to that found in the monkey and cat, with irregularly distributed half-rotation singularities and periodically spaced iso-orientation domains whose direction of elongation was independent of the orientation represented within them. Results overall were similar to those obtained with a low-dimensional version of the Kohonen algorithm (Obermayer *et al* 1991, 1992b). This algorithm is described in more detail in the following section.

9. Dimension-reduction models for cortical development

An important and successful class of models has stemmed from the idea that the visual cortex is a dimension-reducing map, i.e. that each point on its two-dimensional surface can be mapped to a corresponding position in a higher-dimensional stimulus space (Kohonen 1982, 1988, Mitchison and Durbin 1986, Durbin and Willshaw 1987, Durbin and Mitchison 1990)†. This can be visualized in abstract terms by imagining a three- (or higher-) dimensional stimulus space, each position in which corresponds to a set of potential receptive field properties (for example, receptive field position (two dimensions), preferred orientation (two dimensions if orientation is represented as a vector) and eye preference (one dimension)). The cortex can then be 'back-projected' into this space in such a way that each position on its two-dimensional surface occupies the position in stimulus space corresponding to its receptive field (figure 12). The way in which the cortex is folded inside and fills stimulus space then defines the overall map of receptive field properties. This map is of course more usually conceived of as a forward projection, i.e. as a mapping of some stimulus dimension onto the surface of the cortex.

† Mitchison (personal communication) has pointed out that algorithms which assign points in the cortex to points in a higher-dimensional space actually perform dimension expansion, rather than dimension reduction. Although the term 'dimension reduction' is now in common use, the fact that it might sometimes be more correct to refer to 'dimension expansion' should be borne in mind.

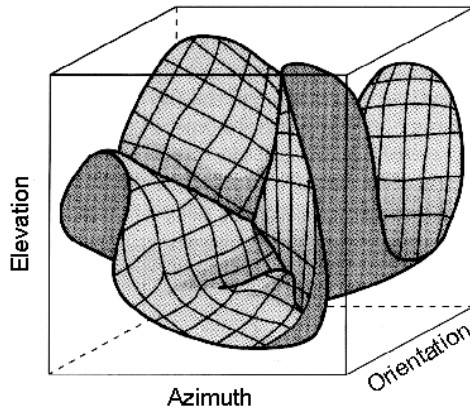


Figure 12. An imaginary projection of the cortex into a stimulus space: the folded sheet is the cortex, with points on the grid representing positions in cortical coordinates. The receptive field properties of each point in the cortex determine the position of the point within the stimulus space. A three-dimensional subset of this space is shown here: receptive field elevation and azimuth, and preferred orientation. The low-dimensional Kohonen and elastic net algorithms work by moving the positions of cortical points within a stimulus space of this kind, in such a way that the folded sheet fills the space, and becomes locally smooth. (Taken from Swindale 1992.)

Although it was not couched in technical language, the idea that the organization of columnar structures in the visual cortex might be a solution to this mapping problem, subject to certain constraints, was also clearly expressed by Hubel and Wiesel (1974b, 1977). They pointed out two important functional considerations which might help in explaining why the cortex has the structure that it does. First, the fact that neurons with similar receptive field properties occur close together in the cortex may help to minimize the total lengths of axonal and dendritic connections, given that more connections are likely to be made between neurons with similar properties than dissimilar ones. This would explain why the map is, at least to some degree, locally continuous. Second, it is presumably an important requirement that the cortex should fill stimulus space as completely and as uniformly as possible. Were this not to happen, certain regions in stimulus space would fail to gain a representation in the cortex and the animal might be blind or relatively insensitive to those particular stimulus combinations. The consequences of these ideas are examined in more detail below, in section 11.

These considerations suggest that the projection of visual cortex into stimulus space is subject to two conflicting requirements:

- (i) the cortical surface should pass through a representative selection of points in stimulus space;
- (ii) the area of the sheet should be kept a minimum, since this will ensure continuity, and hence minimize wiring length.

An analogous problem is the travelling salesman problem (TSP), where the shortest route connecting a set of cities must be found. The problem of minimizing the length of the salesman's one-dimensional tour of a set of cities, which occupy positions in a two-dimensional space, is essentially the same, computationally, as minimizing the area of a sheet which must visit each of a number of points in a three- (or higher-) dimensional space.

Although this problem is simple to state, the task of solving it is not easy: even apparently trivial examples, involving as few as 30 cities, cannot be solved by simply trying all the combinations in sequence and selecting the shortest[†]. Attention has therefore been devoted to finding algorithms which give solutions which can be calculated in a practicably short period of time and which, although not provably optimal, are probably close to the best solution. Two such algorithms have been applied to the problem of visual cortex organization, and will be discussed here: the first is based on the behaviour of a simulated elastic net (Durbin and Willshaw 1987); the other is derived from the self-organizing feature map (SOFM) algorithm proposed by Kohonen (1982) and described in the preceding section. The interest of these models is two fold: first, given a suitably chosen stimulus space, the maps calculated with them closely resemble those found in the visual cortex and, second, strong formal similarities can be found between the behaviour of the algorithms and more 'realistic' neural net models, e.g. the competitive Hebbian mechanisms used by Obermayer *et al* (1990) and Goodhill (1993).

9.1. Elastic net models

In this type of model, first proposed by Durbin and Willshaw (1987), the salesman's tour (or, analogously, the cortical map) is represented conceptually by a string of beads joined by an elastic thread. For the two-dimensional cortical analogy one can think of a square two-dimensional lattice of points, i.e. a net, connected by elastic. It is important to remember that each lattice point corresponds to a single fixed position on the cortical surface; although the separation of adjacent lattice points in stimulus space can vary, the closer they are in stimulus space, the more similar are the receptive fields of the two corresponding points in the cortex. In both the one- and the two-dimensional cases, the net has a certain energy, which will be lower, the closer the beads or lattice points are to one another. The cities (or analogously, points in stimulus space) exert attractive forces on the beads or lattice points, which are thereby drawn closer to the cities. As the beads approach the cities, the distances over which the attractive forces are exerted are made smaller and, eventually, each city (or stimulus point) will capture a bead, provided the number of beads is initially chosen to be greater than or equal to the number of cities.

The behaviour of this system can be described more formally as follows. Let \mathbf{y}_j be a vector which describes the position of cortical point j (or the j th bead) in stimulus space, i.e. \mathbf{y}_j is the receptive field of point j . Let the position of each stimulus (or city) i be the vector \mathbf{x}_i and let the magnitude of the attractive force exerted by stimulus i on cortical point j be proportional to the following Gaussian function of the distance between points i and j :

$$w_{ij} = \exp(-|\mathbf{x}_i - \mathbf{y}_j|^2/2K^2) \bigg/ \sum_p \exp(-|\mathbf{x}_i - \mathbf{y}_p|^2/2K^2). \quad (22a)$$

K is a distance scaling parameter and the summation over p in the denominator is over all the cortical units. Although w_{ij} is analogous to a force, it can also be interpreted as the response of cortical unit j to stimulus i , assuming that receptive fields have a Gaussian profile (often a good approximation), normalized by dividing by the sum of the responses of all the cortical units to stimulus i (i.e. the term in the denominator). This normalization is important to the operation of the algorithm because it ensures that stimuli which are a long way from the cortex (equivalently, cities which are far away from tour points)

[†] The number of combinations is $(N - 1)!/2$. For $N = 30$ this is approximately 10^{31} combinations.

evoke responses which are as strong, on average, as those evoked by closer stimuli. As a consequence, it can be guaranteed that each stimulus will gain a representation in the cortex (i.e. the salesman's tour will visit all the cities).

At each iteration of the model, the \mathbf{y}_j 's are changed by an amount

$$\Delta \mathbf{y}_j = \alpha \sum_i w_{ij} (\mathbf{x}_i - \mathbf{y}_j) + \beta K \sum_{k \in N} (\mathbf{y}_k - \mathbf{y}_j) \quad (22b)$$

where α and β are rate constants and the values of k over which the summation in the second term is taken are the nearest neighbours of point j . The first summation term on the right-hand side represents the net force exerted by all the stimuli on point \mathbf{y}_j , while the second term represents the elastic pull of adjacent points. As the iterations proceed, the value of K is slowly reduced, causing the elastic forces between neighbouring cortical points to become weaker and the attractive effect of each stimulus to be increasingly local. Equivalently, the receptive fields of the cortical units become more selective in their responses to different stimuli. This has two effects: the receptive fields of the cortical units tend to become more similar to those stimuli to which they are already most responsive, while the elastic forces tend to make neighbouring cortical locations respond to similar stimuli. It will be recognized that these behaviours are features of almost all the models discussed so far.

Goodhill and Willshaw (1990) applied this algorithm to the problem of forming a retinotopic map from the two eyes onto the cortical surface. They studied a simplified one-dimensional version of the problem, in which two one-dimensional retinas projected to a one-dimensional cortex, as well as a more realistic implementation in which two two-dimensional retinas projected onto a two-dimensional cortex. For the one-dimensional case, the stimuli, which Goodhill and Willshaw identified with retinal neurons, formed two parallel rows, one for each retina (figure 13). The neurons in each row were spaced a distance $2d$ apart in a horizontal direction and the rows were a distance $2l$ apart in the vertical direction (the physiological interpretation of vertical distance in this framework is discussed below). Cortical points were initially positioned randomly between the two rows with a small amount of systematic bias applied to the horizontal position components to ensure a determinate orientation of the final retinotopic map. There were typically between one and three times as many cortical points as retinal neurons.

Development in this model goes through a number of characteristic stages. Initially, the cortex flattens out and lies equidistant between the two rows of retinal neurons with the ends pulled in from the edges of the rows (figure 13(a)). This corresponds to the establishment of an ordered retinal topography (with some distortion at the edges of the cortex) and the presence of large binocular receptive fields. As K is reduced (below a value of about 0.5) a critical stage is reached and periodic fluctuations in the vertical positions of the cortical points start to develop (often nucleating from the ends or other positions along its length). These grow rapidly (figure 13(b), (c)) and the cortex eventually approaches and connects together all the points in the two retinas (figure 13(d)). Physiologically, this corresponds to the formation of smaller, monocular, receptive fields, with the exception of a few binocular points at ocular dominance borders. Geometrically, the path taken by the cortex through the retinal units corresponds (approximately) to the shortest line connecting all the units in both retinas. The frequency with which the path crosses from one retina to the other depends upon the values of l and d and it can be shown that the path length is a minimum when the number of retinal cells per ocular dominance 'stripe' is $n = 2l/d$ (Goodhill 1992).

In the two-dimensional version of the model, the cortex was represented by a sheet of points, each of which interacts with its four nearest neighbours; the retinas are likewise two-dimensional sheets of cells separated by a fixed vertical distance. Realistic-looking

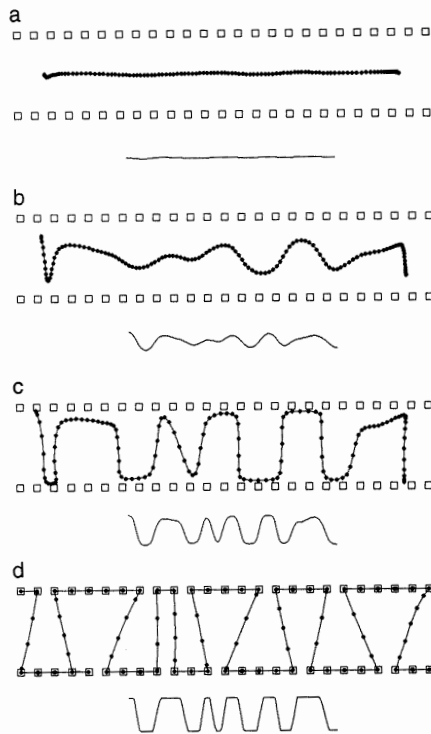


Figure 13. Illustration of the behaviour of the elastic net algorithm when applied to a one-dimensional model of ocular dominance column formation. The ‘stimuli’ in the model are represented as two rows of squares: each row corresponds to a single eye, although the squares are not labelled in any way, except by their position. The ‘stimuli’ can also be thought of as retinal units embedded in a space whose metric is inversely related to the correlation between them. The cortex is represented as an elastically connected string of beads, which initially lies midway between the two sets of stimuli. Initially (*a*) the elastic forces between the beads cause the string to flatten and contract; the attractive forces exerted by the stimuli also cause the string to lie midway between the two rows. As the distance over which the forces are exerted is reduced (i.e. the value of K in equation (22*a*)) instability develops and cortical points start to move towards the stimuli (*b*) and (*c*). Finally (*d*), each stimulus has captured a cortical point. The algorithm has also solved (approximately) the travelling salesman problem for the set of stimuli, i.e. the beads connect them by approximately the shortest route. The line below each panel shows ocular dominance as mapped onto the cortex. Note the resemblance between the retinotopic arrangement in (*d*) and the probable arrangement in monkey cortex illustrated in figure 4.

ocular dominance stripes are formed (figure 14(*a*)), the spacing of which depends upon the separation of the two retinal layers: the larger the separation, the wider the stripes.

Durbin and Mitchison (1990) applied the same algorithm to the problem of mapping orientation and retinotopic position onto the cortical surface, ignoring binocularity. They defined a four-dimensional stimulus space, with coordinates (x, y, η, χ) where x and y specified the centre of the receptive field in visual space and η and χ specified orientation as a point on the circle defined by $\eta = r \cos(2\theta)$, $\chi = r \sin(2\theta)$ where r is a constant, and θ is the preferred orientation (the orientation angles are doubled to reflect the fact that orientation preference is cyclic over the range $0-\pi$). Cortical units and stimuli were

initially randomly positioned in stimulus space and iterations were continued until a stable configuration was found. The resulting distribution of orientation preferences (figure 14(d)) exhibited many of the features found in monkey and cat visual cortex, including periodicity, half-rotation singularities and periodic variations in the orientation gradient. An interesting observation was that the retinotopic map contained variations in magnification factor which were correlated with the variations in orientation gradient: specifically, in cortical regions where orientation preferences changed rapidly, retinal positions changed slowly, and *vice versa*.

Erwin *et al* (1995) combined the models of Durbin and Mitchison (1990) and Goodhill and Willshaw (1990) into a five-dimensional feature space in which binocularity, retinotopic position and orientation were all represented. The resulting output (obtained after 2×10^6 iterations of equation (22b)) was highly realistic and, with an appropriate choice of parameters l and r , successfully reproduced the known relations between ocular dominance stripes and orientation columns, with orientation singularities located in the centres of ocular dominance stripes and local orthogonality between orientation and ocular dominance columns. This is another example of the type of correlation described in the previous paragraph where a rapid change in one parameter as a function of cortical distance is associated with a slow change in a different parameter. This relation is in fact a simple consequence of dimension reduction. For example, if distance along a straight line is measured by l and the line is projected onto a two-dimensional space (x, y) at different angles, the gradients dx/dl and dy/dl will be inversely correlated.

The elastic net algorithm has been further analysed by Durbin *et al* (1989), Yuille (1990), Yuille *et al* (1991) and Dayan (1993). These papers suggest ways of interpreting distances in stimulus space in terms of correlations between input neurons and show how the algorithm can be interpreted in terms of more conventional Hebbian models, such as that of Miller *et al* (1989).

9.2. Low-dimensional self-organizing feature map (SOFM) models

Applications of Kohonen's SOFM algorithm to visual cortex map formation have been described above, in section 8, where they were characterized as competitive Hebbian mechanisms. A slightly different version of Kohonen's algorithm was applied to the problem of visual cortex organization by Obermayer *et al* (1991, 1992a, b). As used by these authors, the algorithm performs dimension reduction in much the same way as the elastic net method and, like the latter, it has an essentially geometric interpretation, which can be described as follows. A two-dimensional cortical sheet fills a stimulus space of equal or higher dimension according to some initial configuration. Points in the stimulus space are chosen one at a time (e.g. at random, or from a predefined fixed set) and for each stimulus the cortical point which is nearest, i.e. responding most strongly, is found. This point is then moved closer to the stimulus. Nearby cortical points are also moved a lesser distance towards the stimulus, which tends to enforce continuity in the cortical representation. After presentation of a sufficiently large number of stimuli, the cortical sheet becomes locally smooth and it fills stimulus space in a manner determined by the initial configuration and the history and probability distribution of stimulus presentation.

The main differences between the low- and high-dimensional implementations of the algorithm are that, in the low-dimensional version, stimulus values such as retinotopic position and orientation are directly encoded by the input vectors, e.g. receptive field position, x , is encoded as an activity value, x , in a single input unit; in addition, the weight values of the winning cortical unit and its neighbours (the weight values are simply the

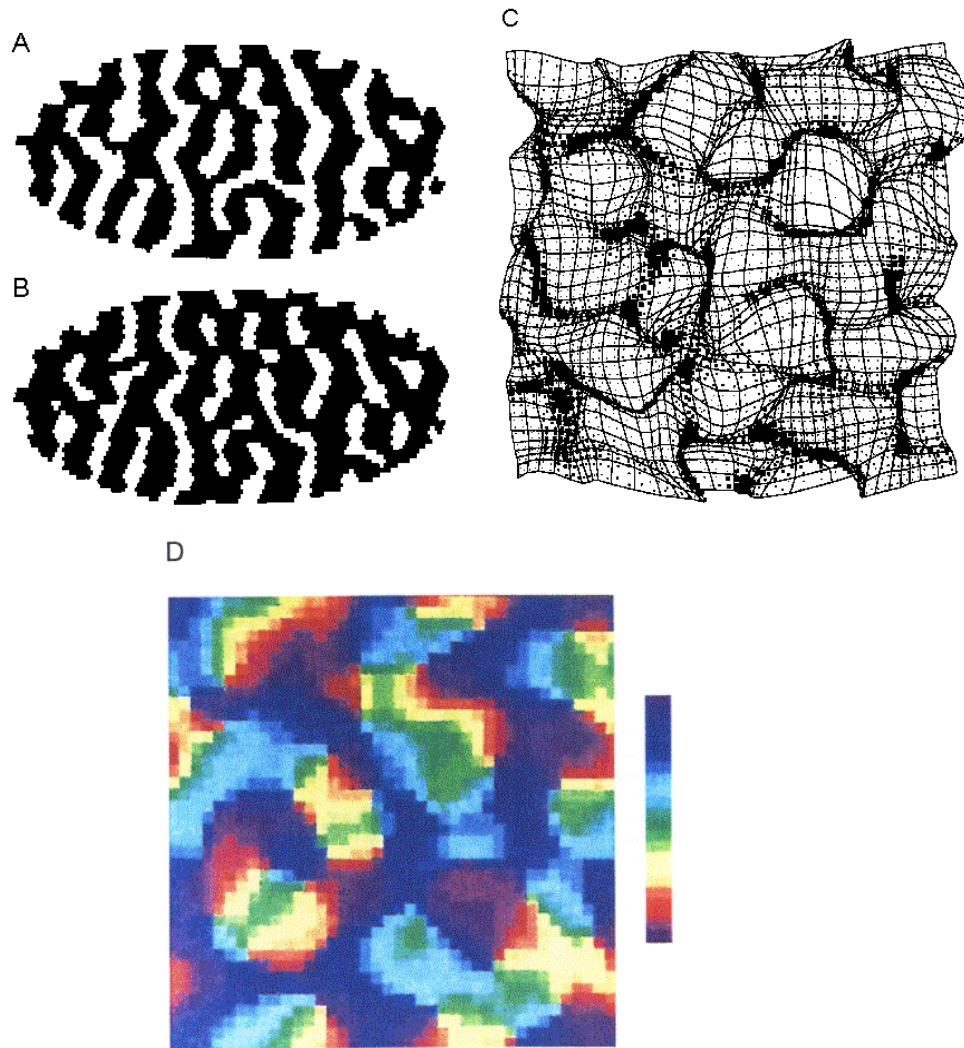


Figure 14. Simulations of cortical topography produced by the elastic net algorithm. (A) Ocular dominance stripes formed when two circular retinas were mapped to an elliptical cortex: this causes the stripes to run perpendicular to the long axis of the ellipse. (B) Monocularly deprived ocular dominance stripes, simulated by reducing the value of α (equation (22b)) for one of the two retinas. (C) Combined formation of retinotopy and orientation columns: the figure shows the projection of the cortex (whose surface is represented by an equally spaced array of grid points) into retinotopic coordinates: thus, the further apart two points in the grid are, the more distant are their receptive fields. The black squares represent the magnitude of the orientation gradient at each cortical location. Notice that there is a strong inverse correlation between the orientation gradient and the retinal magnification factor: in regions where cortical points are far apart in retinotopic space the orientation gradient value is small, and vice versa. (D) The corresponding map of orientation preference in the cortex. The strip on the left shows the colours used to code orientations. (Parts (A) and (B) are reprinted from Goodhill and Willshaw (1994) with permission from MIT Press © 1994 Massachusetts Institute of Technology; parts (C) and (D) are reprinted from Durbin and Mitchison (1990) with permission from *Nature* © 1990 Macmillan Magazines Limited.)

position of the unit in stimulus space) are made more similar to the input vector, rather than increased in value in the normal Hebbian way (and subject to normalization constraints).

Thus, for the low-dimensional case (cf equation (21) which is the high-dimensional case) after the presentation of a stimulus vector \mathbf{v} , the cortical receptive fields (or weight values) \mathbf{w}_j change by an amount

$$\Delta \mathbf{w}_j = \varepsilon h(j, j^*) (\mathbf{v} - \mathbf{w}_j) \quad (23)$$

where ε is a rate constant, j^* is the cortical point closest to \mathbf{v} , and $h(j, j^*)$ is a decreasing function of the cortical distance r between points j and j^* . For this, Obermayer *et al* (like Goodhill (1993)) used a radially symmetric Gaussian function $h(r) = \exp(-|r|^2/2\sigma^2)$, although for some simulations $h(r)$ was anisotropic, i.e. oval rather than circular.

Obermayer *et al* (1991, 1992a, b) applied this algorithm to a five-dimensional feature space, with components $(x, y, q \cos(2\phi), q \sin(2\phi), z)$. Parameters x and y correspond to retinotopic position, q describes orientation selectivity (a value of $q = 0$ indicates a circularly symmetric receptive field), ϕ is preferred orientation and z is an ocular dominance value. Stimuli were chosen with a uniform probability distribution, $P(\mathbf{v})$, from the manifold

$$V = \{ \mathbf{v} | x, y \in [0, d], \phi \in [0, \pi], q < q_{\text{pat}}, |z| < z_{\text{pat}} \}.$$

The size of the Gaussian neighbourhood function, σ , was gradually reduced during the simulations.

Figure 15 shows the results from one such mapping obtained with this method†: the experimental data on orientation and ocular dominance maps were reproduced in almost every detail (e.g. those listed in table 1); in addition, a good agreement between the shapes of the power spectra and the auto- and cross-correlation functions for real and modelled results was found. As an expected general consequence of the dimension-reduction approach, inverse correlations between local magnification factors along the different stimulus dimensions were found. One example of this was that orientation selectivity varied most rapidly in regions of constant ocular dominance. As a result, singularities were concentrated in the middle of the stripes and the orientation gradient was maximum along directions perpendicular to the stripes. In other words, there was a locally orthogonal relationship between iso-orientation slabs and ocular dominance columns at stripe borders. This latter relationship was investigated in more detail (Obermayer *et al* 1992, Obermayer and Blasdel 1993) by extracting the local orientations of iso-orientation and iso-ocular dominance domains‡. A plot of the difference angles in the modelled maps showed a bias towards orthogonal values, similar to that observed in the data obtained from optical maps in four adult monkeys. As with mappings obtained using the elastic net method (Durbin and Mitchison 1990), retinotopic position varied most rapidly in regions of low rates of change of orientation preference and *vice versa*. Elongating the neighbourhood function, $h(r)$, had the effect of making the iso-orientation domains run parallel to the direction of elongation.

Obermayer *et al* (1992a) carried out a statistical mechanical analysis of the behaviour of the model, investigating the conditions (determined by the values of d , q_{pat} , z_{pat} and σ) under which stable patterns of fluctuating orientation and eye preference could be predicted to emerge. The analysis, however, could only be carried out in the regime in which spatially fluctuating patterns of orientation and ocular dominance fail to emerge; thus, the biologically interesting behaviours of the system had to be investigated by numerical simulation.

† Obtained after about 10^6 iterations of equation (23). This required about 30 hours of computation on a CM-2 connection machine (Obermayer, personal communication).

‡ These angles were calculated from the positions of the peaks in Fourier spectra obtained from numerous small regions (masked with a narrow Gaussian) in the maps.

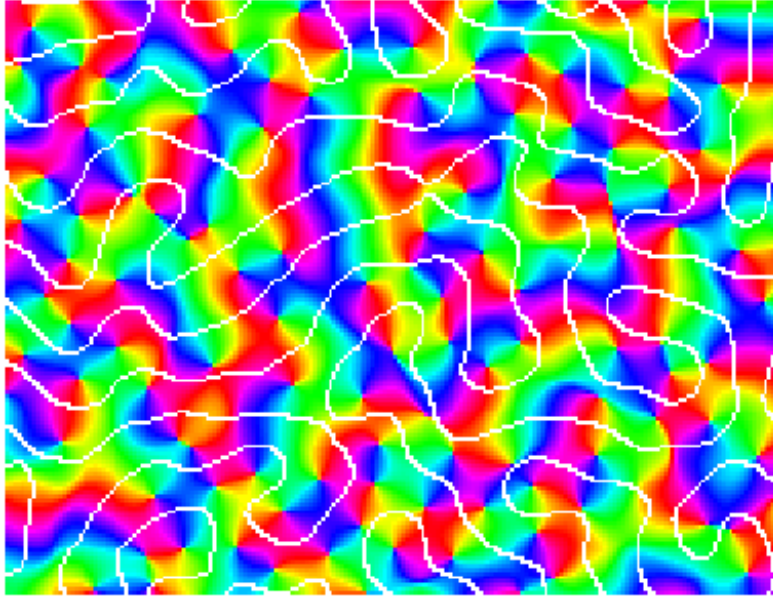


Figure 15. Orientation and ocular dominance maps produced by the low-dimensional Kohonen algorithm for dimension reduction. As in figure 3, the white lines indicate the boundaries of ocular dominance stripes, and a similar colour scheme is used to code orientations. As in the experimental data, singularities tend to lie in the centres of ocular dominance stripes and iso-orientation domains intersect ocular dominance boundaries at right angles. (Figure provided by K Obermayer; details of the model parameters are given in Blasdel and Obermayer (1994).)

9.3. Strengths and weaknesses of the dimension-reduction approach

The similarity of the maps generated by dimension-reduction models to real cortical maps is impressive. This suggests that the constraints of continuity and completeness operating in the models are similar to those operating during cortical development. Given the demonstration that the cortex seems to come reasonably close to an optimal solution to this problem, and assuming that all the near-optimal solutions look similar, then any model or algorithm which solves this problem (which is essentially the travelling salesman problem) can be expected to produce realistic cortical maps. Thus, in principle, the operation of a successful algorithm in this context need not necessarily bear any relation to actual biological developmental mechanisms[†].

It is reasonable to ask, therefore, whether the models of Durbin and Mitchison (1990), Goodhill and Willshaw (1990) and Obermayer *et al* (1991) can be considered to be models of development, or whether they are best regarded simply as existence demonstrations. The answer to this question is not entirely clear. Both algorithms have a rough biological interpretation: e.g. the ‘forces’ attracting cortical points to stimuli are essentially Hebbian, given that the net effect of Hebbian modification (in any model) is to make cells more responsive to stimuli to which they already respond well. The cortical neighbourhood

[†] As an example of different mechanisms having a similar end result, local orthogonality between orientation and ocular dominance columns in Swindale’s (1992) model results from an interaction (slowing the rate of emergence of orientation selectivity in regions where the rate of growth of ocular dominance is high) which cannot be straightforwardly derived from any of the behaviours of dimension reduction models, although the end result appears to be similar.

function can also be implemented biologically in various ways, e.g. by means of lateral connections between cells or by the local spread of substances which modify synaptic strengths. It is less clear how the geometrical construction of the low-dimensional stimulus space, used in an identical fashion in both the elastic net and Kohonen approaches, might be interpreted. Thus, the values of d , q_{pat} , z_{pat} and σ are not straightforwardly derivable from measurable quantities and, at present, are simply chosen to give the best-looking results. For the case of ocular dominance and retinotopy, Goodhill and Willshaw (1990) proposed that distances between individual units within and between the two layers could be identified with a measure of the correlation in the activities of pairs of units. Thus, an increase in the distance between the layers could be identified with a decrease in the correlation in the two eyes' activities. But a metric defined in this way does not necessarily produce a Euclidean space: for example, it is not immediately clear how zero or negative correlations might be represented. This problem is, of course, avoided in 'high-dimensional' models where neural activities are represented explicitly in the input layer.

As an empirical matter, the question of how closely the intermediate and final stages of development in the models resemble those of the real cortex deserves further examination, as does the extent to which the models are able to replicate species differences, the effects of manipulations such as monocular deprivation, and very non-uniform distributions of input stimulus features. These questions have not been fully addressed yet, although Goodhill and Willshaw (1994) were able to model the effects of monocular deprivation (figure 14(b)) and strabismus[†] and a case could probably be made that the later developmental stages of the algorithms resemble normal development. A distinctive aspect of the algorithms' initial behaviour is a phenomenon referred to as 'collapse' (Kohonen 1982): receptive fields rapidly become similar over the whole cortex and approximate to the centre of stimulus space. To the extent that relatively large areas of the cortex may take on a similar preferred orientation and receptive field position, this behaviour does not seem particularly realistic. Finally, the predicted inverse correlation between the local magnification factors for orientation and retinotopic position has yet to be confirmed. In cat area 17, preliminary evidence (Das *et al* 1995) indicates a positive correlation, i.e. receptive field positions were found to change more rapidly in regions of discontinuous orientation change. If this turns out to be true it would undermine the generality of the ideas underlying dimension-reduction theories and the suggestion that the cortex optimizes coverage.

10. Other models

10.1. The tea-trade model

This model, which was devised by von der Malsburg and Willshaw (1977), took its name from an analogy with a hypothetical situation in which one might be able to decide on the exact geographical origin of a particular blend of tea based only on a knowledge of the relative proportions of the different individual tea types making up the final blend[‡]. This would be possible if tea-blenders' use of any particular tea decreased with increasing distance of the source of the tea from the blending site. The application of this basic idea to the problem of map formation went as follows: assume that in the retina there exist sources, in various positions, of a number of different chemical markers which diffuse laterally through the retina. These are taken up (i.e. blended) by individual ganglion cells

[†] Monocular deprivation was modelled by reducing the value of α (equation (22b)) for the deprived eye and strabismus was modelled by increasing the distance between the two sheets of retinal units.

[‡] This is an extremely uninteresting problem, even for an English scientist.

and transported to the target structure (i.e. optic tectum or visual cortex) where they cross synapses and enter postsynaptic cells. The markers are then transported laterally (e.g. by diffusion within dendrites) through cells in the postsynaptic layer. Synapses are increased in strength and/or number based on a measure of how similar the blend of markers in the presynaptic terminal is to the blend present in the postsynaptic element. The modification rule tends to maximize the similarity between pre- and postsynaptic marker sets and can account for the formation of topographic projections and a variety of experimental data on retino-tectal mappings (Willshaw and von der Malsburg 1979). The model can also be applied to the problem of ocular dominance stripe formation (von der Malsburg 1979) given identical markers in the two eyes except for two unique to each eye.

The tea-trade model is unusual in that there is no explicit dependence upon neural activity. This may be useful in situations where it can be shown that neural activity is unnecessary for topographic map formation. The idea that ocular dominance column formation relies entirely on a chemical difference between the two eyes is probably not correct because projections from genetically identical eyes can segregate into stripes (Fawcett and Willshaw 1982, Ide *et al* 1983). No application to orientation column formation has been proposed.

Although the resemblance is not at first obvious, the tea-trade model behaves in a way which is like that of the elastic net algorithm (Durbin and Willshaw 1987) and was the inspiration for it. Thus, a given mixture of markers in a pre- or postsynaptic element can be represented as a position in a space whose axes are the concentrations of the different chemical markers. The synaptic modification rule has the effect of moving the positions of the postsynaptic elements towards nearby presynaptic elements. The diffusion of markers laterally through the postsynaptic sheet is analogous to the elastic forces in the net and has the same effect of enforcing continuity in the postsynaptic sheet.

10.2. *The diffusion-based model of Montague et al*

The model of Montague *et al* (1991), which is based on an earlier proposal by Gally *et al* (1990), postulates that the development of topographic projections in the visual cortex and in other neural structures is determined by a mechanism in which synaptic strengths are changed depending upon presynaptic activity and the concentration of a molecule which is released in amounts proportional to the local postsynaptic activity and diffuses extracellularly through tissue. If the concentration of the signal is high, active synapses are strengthened and inactive ones weakened; if the concentration is low, active synapses are weakened and inactive ones are left unchanged; at intermediate levels of the signal, strengths are left unchanged. This mechanism has since been referred to as 'volume learning' (Montague and Sejnowski 1994).

The function of this signalling molecule (or molecules) is similar to that of the locally excitatory connections between cortical neurons assumed by most other models: it provides a mechanism by which the strengthening of connections between one afferent and a postsynaptic cell will be accompanied by the strengthening of connections from a second afferent to the same, or nearby cells, if the firing of the first afferent is correlated with the firing of the other. The two mechanisms are not entirely equivalent however: while lateral neural connections usually integrate the postsynaptic response within some local region in space and a fixed, short time interval, the diffusion mechanism integrates over both space and time, with scales determined by the diffusion constant of the molecule and the rates of its production and removal. The mechanism will therefore only be able to detect input correlations at spatial and temporal scales which are similar to those imposed by the

kinetics of the accompanying diffusive signal. Gally *et al* (1990) suggested that the signal might be a small, rapidly diffusing molecule, such as nitric oxide, which is released from dendrites in response to neural activity and has been shown to gate synaptic plasticity in other systems (Schuman and Madison 1994). Other candidate molecules include arachidonic acid, carbon monoxide and hydrogen peroxide, as well as members of the neurotrophin family (Thoenen 1995).

Montague *et al* applied their model to the problems of barrel formation in rodent somatosensory cortex and to ocular dominance column development. The simulations were more realistic than any others discussed here and included the specification of individual axonal and dendritic arbors within a three-dimensional neuropile. Axons could actively grow through the neuropile, occupying neighbouring vacant sites by probabilistic sprouting. To simulate ocular dominance column formation, a crude initial topography was assumed and patterns of retinal activation were modelled as travelling waves of synchronous cell firing, similar to those thought to be present prenatally. Whenever one retina was active the other was silent. These waves caused a progressive refinement of topography as well as the final emergence of a realistic pattern of ocular dominance stripes.

The volume learning hypothesis may turn out to be correct, given the evidence for non-local (or 'distributed') Hebbian plasticity in both visual cortex (Kossel *et al* 1990) and hippocampus (Bonhoeffer *et al* 1989), and for the role of a variety of candidate extracellular molecules in modulating long-term potentiation and depression (LTP and LTD). Evaluating the simulation results is hard however: partly because of the large number of details which had to be specified, the model has more free parameters than most and the influence of these on the behaviour of the model and the periodicity of the ocular dominance stripes was not examined. It remains to be seen whether the space and time constants of likely diffusing molecules are in the same range as those which distinguish neural activity in the two eyes and whether they can produce structures of the right size. A simplified implementation of the model, together with a further examination of parameter dependence, would probably be worthwhile.

10.3. Tanaka's thermodynamic approach

The basic ingredients of Tanaka's models (Tanaka 1989, 1990a, b, 1991a, b, 1995) are similar to those in most non-competitive Hebbian models (e.g. von der Malsburg, Miller and Linsker) and include spatially correlated activity in one or more input layers, lateral intracortical interactions, Hebbian learning and input normalization. Tanaka's mathematical treatment of his learning equations is novel and complex, and draws heavily on an analogy with the physics of systems, such as magnetic domain formation, which can be characterized by a discrete state variable known as Potts spin. Tanaka justifies this analogy quite rigorously by mathematical analysis (Tanaka 1990) of a system, inspired by the speculations of Changeux and Danchin (1976), which assumes the presence of:

- (i) a postsynaptic factor which is available in limited amounts and is essential for synaptic stabilization;
- (ii) a presynaptic stabilizing factor, transported anterogradely from the cell body;
- (iii) a Hebbian modification rule which allows the weakening or destabilization of active synapses in the presence of postsynaptic hyperpolarization, as well as the more normal strengthening in the presence of depolarization.

Analysis of the resulting learning equation shows that in a stable equilibrium the synaptic strengths tend to assume upper or lower limiting values (this is also true of the weight

values in other models, such as Linsker's). The resulting binary state variable is the Potts spin of the system, and from it an associated temperature, which is related to the lifetime of an average synapse, and Hamiltonian function (analogous to Linkser's energy function for orientation columns) can be derived. A standard Monte Carlo technique is used to find configurations of the system for which the value of the associated Hamiltonian is a minimum.

Tanaka modelled separately the formation of ocular dominance columns, orientation columns and the barrel map in somatosensory cortex. All these models produce realistic results. His model for ocular dominance (Tanaka 1989, 1991a, b), although derived independently, is formally similar to that of Miller *et al* (1989), inasmuch as Tanaka's Hamiltonian for ocular dominance is the same as the right-hand side of Miller *et al*'s equation for synaptic growth (19). One difference is that Miller *et al* did not assume the possibility of spontaneous formation and removal of synapses. This means that Miller *et al*'s system has a temperature of zero in Tanaka's formulation. Tanaka's model for orientation columns (Tanaka 1990, Miyashita and Tanaka 1992) is closely related to those of Swindale (1982a) and Linsker (1986c). In fact, Tanaka's Hamiltonian for orientation is identical to Linsker's energy function if an isotropic Q^G is assumed. Thus, like Swindale, Tanaka assumes that the interaction between orientations depends only upon the distance between them and not the direction. Consequently, his iso-orientation columns are elongated in directions that do not depend upon the orientation represented within them. Tanaka has recently tackled the problem of the simultaneous emergence of retinotopy, ocular dominance and orientation selectivity (Tanaka 1996).

10.4. Band-pass filter models

A number of authors have shown that realistic patterns of ocular dominance and orientation can be obtained by simply band-pass filtering a random noise pattern. For example, Rojer and Schwartz (1990) simulated ocular dominance columns by first band-pass filtering a two-dimensional scalar noise pattern and then applying a threshold. Orientation columns were simulated by applying a gradient operator to filtered noise, from which they calculated an orientation map, $\theta(x, y) = \frac{1}{2} \arctan\{v/u\}$ where $z(x, y)$ is the filtered noise, x and y are position values, and $u = \partial z/\partial x$ and $v = \partial z/\partial y$. If, as suggested by Erwin *et al* (1995), a single filtered scalar noise pattern is used to generate both ocular dominance stripes and orientation columns, additional points of similarity with experimental data are found: orientation singularities lie in the centres of ocular dominance columns and, as a simple consequence of the gradient operation, the locally orthogonal relationship between ocular dominance and orientation columns is reproduced. Computationally, Rojer and Schwartz's model for ocular dominance has little to distinguish it from a simplified implementation of Swindale's (1980) model for ocular dominance. The derivation of preferred orientation from a gradient operation is novel but, as pointed out by Erwin *et al* (1995), the vectors produced by this operation have the unrealistic property that for any closed loop, $\int (v dx + u dy) = 0$. (Equivalently, $\text{curl grad } z = 0, \forall x, y$.) This is not a property of real orientation maps or of the maps produced by other models, although the difference is hard to detect visually.

Niebur and Wörgötter (1993) calculated patterns of orientation preference directly from the frequency domain, assuming zero energy at all frequencies except at up to three discrete positions in frequency space at similar distances from the origin. Fixed amplitudes and random phases were assigned to these positions and the orientation pattern calculated by back-transforming into spatial coordinates and calculating an orientation angle in the usual way from the real and imaginary components of the signal. Some support for their approach

comes from the observation that orientation power spectra in the cat visual cortex (Diao *et al* 1990) often consist of a small number of relatively discrete-looking peaks. However, this may be because the maps come from small regions of cortex: spectra from larger areas of monkey cortex tend to be more uniformly annular in shape (Obermayer *et al* 1991, 1992a, Blasdel *et al* 1995).

Grossberg and Olson (1994) proposed a filtering algorithm based on the idea that where a number of different features are represented on the surface of the cortex, large values of one feature may correlate with small values of the other features. There is some evidence for this, which they refer to as competitive normalization, inasmuch as orientation selectivity seems to be reduced in regions of extreme ocular dominance. A simple way of imposing this normalization is to impose the restriction that $x_1^2 + x_2^2 + x_3^2 = 1$, where x_1 , x_2 , and x_3 are the feature values in question, i.e. to map the feature space to the surface of the unit sphere. This constraint means that any point on the cortex can be uniquely determined by the values of two angles, α and β , for which the corresponding values of x_1 , x_2 and x_3 are determined by the relations $x_1 = \cos \alpha \cos \beta$; $x_2 = \sin \alpha \cos \beta$; and $x_3 = \sin \beta$. The algorithm works by first assigning a random set of values to α and β , from which values of x_1 , x_2 , and x_3 are then calculated. Each set of x values is then filtered with an annular band-pass filter, which may or may not be the same for each feature. (It may be noted that once this filtering has taken place the normalization constraint no longer holds). Preferred orientation is then defined as $\theta = \frac{1}{2} \arctan\{x_1/x_2\}$ and ocular dominance by the value of x_3 . This model generates realistic orientation columns (for which curl $(x_1, x_2) \neq 0$) in which the orientation singularities occupy the centre of ocular dominance patches. No locally orthogonal bias in the intersection angles of iso-orientation and ocular dominance borders is obtained unless an anisotropic filter is used to make the ocular dominance bands run in one direction. The ocular dominance maps produced by this model, as in Rojer and Schwartz's, are somewhat unrealistic because well-defined stripes of uniform width are never present unless a strongly anisotropic filter is used.

10.5. The relationship between visual cortex shape and ocular dominance column morphology

Most of the models for ocular dominance column formation discussed so far have simulated only small regions of cortex and none have considered in any detail the global properties of ocular dominance columns and their overall relationship with the retinotopic map. An exception to this is a computational study by Jones *et al* (1991) which suggests that the morphological differences between cat and macaque monkey ocular dominance stripes may be the result of two constraints:

- (i) a fixed overall shape of LGN and visual cortex;
- (ii) a locally isotropic magnification factor within individual ocular dominance stripes.

This approach stands in contrast to other models (see e.g. Swindale (1981a)) which explain the feature variations (overall orientation, spots versus stripes, etc) in an *ad hoc* fashion by simply varying parameter values to obtain the desired resemblance.

Jones *et al* suggest that the overall shape of the visual cortex may be relevant to the problem, for the following reasons. Cat and monkey LGNs and visual cortices differ in shape (LeVay *et al* 1985, Anderson *et al* 1988): the monkey LGN is roughly circular, but the visual cortex to which it projects is elliptical, with a roughly 2:1 length-width ratio. In the cat, both the LGN and cortex are elliptical, with similar length-width ratios. Jones *et al* calculated mappings between regions with these shapes, first simplifying the problem by dividing the

LGN and cortical areas into a small number of hexagons, the width of each corresponding to the diameter of a single ocular dominance column. This automatically enforces the constraint of isotropic magnification within ocular dominance columns. Mappings between pairs of LGN layers (i.e. left and right eyes) and the cortex were calculated, subject to the constraint of minimizing the maximum cortical distance between representations of neighbouring LGN points, as well as the number of points that are this distance apart. An exact solution to this minimization problem, which is NP complete, was obtained using an algorithm for subgraph isomorphism. The resulting interdigitating arrangement of left- and right-eye hexagons of the surface of the cortex (figure 16) was different, depending upon whether macaque monkey or cat LGN and cortex shapes were simulated. For the monkey, the algorithm produced more or less parallel stripes, running perpendicular to the long axis of the simulated cortex. For the cat, where two elongated LGNs projected to an elongated cortex, the arrangement was less regular, with more branching and no consistent overall direction of stripe elongation. The results show, therefore, that global mapping constraints may provide an explanation for some of the morphological differences between cat and macaque monkey ocular dominance columns. More recently, the elastic net algorithm has been applied to the same problem, with essentially similar results (Goodhill and Willshaw 1994, Bates *et al* 1995): in these instances, two circular retinas projected to either a circular or an elliptical cortex.

It is possible to see why these results were obtained, for the following general reasons, given by Jones *et al*. First, assume that magnification factor in the macaque LGN is isotropic (Connolly and Van Essen 1984) and that magnification factor within ocular dominance stripes is also isotropic. Then, if each of two circular LGN layers is cut into a series of stripes which are laid alternately side by side, the resulting area covered will be approximately elliptical, with each stripe running perpendicular to the long axis (LeVay *et al* 1985). This also means that overall magnification factor in the cortex must be anisotropic, a conclusion which was reached by Hubel and Wiesel (1977) and seems to be supported by experimental measurements (Tootell *et al* 1988b)†. It is obvious that two elliptical LGNs cannot be similarly divided into uniform stripes and overlaid on an ellipse with a similar length–width ratio, without either compressing the retinal map within each stripe, or, as demonstrated by Jones *et al*, adopting a much more disordered stripe topology.

These arguments lose their force if magnification factor within ocular dominance stripes is not constrained to be isotropic, because the within-stripe retinal map can then be compressed to accommodate any desired combination of LGN, cortical and stripe morphologies. If magnification factor is so constrained, however, then it is clear that stripe morphology and cortical shape will not be independent of each other. This raises an intriguing question. Is the overall shape of striate cortex innately prespecified and determinative of overall column morphology, or do local factors, perhaps dependent upon the density and spread of lateral cortical connections, determine the morphology of the columns and secondarily the overall shape of the cortex? The latter possibility should not be dismissed, as it is currently a matter of active debate (Innocenti and Kaas 1995) whether cortical areas and their boundaries are prespecified within the cortex (Rakic 1988), or determined interactively with the thalamus (O’Leary 1989, O’Leary *et al* 1994).

† It is interesting that cortical magnification factor in the squirrel monkey, which lacks ocular dominance columns, is isotropic (Campbell and Blasdel 1995).

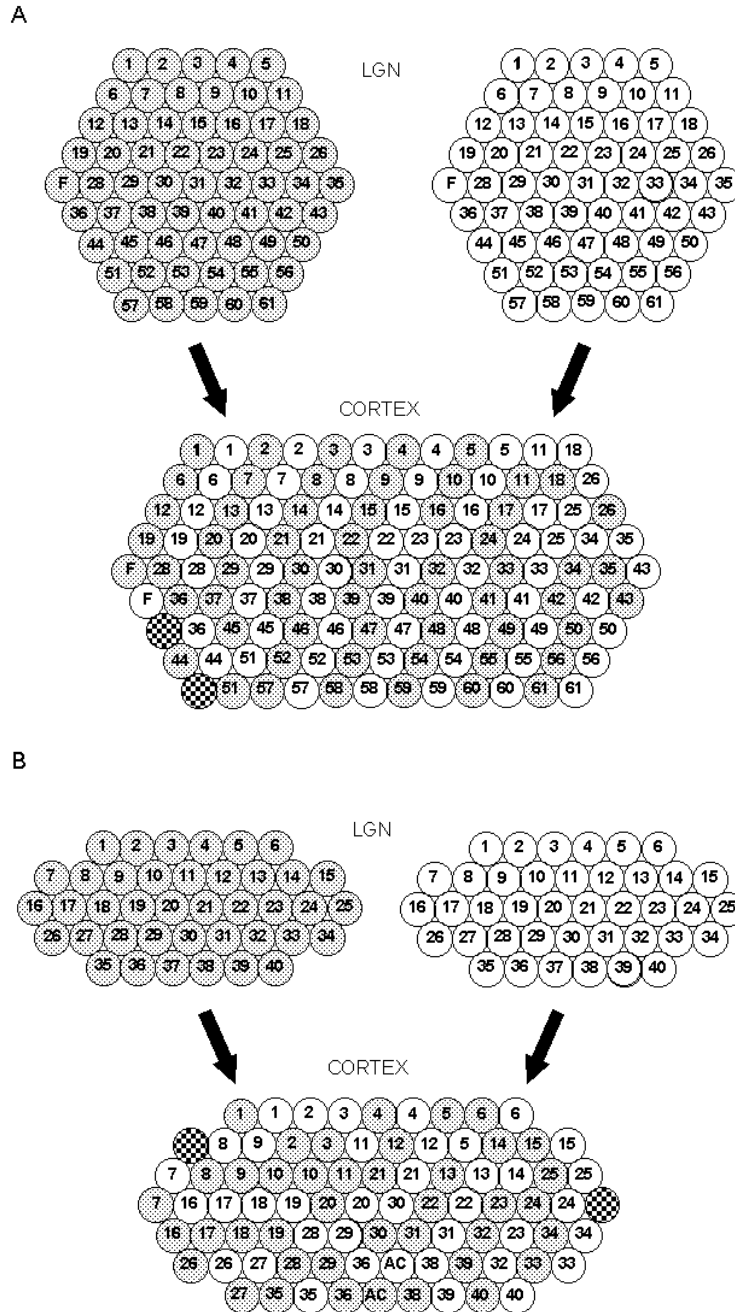


Figure 16. Illustration of the influence of visual cortex shape on ocular dominance stripe morphology. (A) The mapping from two approximately circular LGNs to an approximately elliptical cortex produced by an exact solution to a distance minimizing algorithm described by Jones *et al* (1991): note that the solution is an orderly pattern of stripes which run perpendicular to the long axis of the cortex. (B) When two elliptical LGNs map to an elliptical cortex the solution is a much less orderly interdigitation of inputs. F = fovea; AC = area centralis. (Redrawn from Jones *et al* 1991.)

10.6. Approaches based on information theory

Although much visual cortical development takes place before the eyes are open, it would be surprising if the early development of receptive field properties was not reflective of fundamental general principles governing the way in which sensory information is coded and represented within the brain. Ideas about sensory coding have a long history (reviewed by Barlow (1989)) and, although they address the question of what the total set of individual receptive field properties might be, rather than how these properties are arranged spatially within the cortex, one does not have to add much to ideas about single-cell behaviour to come up with a topography. Nor can one address the issue of topography without first considering what properties are, or might be, represented in the map as a whole. Consequently, a number of authors have suggested that information theory (Shannon and Weaver 1949) may be able to explain some of the properties of the visual cortex. One idea (Barlow 1959) is that visual cortex recodes the visual image, detecting and removing redundancies in the firing pattern of retinal neurons, so that the information in it can be represented by the firing of a smaller number of neurons in the cortex. The sensory image may also be transformed in such a way as to render the information in it robust to transmission along noisy channels with limited dynamic range. It is also probable that a function of cortical processing is the removal of information which is irrelevant, or relatively unimportant, to the processing that goes on at higher levels.

Application of these ideas has produced some interesting results. For example, Daugman (1989) has shown that a highly effective compression of visual images can be achieved if the image is represented by the outputs of oriented two-dimensional Gabor filters whose sensitivity profiles resemble the receptive fields of cortical simple cells. This finding, which is essentially a statement concerning the mathematical properties of natural visual images (see also Baddeley and Hancock 1991), suggests that a goal of cortical processing might be to achieve a faithful representation of the visual image with a small number of neurons. In a series of papers, Linsker (1988a, b, c, 1989a, b, 1990, 1992) has argued, along somewhat similar lines, that the cortex develops in such a way as to maximize the amount of mutual information between the input signal (e.g. at the retina) and the output (in the visual cortex). Application of this principle, namely gradient ascent on a mutual information measure (Linsker 1989b), leads to a Hebbian-like learning rule which can result in the formation of topographic mappings with many of the properties of visual cortex maps. Hesselroth and Schulten (1994) obtained a similar result and showed that topographic representations of oriented simple cell-like receptive fields could be obtained.

The fact that Hebbian rules can lead to the development of representations that reduce redundancy should not be surprising. Inputs whose firing patterns tend to be correlated will tend to converge on the same postsynaptic cell (as happens, for example, in von der Malsburg's network for orientation preference), i.e. their signals will be pooled, rather than kept separate. Many neural nets incorporating Hebbian learning rules (see e.g. Oja 1982, Sanger 1989, Földiák 1989) are able to find the principal component vectors of the data sets on which they have been trained and are, therefore, capable of reducing redundancy. Application of a competitive Hebbian learning rule to a network trained with natural images (Barrow 1987, Barrow and Bray 1992) gave rise to the formation of receptive fields with Gabor-like sensitivity profiles, a finding which is consistent with Daugman's (1989) results.

Information theory is potentially a powerful tool for the study of visual cortex organization and it is a help that the mathematical foundations of the subject are well established. However, its application to biological problems is not straightforward. The fact that there are many more cells in the visual cortex than in the two retinas means that it

is not *a priori* necessary to recode the image in a compact form. Removal of redundancy might seem an obviously worthwhile thing to do, but it is also the case that adding certain forms of redundancy to the representation might make it less sensitive to added noise or loss of neurons. Information theory also says nothing about the relative importance of different kinds of information, or what information it might be possible to discard during sensory processing. For this, ideas derived from biological considerations are necessary. Barlow (1986) has suggested that a task of sensory processing is the detection of ‘suspicious coincidences’, that is, pairs of sensory events whose co-occurrence is greater than chance and suggestive of a causal relationship. Cortical maps may explicitly represent such pairings by ensuring that the cells involved in detecting the pairing are close together. Although this may seem like a biological constraint, it is perhaps not all that different from straightforward redundancy reduction. Marr’s (1970) ‘fundamental hypothesis’[†] is arguably the right kind of idea, as it is a speculation about a specific type of redundancy which may be a property of the real world and which might be important in learning and perception. As far as I am aware, this idea has not yet been implemented as a model for visual cortical receptive field organization and topography: it, and ideas like it, might be worth exploring in this context.

11. Coverage, continuity and wirelength

11.1. Coverage

The idea that uniform representation of visual features within area 17 might be an important constraint on columnar structure is due to Hubel and Wiesel (1974b, 1977). They suggested that columns in the striate cortex appeared to be laid out in such a way as to ensure that all combinations of eye and orientation preference occurred at least once within any region equal in size to the cortical point image. This could be an important constraint on the evolution of the mechanisms of columnar development in the cortex, because an absence of certain combinations of receptive field properties might render the animal perceptually blind or less sensitive to the unrepresented stimulus. Swindale (1991) suggested that coverage might be measured by calculating, for each point in a suitably defined stimulus space, the total amount of neural activity evoked in the cortex. This was given by the expression

$$A(\theta, \phi, \psi, e) = \int n_e(x - x', y - y') \Omega \{ \theta - \theta_c(x - x', y - y') \} P(x', y') dx' dy' \quad (24)$$

where θ is stimulus orientation; (ϕ, ψ) is retinotopic position, assumed to map to positions (x, y) in the cortex; $n_e(x, y)$ is the cortical response to eye $e \in \{L, R\}$; $\Omega(\theta)$ is the orientation tuning function (assumed to be the same at all points in the cortex) and $P(x, y)$ is the cortical point image. A normalized measure of uniformity was defined as $c' = \text{standard deviation}(A)/\text{mean}(A)$. A similar measure has been termed feature normalization by Grossberg and Olson (1994). There is a close similarity between the calculation of coverage, which takes a cortical map of stimulus properties and projects it as neural activity in stimulus space, and the maps produced by the elastic net and Kohonen algorithms, since the latter also map each position in the cortex into the location in stimulus space corresponding to the centre of the receptive field at that cortical location. In the limit that receptive field widths and point image size are delta functions, the two maps are identical.

Although calculations of coverage have not been made for the maps generated by the elastic net or Kohonen algorithms, it is easy to see that these algorithms will tend to ensure

[†] ‘Where instances of a particular collection of intrinsic properties (i.e. properties already diagnosed from sensory information) tend to be grouped such that if some are present, most are, then other useful properties are likely to exist which generalize over such instances. Further, properties are often grouped in this way’.

uniform coverage, provided that a sufficiently large number of stimuli, uniformly distributed in stimulus space, are presented during the training process. When only a small number of stimuli are presented, the two algorithms behave differently: the elastic net method will interpolate between stimuli and produce a map in which positions between the stimuli are represented, whereas the Kohonen map will represent, over larger cortical areas, only the stimulus values which were presented. It is not clear at present which of these behaviours (if either) corresponds more closely with the behaviour of the cortex, although it is not hard to envision experimental tests of the differences.

Calculations based on simulated visual cortex maps (Swindale 1991) allowed an analysis of some of the parameters that are likely to affect coverage uniformity, i.e. the amount by which coverage varies with position within stimulus space. Coverage was found to be most uniform when the period of the orientation columns was about half that of the ocular dominance columns and when the point image was no smaller than about twice the period of the ocular dominance columns. This is, at least approximately, in agreement with the measurements of these parameters that have been made in macaque striate cortex, where orientation columns, ocular dominance columns and point image sizes are about 0.6, 0.8 and 1–2 mm, respectively. This suggests that completeness may be an important constraint on striate cortex organization, at least for the simple stimulus space defined by orientation, ocular dominance and receptive field position.

It is an open question, however, as to whether uniform coverage is always necessary, or is always obtained. One possibility is that higher cortical areas are able to interpolate between incomplete representations in lower cortical areas. This must ultimately be true, because, as has often been pointed out, there are not enough neurons to represent every possible combination of stimulus features, even though these combinations can all be perceived as unique. It is possible that complete representations of even low-level visual features are not obtained, because human psychophysical evidence shows that there are irregular variations in sensitivity across the visual field for simple stimuli, such as gratings of particular orientations (Regan and Beverly 1983), for positional hyperacuity thresholds (Jiang and Levi 1991) and for motion in depth (Hong and Regan 1989). These variations are idiosyncratic and unpredictable in their location in the visual field, suggesting that they might be a correlate of uneven representation of stimulus responsiveness in lower visual cortical areas.

11.2. Continuity

The observation that the receptive fields of neighbouring cortical neurons tend to be similar was one of the first significant discoveries made about the physiological organization of the cortex (Mountcastle 1957). One way to quantify the similarity is to calculate the surface area of the cortex as projected into a suitably defined stimulus space (figure 12), e.g. by

$$C = \sum_{i,j} |\mathbf{y}_{i,j} - \mathbf{y}_{i+1,j}| |\mathbf{y}_{i,j} - \mathbf{y}_{i,j+1}|$$

where $\mathbf{y}_{i,j}$ is the receptive field of the point in the cortex with location (i, j) . The lower the value of C , the more continuous the cortical map. The constraints of continuity and completeness conflict: it is obvious that the cortical map can be completely continuous only at the expense of completeness, i.e. all receptive fields the same, while completeness is easily obtained at the expense of continuity, e.g. by assigning receptive field values at random to different cortical locations. It has been suggested by several authors (see e.g. Niebuhr and Wörgötter (1993), Yuille *et al* (1991), Erwin *et al* (1995)) that a common principle underlying most models of visual cortex topography is that they maximize some

combination of continuity and completeness, making use of the fact that increasing one will tend to decrease the other.

This can be illustrated, as follows, by the behaviour of the elastic net algorithm. The learning rule for the algorithm is given in (22b), that is, an expression for the change in receptive field properties $\Delta \mathbf{y}_j$ in terms of the distances between neighbouring cortical locations and their distances from a set of stimulus values \mathbf{x}_i . If the expression for $\Delta \mathbf{y}_j$ is integrated with respect to \mathbf{y}_j , an energy, or cost function, E , is obtained (Durbin and Willshaw 1987, Yuille 1990) as the sum of two terms:

$$E = -\alpha k \sum_i \log \sum_j \exp \left\{ -|\mathbf{x}_i - \mathbf{y}_j|^2 / 2k^2 \right\} + \frac{1}{2} \beta \sum_j |\mathbf{y}_j - \mathbf{y}_{j+1}|^2. \quad (25)$$

This function (by definition) has the property that $\Delta \mathbf{y}_j = -k \partial E / \partial \mathbf{y}_j$. Thus, at each iteration of the algorithm, $\partial E (= -\Delta \mathbf{y}_j \partial \mathbf{y}_j / k)$ is guaranteed to be negative (provided that $\Delta \mathbf{y}_j$ is small enough that its sign is always the same as $\partial \mathbf{y}_j$) and so the learning rule explicitly minimizes the function given by E . The first term in E is essentially the completeness constraint, i.e. minimizing its value will tend to ensure that each stimulus \mathbf{x}_i is represented in the cortex, i.e. that there is a $\mathbf{y}_j = \mathbf{x}_i$, $\forall i$. If k is interpreted as the width of the receptive field (e.g. in visual space or along the orientation axis) then this part of the expression is analogous to the definition of coverage in (24), if both orientation tuning curves and point-image profiles are assumed to be Gaussian in stimulus space[†]. Orientation tuning curves are often well described by a Gaussian function, while if locally uniform and isotropic retinal magnification factors are assumed, then the point image will be Gaussian in stimulus space, as well as on the surface of the cortex. The term $\sum_j \exp \left\{ -|\mathbf{x}_i - \mathbf{y}_j|^2 / 2k^2 \right\}$ is thus a good approximation to the total response given by the cortex to a stimulus \mathbf{x}_i . The second term in the expression measures continuity, since its value will be small when the receptive field values of adjacent cortical locations are similar. The trade-off between completeness and continuity is then determined by the relative values of the parameters α and β .

Energy or cost functions can be defined on the basis of many different considerations and learning rules can be derived from them by differentiating with respect to the parameter(s) which will be changed by the resulting algorithm. This is a widely used tool in computational neuroscience (Hertz *et al* 1991, Haykin 1994, Anderson 1995), and often reveals similarities between models (see e.g. Yuille *et al* (1991), Yuille (1990), Mitchison (1995)). However, if the resulting learning rule is to be useful as a model of real development, both it and the associated energy function have to have some biological plausibility.

While continuity is generally assumed to be important, the biological reasons for it are still a matter for speculation. One possibility, discussed in the following section, is that continuity minimizes the length of connections in the cortex, assuming that the net length of the axonal and dendritic connections between any two cells is proportional to the similarity in their receptive field properties as well as to their physical separation in the cortex. Another possibility is that regulation of the supply of blood-borne nutrients to nerve cells may be simplified if neurons which are likely to respond simultaneously are grouped together. The success of functional magnetic resonance imaging methods (which detect local variations in blood flow within the brain) bears witness to the fact that blood flow within small brain regions is precisely regulated by neural activity. Another possibility (Swindale *et al* 1990) is that the transmission of signals from one cortical region to another may be easier if neural activity patterns are band limited or band pass in the spatial domain: this will be achieved if nearby neurons have similar response properties, so that they tend to be simultaneously active. Because transmission of information in spatially band-pass

[†] This was pointed out to me by Graeme Mitchison.

signals can be achieved with a relatively coarse set of samples, continuous representations may allow information to be transmitted to higher cortical areas by smaller numbers of neurons than would be required otherwise.

11.3. Wirelength

The possibility that continuity in cortical topography might be explained as the outcome of the requirement to minimize the total volume of axons and dendrites was suggested by Cowey (1979) and has been studied in more detail by Mitchison and Durbin (see Mitchison and Durbin 1986, Durbin and Mitchison 1990, Mitchison 1991, 1995). Although the biological appeal of this idea is obvious, it is hard to explore its consequences with any certainty, partly because any calculations will depend upon presently very incomplete knowledge of the rules governing the connections between cortical neurons. One simple assumption, however, is that connections are likely to be made preferentially between regions of cortex with similar response properties, i.e. those that can be mapped to neighbouring regions in stimulus space. Given this, Mitchison and Durbin (1986) proposed a ‘wiring cost function’, defined (for a two-dimensional stimulus space) by

$$C = \sum_{i,j} \{ |\mathbf{f}(i, j) - \mathbf{f}(i + 1, j)|^p + |\mathbf{f}(i, j) - \mathbf{f}(i, j + 1)|^p \} \quad (26)$$

where $\mathbf{f}(i, j)$ is the location in the cortex corresponding to the position (i, j) in stimulus space and the exponent p is used as way of weighting the cost function more or less heavily in terms of long versus short connections. Thus, when $p = 1$, the cost is simply the net length of the wires, when $p < 1$, the cost is dominated by the number of short connections, while if $p > 1$, longer connections dominate the cost.

Given this (arguably somewhat simple[†]) estimate of a wirelength cost, it is of interest to ask what types of map will minimize C . For the simple case where the stimulus space is a two-dimensional $N \times N$ array, and the cortex is a straight line (i.e. the integers $1, \dots, N^2$), it is possible to find provably optimal solutions, i.e. numberings of the array which minimize the sum of the absolute values of the differences between neighbouring array points (Mitchison and Durbin 1986, Durbin and Mitchison 1990). For values of $p < 1$, these solutions resemble those produced by the elastic net algorithm, which suggests, but does not prove, that when the algorithm is applied to the task of producing more realistic simulations of visual cortex structure, the wirelength measure of (26) is also being minimized.

Despite this similarity, it cannot be claimed with certainty that the elastic net algorithm explicitly minimizes C : as shown in the preceding section, what the algorithm actually does is minimize the term $\sum_j |\mathbf{y}_j - \mathbf{y}_{j+1}|^2$ which is the inverse of C , i.e. the sum over the cortex of the squares of the distances, in stimulus space, between adjacent cortical points. The two expressions are not the same, although they might be expected to behave similarly in most instances. More recently, Mitchison (1995) has argued that maps produced by the Kohonen algorithm minimize a measure that is closely related to wirelength. This argument makes use of the demonstration by Luttrell (1989, 1990) that the Kohonen algorithm can be approximated by a procedure which performs gradient descent on a quantity known as a minimum distortion functional. Mitchison shows that this functional can be generalized to resemble a wirelength measure.

[†] The calculation takes into account only connections made between cells with neighbouring receptive field positions, i.e. for stimulus values i and $i + 1$, etc, and also requires quantization of stimulus space into discrete values. While the definition could be broadened to include (potential) connections made by neurons with more dissimilar receptive field properties, this would require further assumptions about how to weight connection lengths in terms of distances in stimulus space.

Mitchison (1991) has also considered the following interesting, and somewhat less abstract, version of a wirelength problem: in this, axonal volume, rather than net length, is the relevant biological variable and relatively subtle factors, such as axonal branching topology and the change in axonal diameter at branch points, turn out to be important. Suppose there are two sets of neurons, *A* and *B*, with fixed rules regarding the number of connections made between neurons of like and unlike types. What spatial arrangement of neurons *A* and *B* minimizes the total volume of connections? One possible layout is for *A* and *B* to be placed in nearby, but physically separate areas: each neuron in *A* can connect efficiently with other neurons in *A* and send a single longer 'commissural' connection to the region in which the *B* neurons are located, with a relatively small penalty in terms of volume, and then make the necessary connections within *B*. At the opposite extreme, neurons *A* and *B* could be interspersed: this would lengthen the connections made between neurons of the same type, since each would be, on average, further apart, but commissural connections would no longer be necessary. It is straightforward to see that the first solution is best if *A* and *B* are weakly, or not at all connected, while the second solution will be best if set *A* connects only with *B*, and *vice versa*, and not with members of itself. More interesting, however, is the existence of intermediate cases, in which the most favourable arrangement is a set of alternating stripes of *A* and *B*. Mitchison shows that there are certain requirements for this: one is that when axons branch, the diameter of each branch should not be much less than that of the parent axon; another is that axons should connect sites efficiently (Mitchison assumed 'minimal spanning trees').

Although none of the preceding arguments constitutes proof, they are all consistent with the idea that retinotopic maps, ocular dominance and other types of functional segregation, are, at least in part, the outcome of an evolutionary process in which developmental mechanisms leading to shorter wiring had a functional advantage. Demonstrations of this which go beyond plausibility may be almost impossible to obtain however, given the complexity of the variables that combine to determine wiring length and volume, and the need to decide on the functional 'penalty' or cost function to assign to these parameters. Models which explicitly minimize wirelength (see e.g. Todorov *et al* (1995)), as well as better definitions of wirelength, may not in the end be all that useful, because (as pointed out by Durbin and Mitchison (1990)) it is unlikely that developmental mechanisms explicitly minimize wirelength in any case: evolution may simply have selected mechanisms which, like the elastic net and related algorithms, produce reasonably good solutions to the problem.

12. Evaluation of assumptions common to most models

A common set of simplifying assumptions underlies most of the models discussed here. Although these will be evaluated more or less critically, it should be remembered that simplification is a necessary ingredient of any model and is often desirable, notwithstanding the probability of criticism on the grounds of unrealism.

12.1. Patterned retinal activity

In evaluating the types of retinal activity that ought to be included in a model, it should be remembered that the basic forms of stimulus specificity (localized receptive fields, orientation specificity and eye preference) and their accompanying topography are all capable of forming in the absence of visual stimulation, although the effects of visually driven inputs after eye opening are almost certain to be important as well. None of the models discussed here deals with this situation in a satisfactory manner, although models

which include both pre- and postnatal patterns of retinal activity are beginning to appear (Berns *et al* 1993, Olshausen and Field 1995). One difficulty is the limited amount of relevant physiological data (Mastrorarde 1983, Galli and Maffei 1988, Meister *et al* 1991, Wong *et al* 1993) which is all from subprimate species. It would be extremely useful to know what patterns of retinal activity are present prenatally and in darkness postnatally in primates, but finding this out is likely to be very difficult.

12.2. Hebb synapses

There is an overwhelming amount of circumstantial evidence for Hebbian synapses of some kind in the visual cortex (reviewed by Constantine-Paton *et al* 1990, Rauschecker 1991, Friedlander *et al* 1993). There is a small amount of direct evidence (Frégnac *et al* 1988, 1992, 1994, Greuel *et al* 1988) showing that stimulation of afferent pathways to a cell in combination with depolarization of the cell will lead to strengthening of the effects of afferent stimulation alone. However, there are still rather few data that would support a choice between different candidate varieties (see Brown *et al* 1990) of Hebbian modification rules. As mentioned above, there is evidence (Kossel *et al* 1990) for the local propagation of Hebbian strengthening through the cortex, as required by volume learning and by competitive Hebbian models. There is also evidence (Reiter and Stryker 1988) for Hebbian weakening of connections which has not been incorporated into most Hebbian models. Uncertainty about the nature of Hebbian modification in the developing visual cortex is arguably the weakest component of most models.

12.3. Radially symmetric, short-range excitatory and long-range inhibitory lateral cortical connections

This is an almost universal ingredient, but is surprisingly difficult to support with physiological or anatomical data. It is well known that lateral connections in the visual cortex are not uniform but patchy and extend over distances of several millimetres (Gilbert and Wiesel 1979, Rockland and Lund 1983, Livingstone and Hubel 1984b). They are often anisotropic in their spread (Luhmann *et al* 1986, Matsubara *et al* 1987, Fitzpatrick *et al* 1993, Yoshioka *et al* 1996). In cats, the pattern of lateral connections is diffuse and extensive in early postnatal life (Callaway and Katz 1990) and connections are selectively eliminated to form patches in an activity-dependent fashion (Luhmann *et al* 1986, Callaway and Katz 1991, Löwel and Singer 1992). The connections which extend furthest are probably mostly excitatory (McGuire *et al* 1991, Hirsch and Gilbert 1991, Kisvárdy and Eysel 1992) and link columns with similar orientation preferences (Gilbert and Wiesel 1989); in contrast, the axons of inhibitory neurons travel shorter distances of up to a millimetre (Kisvárdy 1992). The models can only be made to fit into the framework of these findings if it is assumed that the long-range excitatory connections do not play a major role in the development of topography and that a second distinct set of short-range ($< 200 \mu\text{m}$) excitatory connections is present. Physiological experiments in cat visual cortex which examined the patterns of spike correlation between pairs of neurons at various distances apart (Hata *et al* 1991) showed that excitatory connections were more common between cells $< 400 \mu\text{m}$ apart, but did not provide convincing evidence that inhibitory interactions were more common for larger separations (figure 7 in Hata *et al* 1991). It is also an open question as to whether the very weak interactions shown by Hata *et al*, and by other cross-correlation studies, are as strong as is required by most models. Whatever the answers to these questions, it seems *a priori* likely that present assumptions (the model of Sirosh and Miikkulainen (1994, 1995) is

an exception) about fixed and radially symmetric lateral cortical interactions will eventually turn out to be only crude approximations to the truth. On the other hand, lateral interactions mediated by the extracellular diffusion of chemical messengers might satisfy this condition reasonably well.

12.4. Normalization of input strengths

Although there is no doubt that there must be upper limits on such things as the total number of connections received by each neuron, the total number of synapses per axon, the total number of synapses per unit area (or volume) of cortex and the maximum strength of an individual synapse, the factors determining the actual values of these parameters in the brain are likely to be diverse and it is possible that none of these upper limits is ever actually reached. Nevertheless, most models impose at least some of them quite rigidly. A common technique is to maintain the sum of input strengths constant for each postsynaptic neuron, but it has not yet been shown experimentally that increasing the strength of one set of connections to a neuron leads to a simultaneous weakening of other connections to the same neuron, nor has a cellular mechanism for such an interaction been demonstrated. Another technique, conservation of the total synaptic strength per axonal arbor, can be supported experimentally, as there is evidence that removal of synapses from one part of an axon can result in an increased density of innervation elsewhere (Pockett and Slack 1982, Sabel and Schneider 1988). But the effects of monocular deprivation clearly show that individual axons have the capacity to form either more or less than their usual number of connections in different circumstances, which means that it is inappropriate to enforce axonal conservation as a rigid constraint. In addition, overall synaptic density increases substantially during the periods of ocular dominance and orientation column formation (Cragg 1975, Rakic *et al* 1986). With the exception of an upper or lower limit on the strength of individual connections, most other constraints are, in effect, lateral interactions occurring over distances equal to the spread of either individual axons or the dendrites of individual neurons. If implemented as such, they do not need to be enforced rigidly.

A similar criticism of the use of normalization rules has recently been made by Elliott *et al* (1996a, b, c) who describe them as 'an unsatisfactory mathematical trick' and suggest an alternative, and more flexible, type of rule based on competition for neurotrophins.

13. Overall evaluation of the different models

13.1. Ocular dominance models

The majority of models proposed for ocular dominance column formation (table 2) produce acceptably realistic branching stripes, so that further differentiation between models on the basis of their stripe morphology alone may not be very useful, unless quantitative morphological indices can be found that are able to differentiate between patterns that are visually similar. As reviewed above, however, there is a considerable between-species variability in the segregation pattern of columns, ranging from no segregation, transient segregation, rather irregularly spaced spots and patches with overlap at the boundaries (in the cat), to the industry standard striped pattern with strongly parallel bands and sharp boundaries found in the macaque monkey. The extent to which the different models can cope with this range of variability has not, for the most part, been tested, although it is suggested above that Swindale's (1980) model can accommodate much of it, while some authors (see e.g. Tanaka 1991a, b, Jones *et al* 1991) have applied their models specifically

to the issue of morphological variability.

Most of the models manage to explain the effects of monocular deprivation in reasonably satisfactory ways. However, no explanation has yet been given for the different effects of binocular visual deprivation in area 17 of the cat, where segregation is impaired, and the apparent lack of effect of it in area 18 of the same species, and in area 17 of the macaque monkey—perhaps because the results from the cat are not universally accepted. While the model of Goodhill (1993) is able to account for the effect of strabismus on the spacing of the columns, the models of Miller *et al* (1989) and Tanaka (1991) probably cannot, because column spacing in these models is determined by intracortical interactions, rather than by intraocular correlations in neural activity. Models based on Hebbian rules which permit only strengthening of synaptic inputs (see e.g. von der Malsburg (1973), Miller *et al* (1989), Goodhill (1993)) cannot explain the results of experiments (Reiter and Stryker 1988) in which the GABA agonist muscimol is infused into the cortex while the animal is monocularly deprived. This leads to a shift in the ocular dominance histogram in favour of the deprived eye. This result suggests a modification of Hebbian rules (see section 2.4.6), which might be worth incorporating into future models.

No attempt has been made to explain the apparent indifference of ocular dominance stripes to the perturbation introduced by the optic disc representation (e.g. figure 2). It might be illuminating to try to model this ‘natural experiment’.

13.2. Orientation column models

There is good agreement among experimenters about the general properties of orientation columns in cat and macaque monkey visual cortices (summarized in table 1) and these properties provide a good basis for judging orientation column models. A number of suggested arrangements, including all those not based explicitly on developmental hypotheses (Hubel and Wiesel 1977, Braitenberg and Braitenberg 1979, Soodak 1987, Götz 1987, 1988, Rojer and Schwartz 1990) have turned out to be incorrect, although partial confirmation might be claimed for some of them. The earliest neural network model proposed to account for the layout of orientation columns (von der Malsburg 1973) was too small to permit a detailed comparison with the experimental data obtained many years later, but it is possible that a larger version would produce realistic results. More recent neural net models have had mixed success: the models of Linsker (1986c) and Miller (1992b, 1994) generate superficially realistic patterns containing half-rotation singularities, but the domains for a given orientation show a strong tendency to run either parallel (Linsker) or orthogonal (Miller) to the direction of the orientation as projected in retinotopic coordinates onto the surface of the cortex. This type of relationship is not observed experimentally (Erwin *et al* 1995). The models of Swindale (1982a, 1992a), Obermayer *et al* (1990, 1991, 1992a, b), Durbin and Mitchison (1990), Tanaka (1990), Miyashita and Tanaka (1992) and Grossberg and Olson (1994) produce orientation maps that have not yet been shown to differ from real maps in any significant detail. This list includes models based on competitive and non-competitive Hebbian mechanisms, as well as the elastic net and low-dimensional Kohonen algorithm.

Many of the models (see e.g. von der Malsburg (1973), Durbin and Mitchison (1990), Obermayer *et al* (1990, 1991, 1992a, b), Tanaka (1990), Miyashita and Tanaka (1992)) assume, either explicitly or implicitly, the existence of oriented patterns of retinal activity. This is a critical detail because it is still an open question as to whether the patterns of activity that are present before the time of eye opening in cats and monkeys have the required properties for the models to work. For this reason, Linsker’s and Miller’s models

are valuable because they show that there are conditions in which radially symmetric patterns of spontaneous activity might, through a symmetry-breaking process, drive the formation of oriented receptive fields.

Finally, while ocular dominance is a property which can very probably be adequately explained as the result of the anatomical distribution of left- and right-eye inputs, orientation selectivity is probably much more complicated. Very few structural correlates of orientation preference have been discovered[†] and the connectivity patterns that might give rise to orientation selectivity are still largely a matter for speculation. Most of the models discussed here assume that the major determinant of preference is the pattern of convergence of geniculate afferents (with perhaps some additional effects provided by radially symmetric Mexican hat lateral interactions within the cortex). However, other factors will probably have to be taken into account. These include antagonism between ON and OFF centre afferents, inhibitory and feedback pathways and lateral cortical interactions that are more complicated than the Mexican hat model (Pei *et al* 1994, Volgushev *et al* 1995). A number of models, exploring how some of these factors might contribute to the response properties of individual neurons, have recently been proposed (see e.g. Heeger (1992), Somers *et al* (1995)). It is likely that realistic models of orientation column structure will eventually have to take into account circuitry that is more complex than simple convergence of geniculate axons onto single cells.

13.3. Combined models of orientation, ocular dominance and retinotopy

The only models developed so far that deal successfully with all three properties are based on either the elastic net or the Kohonen approaches (Obermayer *et al* 1991, 1992a, b, Erwin *et al* 1995). These alternatives appear to perform equally well in respect of the separate retinal, orientation and ocular dominance maps and they reproduce the known structural relations between orientation and ocular dominance. The success of these models is impressive, given their underlying simplicity. There may be few other areas of neurobiology where a relatively straightforward mathematical procedure has been able to accurately reproduce such an apparently complex set of data. The success of the models will be further enhanced if the predicted inverse relation between orientation gradient magnitude and retinal magnification factor can be confirmed; it will be puzzling, in fact, if it is not.

13.4. Competitive Hebbian models versus linear Hebbian models

The Hebbian rules used in the models discussed here fall into two main classes: competitive (see e.g. Durbin and Mitchison (1990), Obermayer *et al* (1990), Goodhill, (1993)) and non-competitive[‡] (see e.g. Linsker (1986a), Miller *et al* (1989), Tanaka (1989)). The mechanisms implied by each are quite distinct. In the non-competitive models, the learning rule is local and the strengths of individual synapses change purely on the basis of their correlation with their postsynaptic cell. Changes are assumed to be slow and governed in a linear way by the time-averaged statistics of the input firing patterns. Competitive Hebbian mechanisms increment the strengths of all the connections in the vicinity of the cortical cell which is firing most strongly in response to a stimulus. Because of the nonlinear nature of this

[†] One recent finding is that in the tree shrew, intracortical connections extend furthest in directions in the cortex which correspond to the orientation preference of the cell as projected onto the retinotopic map (Fitzpatrick *et al* 1993). This result may turn out to be true for other species as well, once local anisotropies in retinal magnification factor are taken into account.

[‡] These terms are less than ideal because all the models implement mechanisms that are competitive in one way or another.

selection process, it is not possible to average over repeated stimulus presentations and stimuli have to be presented one at a time to the network while it learns. The mechanism for the local strengthening (Kohonen 1993) might involve the release and lateral diffusion of one or more 'modification inducing substances' triggered in an all-or-none fashion by suprathreshold activity in a set of strongly responding neurons.

Judged by results, competitive Hebbian models seem to perform somewhat better than non-competitive ones, although it is not improbable that equally good non-competitive models may be devised in future. Although there is experimental evidence (reviewed in sections 8.2 and 10.2) suggestive of the existence of a diffusive extracellular signal like that implied by the Kohonen model, this evidence is, so far, equally consistent with the volume learning hypothesis proposed by Montague *et al* (1991): in the latter case, the relevant signal is presumed to be released in amounts linearly proportional to postsynaptic activity, rather than in a nonlinear, all-or-none fashion.

14. Comments on the field as a whole

14.1. How similar are the different models?

As pointed out by several authors (see e.g. Niebuhr and Wörgötter (1993), Grossberg and Olson (1994), Erwin *et al* (1995)) almost all models of visual cortex organization implement, in one way or another, two conflicting constraints: continuity and completeness. Analogous terms with essentially similar interpretations, such as coverage (Swindale 1991), feature normalization (Grossberg and Olson 1994), far-field diversity and near-field conformity (Götz 1988), and so forth, have also been used. In most models, continuity is imposed by assuming lateral excitatory connections between cortical neurons, fixed local axonal arbors, or lateral diffusion of chemical messengers. Completeness is attained in most models by presenting them with enough stimuli, and also indirectly by the use of normalization rules and/or lateral inhibition. Because they are very general in nature, continuity and completeness constraints can be implemented in many different ways and this is undoubtedly one of the reasons for the plethora of successful models.

The models should not, however, be dismissed as merely superficial variations on a common theme, although that may, by now, seem tempting. First, even if the continuity and completeness constraints can be applied in a relatively 'pure' form in a model (this is perhaps most obvious in the elastic net formulation discussed in section 11.2), questions remain, such as what determines the relative importance of continuity versus completeness and how to perform the optimization. This latter issue may be non-trivial because, for problems of this complexity, no practical method exists which is able to find the single optimal solution. This may not be a disadvantage because it is unlikely that the cortex will achieve the optimum solution in any case. But it then becomes important to consider the variety of near-optimal solutions which may exist and the possibility that these do not all resemble the cortex, in spite of yielding similar energy or cost values. If this is so, then even if the different models can be shown to be related, in the sense that they minimize the same things, the ways in which they perform the minimization may be significant: different algorithms (or developmental mechanisms) may leave their own signature on the final patterns they produce, even if, from a computational perspective, they are doing the same thing. This could provide a further basis for distinguishing between models that otherwise might seem to be equivalent. A somewhat more obvious, and related, requirement, is that the intermediate stages of the models should resemble those of real development. In other words, models may be differentiable, even in cases when they implement similar

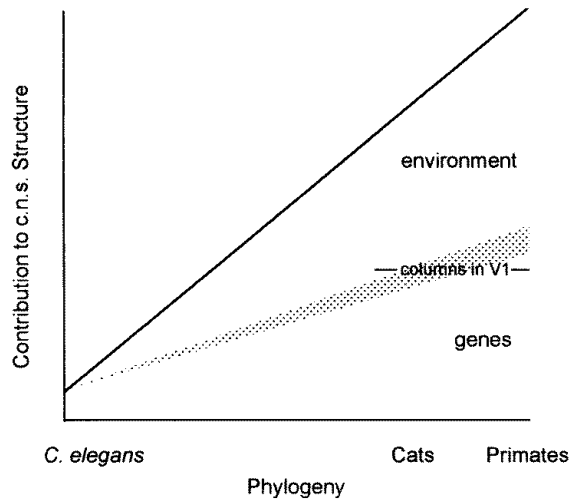


Figure 17. A diagram illustrating the concepts of complementarity and anticipation. The shaded region indicates the presence of a smooth transition between genetic and environmental contributions to central nervous system structure: close to the boundary (shaded region), both mechanisms may be capable of determining certain structures and it may be hard to distinguish between them. As one ascends the phylogenetic scale, genetic mechanisms are increasingly able to determine structure, because they are able to anticipate the consequences of learning which would otherwise occur later in development. (Mechanisms that utilize spontaneous neural activity are defined here as genetic: their operation is regarded as, in principle, different from those that rely upon environmentally driven neural activity, even though, in practice, the actual machinery might be similar, or even identical.)

principles and approach similar end points.

The mathematical analyses of models performed by Yuille *et al* (1991) and Mitchison (1995) are for the most part demonstrations of similarity, rather than formal proofs of equivalence. This, and the preceding arguments, suggest why, even if many of the models are formally similar, they are not identical and do not all make the same predictions. Even the two which seem most likely to be related, the elastic net, and low-dimensional Kohonen algorithms, behave differently when, for example, they are presented with non-uniform stimulus distributions. Thus, while it is clearly important to draw attention to and to explore the formal similarities between models, it may also be illuminating to concentrate on the differences between them, since this process is more likely to lead to useful experimental tests.

14.2. Complementarity and anticipation

While not all the models are the same, it is clearly the case that many of them can be implemented in different ways, e.g. by mechanisms based on chemical diffusion, spontaneous activity and visually driven neural activity. It may be significant that these biologically distinct mechanisms can lead to similar end results. Development of the brain proceeds through a variety of stages in which the earliest events are programmed at the genetic level, while later ones are increasingly a function of neural activity, at first spontaneous in origin and finally resulting from environmental stimulation. An analogous

progression occurs in phylogeny, with the connections in the simplest nervous systems being almost completely specified genetically (e.g. in *C. elegans*) while in the most complex, genetic information is clearly inadequate as a means of specifying all the connections. Successful development of the cortex in individual animals may require a smooth transition between these stages and this may be simpler if genetic and neural activity based mechanisms behave similarly and can coexist. The possible existence of such a ‘complementarity principle’ (analogous to Bohr’s principle that quantum and classical mechanics should blend smoothly at intermediate size scales) was suggested by Grossberg (1976) and a related idea has been discussed by Kandel and O’Dell (1992). It means that a biologically realistic model of visual cortex development may have to incorporate many different mechanisms. The awkwardness of this, from a practical standpoint, and the difficulties it poses for getting a realistic model right in the long run, should not hide the interest of the underlying reasons for it.

Complementarity may confer another advantage. Other things being equal, it is probably better for an organism if the connections in its nervous system can be specified genetically, rather than environmentally: genetic (or epi-genetic mechanisms utilizing spontaneous neural activity patterns) may be more reliable, and the necessary connections can be made before birth, giving the animal an advantage—providing of course that genetic mechanisms can reliably anticipate the patterns of natural stimulation that will occur later. This is very likely to be the case for V1 development, since the low-level visual features that are represented in V1 topographic maps are dependable properties of the world. In such circumstances, there may be an evolutionary pressure for genetic mechanisms to take over, or anticipate, what might later have been achieved by environmentally driven patterns of neural activity. Thus, homologous neural structures (e.g. area 17 in cats and monkeys) are more likely to be genetically determined in the phylogenetically more advanced species. Figure 17 attempts a visual representation of these ideas. They may explain some of the species variability, e.g. between cats and monkeys, which has bedevilled attempts to disentangle genetic and environmental contributions to the early development of topography in the striate cortex.

15. Future directions

15.1. Questions for experimenters

- What are the pre- and postnatal temporal and spatial dynamics of spontaneous and visually driven activity in retino-geniculate and geniculo-cortical afferents?
- What are the temporal dynamics of axonal and dendritic growth and of synapse formation in early cortical development? How do growing axons behave and what are the chemical and electrical signals to which they respond?
- When a connection between an axon and a cell is removed, or strengthened, what happens (i) to the other connections to the cell, (ii) to other connections made by the axon?
- What kind of topology, if any, is present in the distribution of axonal inputs within the dendritic arborization of individual neurons?
- How accurate is the retinal topography at the time when axons leave the subplate and invade the cortex?
- How accurate is retinal topography at the stage when ocular dominance and orientation columns begin to emerge?

- Is retinal magnification factor locally uniform in the visual cortex? If not, is there a correlation between orientation gradient and retinal magnification factor?
- Please provide a ‘movie’ of columnar structures forming in young animals, or a description as close to a movie as possible!
- Is there a systematic variation in the spatial phase of simple cell receptive fields with tangential position in the cortex?
- Please continue to provide detailed quantitative information on the effects of different manipulations of the visual environment on columnar periodicity and structure!

15.2. Suggestions for modellers

- Include receptive field scatter and the point image; this will mean modelling several cortical units at each location rather than just one.
- Include intracortical synaptic modification rules, including modification of inhibitory synapses.
- Include patterns of retinal activation likely to exist pre- and postnatally, if necessary as separate pre- and postnatal phases.
- Include stimulus properties, additional to the three discussed here, which appear to have orderly columnar representations in the cortex, e.g. spatial frequency and colour in the macaque and direction preference in the cat: the latter will require one to address the problem of temporal dynamics of the correlations in retinal activity patterns.
- Take into account the fact that connections are made, at least initially, by axons branching and growing in response to directional cues, e.g. chemical concentration gradients (Gierer 1987). Directed sprouting and axonal growth are almost certainly important components of early neural development and may also be important at later stages.
- Do not ignore the fact that neurons have dendrites: although the dendritic fields of many cells are extremely restricted in the tangential direction (i.e. a radius $\leq 100 \mu\text{m}$), and axons do, in general, extend over much larger distances, there is an increasing amount of evidence for activity-dependent plasticity of dendrites (e.g. Bodnarenko and Chalupa (1993), McAllister *et al* (1995)); furthermore, the dendrites of some cells extend over distances that can be significant (e.g. $> 100 \mu\text{m}$) on the scale of column structure.
- Do not incorporate normalization constraints rigidly: instead incorporate them into an overall description of pre- and postsynaptic trophic factors controlling the growth and survival of axonal connections.
- The continuity constraint has proved powerful in explaining much of visual cortex structure, but more work needs to be done to explain why continuity might be important biologically. Explanation in terms of economy of wiring might not always be correct, e.g. some types of computation might involve shorter wiring if cell types with different receptive field properties are close together. It remains to be shown that the wiring involved in generating orientation selectivity (which is at present unknown) is minimized by the known pattern of columns.
- Remove as much detail as possible from your model, without reducing its descriptive scope.

16. General conclusions

Many aspects of visual cortex topography, including the patterns of ocular dominance and orientation columns, can be satisfactorily explained as the outcome of a self-organizing process in which most of the initial conditions are random, and in which Hebbian learning mechanisms and cortical interactions with laterally excitatory and inhibitory components enforce local continuity and global completeness on the resulting topographic maps. Many models incorporating these basic assumptions have been proposed and the best of them are capable of generating patterns of retinal topography, eye dominance and orientation selectivity which do not differ from the experimental data from macaque monkey in any currently known detail.

Further progress in the field will depend upon:

- (i) obtaining more complete and accurate data sets from the macaque and other species;
- (ii) developing new ways of describing cortical structures quantitatively, so that more detailed comparisons between model output and data can be made;
- (iii) revising and extending the models to incorporate knowledge, or experimentally inspired ideas, about the multiple factors that determine the growth of axons, dendrites and synapses in the cortex; and
- (iv) demonstrating that the models can satisfactorily explain experimental data on inter-species variability and the effects of environmental manipulation during development.

Extension of the models to the description of different types of surface maps of response properties currently being revealed in cortical areas such as V2 (Roe and Ts'o 1995, Gegenfurtner *et al* 1996), MT (Malonek *et al* 1994) and infero-temporal cortex (Fujita *et al* 1992) promises to provide a major and rewarding challenge to theoreticians.

Acknowledgments

I thank Geoff Goodhill, Graeme Mitchison and Ken Miller for reading and commenting on the manuscript: I nevertheless take responsibility for the remaining errors of fact and interpretation and will be grateful if readers take the trouble to point these out to me. I also thank Klaus Obermayer, Terry Elliott and Geoff Goodhill for sending unpublished manuscripts and Klaus Obermayer for providing figures 3 and 15. This work was supported by grants from the Canadian Medical Research Foundation and the Natural Sciences and Engineering Research Council of Canada.

References

- Albus K 1975a A quantitative study of the projection area of the central and paracentral visual field in area 17 of the cat. I. The precision of the topography *Exp. Brain Res.* **24** 159–79
- 1975b A quantitative study of the projection area of the central and paracentral visual field in area 17 of the cat. II. The spatial organization of the orientation domain *Exp. Brain Res.* **24** 181–202
- 1979 14C-Deoxyglucose mapping of orientation subunits in the cat's visual cortical areas *Exp. Brain Res.* **37** 609–13
- Albus K and Wolf W 1984 Early post-natal development of neuronal function in the kitten's visual cortex: a laminar analysis *J. Physiol. (Lond.)* **348** 153–85
- Allendoerfer K L and Shatz C J 1994 The subplate, a transient neocortical structure: its role in the development of connections between thalamus and cortex *Ann. Rev. Neurosci.* **17** 185–218

- Anderson J A 1995 *An Introduction to Neural Networks* (Cambridge, MA: MIT Press)
- Anderson P A, Olavarria J and Van Sluyters R C 1988 The overall pattern of ocular dominance bands in cat visual cortex *J. Neurosci.* **8** 2183–200
- Arnett D W 1978 Statistical dependence between neighbouring retinal ganglion cells in goldfish *Exp. Brain Res.* **32** 49–53
- Arnett D W and Spraker T E 1981 Cross-correlation analysis of the maintained discharge of rabbit retinal ganglion cells *J. Physiol. (Lond.)* **317** 29–47
- Baddeley R J and Hancock P J 1991 A statistical analysis of natural images matches psychophysically derived orientation tuning curves *Proc. R. Soc. B* **246** 219–23
- Baier H and Bonhoeffer F 1994 Attractive axon guidance molecules *Science* **265** 1541–2
- Barlow H B 1959 Sensory mechanisms, the reduction of redundancy, and intelligence *NPL Symp. No 10, The Mechanisation of Thought Processes* (London: HMSO)
- 1975 Visual experience and cortical development *Nature* **258** 199–204
- 1986 Why have multiple cortical areas? *Vision Res.* **26** 81–90
- 1989 Unsupervised learning *Neural Comput.* **1** 295–311
- Barlow H B and Pettigrew J D 1971 Lack of specificity of neurones in the visual cortex of young kittens *J. Physiol. (Lond.)* **218** 98–100
- Barrow H G 1987 Learning receptive fields *Proc. IEEE 1st Int. Conf. on Neural Networks* vol IV, pp 115–21
- Barrow H G and Bray A J 1992 An adaptive neural model of early visual processing *Artificial Neural Networks II: Proc. Int. Conf. on Artificial Neural Networks* ed I Aleksander and J Taylor (Amsterdam: Elsevier) ch 26
- Bates K, Goodhill G J, Assad J and Montague P R 1995 A theoretical study of the influence of correlated activity on the global structure of ocular dominance stripes *Soc. Neurosci. Abstr.* **21** 392
- Bear M F, Kleinschmidt A, Gu Q and Singer W 1990 Disruption of experience-dependent synaptic modifications in striate cortex by infusion of an NMDA receptor antagonist *J. Neurosci.* **10** 909–25
- Bear M F and Singer W 1986 Modulation of visual cortical plasticity by acetylcholine and noradrenaline *Nature* **320** 172–6
- Berns G S, Dayan P S and Sejnowski T J 1993 A correlational model for the development of disparity selectivity in visual cortex that depends on prenatal and postnatal phases *Proc. Natl Acad. Sci. USA* **90** 8277–81
- Bienenstock E L, Cooper L N and Munro P W 1982 Theory for the development of neuron selectivity: orientation specificity and binocular interaction in visual cortex *J. Neurosci.* **2** 32–48
- Blakemore C 1978 Maturation and modification in the developing visual system *Handbook of Sensory Physiology vol VIII: Perception* ed R Held *et al* (Berlin: Springer) pp 377–436
- Blakemore C and Cooper G F 1970 Development of the brain depends on the visual environment *Nature* **228** 477–8
- Blakemore C and Van Sluyters R C 1975 Innate and environmental factors in the development of the kitten's visual cortex *J. Physiol. (Lond.)* **248** 663–716
- Blasdel G G 1992a Orientation selectivity, preference, and continuity in monkey striate cortex *J. Neurosci.* **12** 3139–61
- 1992b Differential imaging of ocular dominance and orientation selectivity in monkey striate cortex *J. Neurosci.* **12** 3115–38
- Blasdel G G and Fitzpatrick D 1984 Physiological organization of layer 4 in macaque striate cortex *J. Neurosci.* **4** 880–95
- Blasdel G and Obermayer K 1994 Putative strategies of scene segmentation in monkey visual cortex *Neural Networks* **7** 865–81
- Blasdel G G, Obermayer K and Kiorpes L 1995 Organisation of ocular dominance and orientation columns in the striate cortex of neonatal macaque monkeys *Vis. Neurosci.* **12** 589–603
- Blasdel G G and Salama G 1986 Voltage sensitive dyes reveal a modular organization in monkey striate cortex *Nature* **321** 579–85
- Bodnarenko S R and Chalupa L M 1993 Stratification of ON and OFF ganglion cell dendrites depends on glutamate-mediated afferent activity in the developing retina *Nature* **364** 144–6
- Bonhoeffer T and Grinvald A 1991 Orientation columns in cat are organized in pin-wheel like patterns *Nature* **353** 429–31
- Bonhoeffer T, Staiger V and Aertsen A 1989 Synaptic plasticity in rat hippocampal slice cultures: local 'Hebbian' conjunction of pre- and postsynaptic stimulation leads to distributed synaptic enhancement *Proc. Natl Acad. Sci. USA* **86** 8113–7

- Braitenberg V and Braitenberg C 1979 Geometry of orientation columns in the visual cortex *Biol. Cybern.* **33** 179–86
- Brown T H, Kairiss and Keenan C L 1990 Hebbian synapses: biophysical mechanisms and algorithms *Ann. Rev. Neurosci.* **13** 475–511
- Burgi P-Y and Grzywacz N M 1994 Model for the pharmacological basis of spontaneous synchronous activity in developing retinas *J. Neurosci.* **14** 7426–39
- Cabelli R J, Hohn A and Shatz C J 1995 Inhibition of ocular dominance column formation by infusion of NT-4/5 or BDNF *Science* **267** 1662–6
- Callaway E M and Katz L C 1990 Emergence and refinement of clustered horizontal connections in cat striate cortex *J. Neurosci.* **10** 1134–53
- 1991 Effects of binocular deprivation on the development of clustered horizontal connections in cat striate cortex *Proc. Natl Acad. Sci. USA* **88** 745–9
- 1992 Development of axonal arbors of layer 4 spiny neurons in cat striate cortex *J. Neurosci.* **12** 570–82
- Campbell D and Blasdel G 1995 Optical measurement of cortical magnification factors in New and Old World primates *Soc. Neurosci. Abstr.* **21** 771
- Casagrande V A and Harting J K 1975 Transneuronal transport of tritiated fucose and proline in the visual pathways of the tree shrew, *Tupaia glis*. *Brain Res.* **96** 367–72
- Changeux J P and Danchin A 1976 Selective stabilization of developing synapses as a mechanism for the specification of neuronal networks *Nature* **264** 705–12
- Chino Y M, Kaas J H, Smith E L, Langston A L and Cheng H 1992 Rapid reorganization of cortical maps in adult cats following restricted deafferentation in the retina *Vis. Res.* **32** 789–96
- Chun J J M and Shatz C J 1988 Distribution of synaptic vesicle antigens is correlated with the disappearance of a transient synaptic zone in the developing cerebral cortex *Neuron* **1** 297–310
- Conley M, Fitzpatrick D and Diamond I T 1984 The laminar organization of the lateral geniculate body and the striate cortex in the tree shrew (*Tupaia glis*) *J. Neurosci.* **4** 171–98
- Connolly M and Van Essen D 1984 The representation of the visual field in the parvocellular and magnocellular layers of the lateral geniculate nucleus in the macaque monkey *J. Comput. Neurol.* **226** 544–64
- Constantine-Paton M 1983 Position and proximity in the development of maps and stripes *Trends Neurosci.* **6** 32–6
- Constantine-Paton M, Cline H T and Debski E 1990 Patterned activity, synaptic convergence, and the NMDA receptor in developing visual pathways *Ann. Rev. Neurosci.* **13** 129–54
- Constantine-Paton M and Law M I 1978 Eye specific termination bands in tecta of three-eyed frogs *Science* **202** 639–41
- Cook J E 1987 A sharp retinal image increases the topographic precision of the goldfish retinotectal projection during optic nerve regeneration in stroboscopic light *Exp. Brain Res.* **68** 319–28
- Cook J E and Becker D L 1990 Spontaneous activity as a determinant of axonal connections *Euro. J. Neurosci.* **2** 162–9
- Cowey A 1979 Cortical maps and visual perception (The Grindley Memorial Lecture) *Q. J. Exp. Psychol.* **31** 1–17
- Cragg B G 1975 The development of synapses in the visual system of the cat *J. Comput. Neurol.* **160** 147–66
- Crick F H C 1970 Diffusion in embryogenesis *Nature* **225** 420–2
- Cynader M S, Swindale N V and Matsubara J A 1987 Functional topography in cat area 18 *J. Neurosci.* **7** 1401–13
- Das A, Crist R E and Gilbert C D 1995 Relationship between discontinuities in visuotopic and orientation maps in cat V1 *Soc. Neurosci. Abstr.* **21** 771
- Daugman J G 1989 Entropy reduction and decorrelation in visual coding by oriented neural receptive fields *IEEE Trans. Biomed. Engng.* **36** 107–14
- Dawson T M and Dawson V L 1995 Nitric oxide: actions and pathological roles *Neuroscientist* **1** 7–18
- Dawson T M and Snyder S H 1994 Gases as biological messengers: nitric oxide and carbon monoxide in the brain *J. Neurosci.* **14** 5147–59
- Dayan P 1993 Arbitrary elastic topologies and ocular dominance *Neural Comput.* **5** 392–401
- Dayan P S and Goodhill G J 1992 Perturbing Hebbian rules *Advances in Neural Information Processing Systems 4* ed J E Moody *et al* (San Mateo, CA: Morgan Kaufman) pp 19–26
- DeBruyn E J and Casagrande V A 1981 Demonstration of ocular dominance columns in a New World primate by means of monocular deprivation *Brain Res.* **207** 453–8
- Diao Y-C, Jia W, Swindale N V and Cynader M S 1990 Functional organization of the cortical 17/18 border region in the cat *Exp. Brain Res.* **79** 271–82

- Dow B M and Bauer R 1984 Retinotopy and orientation columns in the monkey: a new model *Biol. Cybern.* **49** 189–200
- Dow B M, Snyder A Z, Vautin R G and Bauer R 1981 Magnification factor and receptive field size in foveal striate cortex of the monkey *Exp. Brain Res.* **44** 213–28
- Dow B M, Vautin R G and Bauer R 1985 The mapping of visual space onto foveal striate cortex in the macaque monkey *J. Neurosci.* **5** 890–902
- Durbin R and Mitchison G 1990 A dimension reduction framework for understanding cortical maps *Nature* **343** 644–7
- Durbin R, Szeliski R and Yuille A L 1989 An analysis of the elastic net approach to the travelling salesman problem *Neural Comput.* **1** 348–58
- Durbin R and Willshaw D J 1987 An analogue approach to the travelling salesman problem using an elastic net method *Nature* **326** 689–691
- Easter S S Jr, Burrill J, Marcus R C, Ross L S and Taylor J S 1994 Initial tract formation in the vertebrate brain *Progr. Brain Res.* **102** 79–93
- Edwards D P and Kaplan E 1992 How sharp is the orientation tuning of single cells in the cytochrome oxidase blobs of primate visual cortex? *Invest. Ophthalmol. Vis. Sci. Suppl.* **33** 1255
- Elliott T, Howarth C I and Shadbolt N R 1996a Neural competition and statistical mechanics *Proc. R. Soc. B* (in press)
- 1996b Axonal processes and neural plasticity I: Ocular dominance columns *Cerebral Cortex* (in press)
- 1996c Axonal processes and neural plasticity III: Competition for dendrites *Cerebral Cortex* (submitted)
- Erwin E and Miller K D 1995 Correlation-based learning model of joint orientation and ocular dominance column formation *Soc. Neurosci. Abstr.* **21** 2025
- Erwin E, Obermayer K and Schulten K 1995 Models of orientation and ocular dominance columns in the visual cortex: a critical comparison *Neural Comput.* **7** 425–68
- Fawcett J W and Willshaw D J 1982 Compound eyes project stripes on the optic tectum of *Xenopus*, *Nature* **296** 350–2
- Fitzpatrick D, Zhang Y and Muly E C 1993 Orientation selectivity and the topographic organization of horizontal connections in striate cortex *Soc. Neurosci. Abstr.* **19** 424
- Florence S L, Conley M and Casagrande V A 1986 Ocular dominance columns and retinal projections in New World spider monkeys (*Ateles ater*) *J. Comput. Neurol.* **243** 234–8
- Florence S L and Kaas J H 1992 Ocular dominance columns in area 17 of Old World macaque and talapoin monkeys: complete reconstructions and quantitative analyses *Vis. Neurosci.* **8** 449–62
- Földiák P 1989 Adaptive network for optimal linear feature extraction *Proc. IEEE INNS Int. Joint Conf. on Neural Networks (Washington DC)* vol 1 pp 401–5
- Frégnac Y, Burke J P, Smith D and Friedlander M J 1994 Temporal covariance of pre- and post-synaptic activity regulates functional connectivity in the visual cortex *J. Neurophysiol.* **71** 1403–21
- Frégnac Y and Imbert M 1984 Development of neuronal selectivity in the primary visual cortex of the cat *Physiol. Rev.* **64** 325–434
- Frégnac Y, Shulz D, Thorpe S and Bienenstock E 1988 A cellular analogue of visual cortical plasticity *Nature* **333** 367–70
- 1992 Cellular analogs of visual cortical epigenesis. I. Plasticity of orientation selectivity *J. Neurosci.* **12** 1280–300
- Friauf E, McConnell S K and Shatz C J 1990 Functional synaptic circuits in the subplate during fetal and early postnatal development of cat visual cortex *J. Neurosci.* **10** 2601–13
- Friedlander M J, Frégnac Y and Burke J P 1993 Temporal covariance of postsynaptic membrane potential and synaptic input—role in synaptic efficacy in the visual cortex *Prog. Brain Res.* **95** 207–23
- Fujita I, Tanaka K, Ito M and Cheng K 1992 Columns for visual features of objects in monkey inferotemporal cortex *Nature* **360** 343–6
- Galli L and Maffei L 1988 Spontaneous impulse activity of rat retinal ganglion cells in prenatal life *Science* **242** 90–1
- Gally J A, Montague P R, Reeke G N and Edelman G M 1990 The NO hypothesis: possible effects of a rapidly diffusible substance in neural development and function *Proc. Natl Acad. Sci. USA* **87** 3547–51
- Gegenfurtner K R, Kiper D C and Fenstemaker S B 1996 Processing of colour, form, and motion in macaque area V2 *Vis. Neurosci.* **13** 161–72

- Ghosh A and Shatz C J 1992 Pathfinding and target selection by developing geniculocortical axons *J. Neurosci.* **12** 39–55
- 1994 Segregation of geniculocortical afferents during the critical period: a role for subplate neurons *J. Neurosci.* **14** 3862–80
- Gierer A 1987 Directional cues for growing axons forming the retinotectal projection *Development* **101** 479–89
- Gilbert C D and Wiesel T N 1979 Morphology and intracortical projections of functionally characterised neurones in the cat visual cortex *Nature* **280** 120–5
- 1989 Columnar specificity of intrinsic horizontal and corticocortical connections in cat visual cortex *J. Neurosci.* **9** 2432–42
- 1992 Receptive field dynamics in adult primary visual cortex *Nature* **356** 150–2
- Gödecke I and Bonhoeffer T 1996 Development of identical orientation maps for two eyes without common visual experience *Nature* **379** 251–4
- Goodhill G J 1992 Correlations, competition, and optimality: modelling the development of topography and ocular dominance *Cognitive Science Research Paper 226* University of Sussex, UK
- 1993 Topography and ocular dominance: a model exploring positive correlations *Biol. Cybern.* **69** 109–18
- Goodhill G J and Barrow H G 1994 The role of weight normalization in competitive learning *Neural Comput.* **6** 255–69
- Goodhill G J and Löwel S 1995 Theory meets experiment: correlated neural activity helps determine ocular dominance column periodicity *Trends Neurosci.* **18** 437–9
- Goodhill G J and Willshaw D J 1990 Application of the elastic net algorithm to the formation of ocular dominance stripes *Network: Comput. Neural Syst.* **1** 41–59
- 1994 Elastic net model of ocular dominance: overall stripe pattern and monocular deprivation *Neural Comput.* **6** 615–21
- Götz K G 1987 Do ‘d-Blob’ and ‘l-Blob’ hypercolumns tessellate the monkey visual cortex? *Biol. Cybern.* **56** 107–9
- 1988 Cortical templates for the self-organization of orientation-specific d- and l-hypercolumns in monkeys and cats *Biol. Cybern.* **58** 213–23
- Greuel J M, Luhmann H J, and Singer W 1988 Pharmacological induction of use-dependent receptive field modifications in the visual cortex *Science* **242** 74–7
- Grossberg S 1976 On the development of feature detectors in the visual cortex with application to learning and reaction-diffusion systems *Biol. Cybern.* **21** 145–59
- Grossberg S and Olson S J 1994 Rules for the cortical map of ocular dominance and orientation columns *Neural Networks* **7** 883–94
- Gu Q and Singer W 1993 Effects of intracortical infusion of anticholinergic drugs on neuronal plasticity in kitten striate cortex *Euro. J. Neurosci.* **5** 475–85
- 1995 Involvement of serotonin in developmental plasticity of kitten visual cortex *Euro. J. Neurosci.* **7** 1146–53
- Harris W A 1980 The effects of eliminating impulse activity on the development of the retinotectal projection in salamanders *J. Comput. Neurol.* **194** 303–17
- Hata Y, Tsumoto T, Sato H and Tamura H 1991 Horizontal interactions between visual cortical neurones studied by cross-correlation analysis in the cat *J. Physiol. (Lond.)* **441** 593–614
- Haykin S 1994 *Neural Networks: A Comprehensive Foundation* (IEEE Computer Society Press, Macmillan)
- Heeger D J 1992 Normalization of cell responses in cat striate cortex *Vis. Neurosci.* **9** 181–97
- Hendrickson A E, Hunt S P, and Wu J-Y 1981 Immunocytochemical localization of glutamic acid decarboxylase in monkey striate cortex *Nature* **292** 605–7
- Hendrickson A E, Wilson J R and Ogren M P 1978 The neuroanatomical organization of pathways between the dorsal lateral geniculate nucleus and visual cortex in Old World and New World primates *J. Comput. Neurol.* **182** 123–36
- Hertz J, Krogh A and Palmer R G 1991 *Introduction to the Theory of Neural Computation (Lecture Notes I, Santa Fe Institute Studies in the Science of Complexity)* (Reading, MA: Addison-Wesley)
- Hess D T and Edwards M A 1987 Anatomical demonstration of ocular segregation in the retinogeniculocortical pathway of the New World capuchin monkey (*Cebus apella*) *J. Comput. Neurol.* **264** 409–20
- Hesselroth T and Schulten K 1994 Receptive field and feature map formation in the primary visual cortex via Hebbian learning with inhibitory feedback *Beckman Institute Technical Report UIUC-BI-TB-94-14*
- Hetherington P A, Swindale N V and Zhao D 1995 Inter-ocular disparity and variation in receptive field position and orientation preference studied by tetrode recordings in cat area 17 *Soc. Neurosci. Abstr.* **21** 1649

- Hirsch J A and Gilbert C D 1991 Synaptic physiology of horizontal connections in the cat's visual cortex *J. Neurosci.* **11** 1800–9
- Hirsch H V B and Spinelli D N 1970 Visual experience modifies distribution of horizontal and vertical oriented receptive fields in cats *Science* **168** 869–71
- Hitchcock P F and Hickey T L 1980 Ocular dominance columns: evidence for their presence in humans *Brain Res.* **182** 176–9
- Hong X and Regan D 1989 Visual field defects for unidirectional and oscillatory motion in depth *Vision Res.* **29** 809–19
- Horner T J and Martin K A C 1978 Morphogenetics as an alternative to chemospecificity in the formation of nerve connections *Cell–Cell Recognition (32nd Symp. Soc. Exp. Biol.)* ed A S G Curtis (Cambridge: Cambridge University Press) pp 275–358
- Horton J C 1984 Cytochrome oxidase patches: a new cytoarchitectonic feature of monkey visual cortex *Phil. Trans. R. Soc. B* **304** 199–253
- Horton J C, Dagi L R, McCrane E P and de Monasterio F M 1990 Arrangement of ocular dominance columns in human visual cortex *Arch. Ophthalmol.* **108** 1025–31
- Horton J C and Hedley-White E T 1984 Mapping of cytochrome oxidase patches and ocular dominance columns in human visual cortex *Phil. Trans. R. Soc. B* **304** 255–72
- Horton J C and Hocking D R 1996 An adult-like pattern of ocular dominance columns in striate cortex of newborn monkeys prior to visual experience *J. Neurosci.* **16** 1791–807
- Horton J C and Hubel D H 1981 Regular patchy distribution of cytochrome oxidase staining in primary visual cortex of macaque monkey *Nature* **292** 762–4
- Hubel D H 1975 An autoradiographic study of the retinocortical projections in the tree shrew (*Tupaia glis*) *Brain Res.* **96** 41–50
- Hubel D H and Livingstone M S 1987 Segregation of form, color, and stereopsis in primate area 18 *J. Neurosci.* **7** 3378–413
- Hubel D H and Wiesel T N 1962 Receptive fields, binocular interaction, and functional architecture of cat striate cortex *J. Physiol. (Lond.)* **160** 106–54
- 1963 Receptive fields of cells in striate cortex of very young, visually inexperienced kittens *J. Neurophysiol.* **26** 994–1002
- 1968 Receptive fields and functional architecture of monkey striate cortex *J. Physiol. (Lond.)* **195** 215–43
- 1972 Laminar and columnar distribution of geniculocortical fibers in the macaque monkey *J. Comput. Neurol.* **146** 421–50
- 1974a Sequence regularity and geometry of orientation columns in the monkey striate cortex *J. Comput. Neurol.* **158** 267–94
- 1974b Uniformity of monkey striate cortex: a parallel relationship between field size, scatter and magnification factor *J. Comput. Neurol.* **158** 295–306
- 1977 Functional architecture of macaque monkey visual cortex *Proc. R. Soc. B* **198** 1–59
- Hubel D H, Wiesel T N and LeVay S 1974 Visual field of representation in layer IVc of monkey striate cortex *Soc. Neurosci. Abstr.* 4th Annual Meeting p 264
- 1977 Plasticity of ocular dominance columns in monkey striate cortex *Phil. Trans. R. Soc. B* **278** 131–63
- Hübener M, Shoham D, Grinvald A and Bonhoeffer T 1995 Spatial frequency, ocular dominance, and orientation maps and their relationship in kitten visual cortex *Soc. Neurosci. Abstr.* **21** 771
- Humphrey A L and Norton T T 1980 Topographic organisation of the orientation column system in the striate cortex of the tree shrew (*Tupaia glis*) I. Microelectrode recording *J. Comput. Neurol.* **192** 531–47
- Humphrey A L, Skeen L C and Norton T T 1980 Topographic organisation of the orientation column system in the striate cortex of the tree shrew (*Tupaia glis*) II. Deoxyglucose mapping *J. Comput. Neurol.* **192** 549–66
- Ide C R, Fraser S E and Meyer R L 1983 Eye dominance columns formed by an isogenic double nasal frog eye *Science* **221** 293–5
- Innocenti G M and Kaas J H 1995 The cortex *Trends Neurosci.* **18** 371–2
- Jiang B and Levi D M 1991 Spatial-interval discrimination in two dimensions: effect of eccentricity *Invest. Ophthalmol. Vis. Sci. Suppl.* **32** 1269
- Jones D G, Van Sluyters R C and Murphy K M 1991 A computational model for the overall pattern of ocular dominance *J. Neurosci.* **11** 3794–808
- Kaas J H, Lin C S and Casagrande V A 1976 The relay of ipsilateral and contralateral retinal input from the lateral geniculate nucleus to striate cortex in the owl monkey: a transneuronal transport study *Brain Res.* **106** 371–8

- Kalil R E 1982 Development of ocular dominance columns in cats reared with binocular deprivation or strabismus *Soc. Neurosci. Abstr.* **8** 4
- Kandel E R and O'Dell T J 1992 Are adult learning mechanisms also used for development? *Science* **258** 243–5
- Kim D-S and Bonhoeffer T 1993 Chronical observation of the emergence of iso-orientation domains in kitten visual cortex *Soc. Neurosci. Abstr.* **19** 1800
- Kisvárdy Z 1992 GABAergic networks of basket cells in the visual cortex *Progr. Brain Res.* **90** 385–405
- Kisvárdy Z and Eysel U T 1992 Cellular organization of reciprocal patchy networks in layer III of cat visual cortex (area 17) *Neurosci.* **46** 275–86
- Kleinschmidt A, Bear M F and Singer W 1987 Blockade of 'NMDA' receptors disrupts experience-dependent plasticity of kitten striate cortex *Science* **238** 355–8
- Kohonen T 1982 Self-organized formation of topologically correct feature maps *Biol. Cybern.* **43** 59–9
 —1988 *Self-organization and Associative Memory* 2nd edn (Berlin: Springer)
 —1993 Physiological interpretation of the self-organizing map algorithm *Neural Networks* **6** 895–905
- Kossel A, Bonhoeffer T and Bolz J 1990 Non-Hebbian synapses in rat visual cortex *NeuroReport* **1** 115–8
- Law M I, Zaks K R and Stryker M P 1988 Organization of primary visual cortex (area 17) in the ferret *J. Comput. Neurol.* **278** 157–80
- Lee B B, Albus K, Heggelund P, Hulme M J and Creutzfeldt O D 1977 The depth distribution of optimal stimulus orientations for neurons in cat area 17 *Exp. Brain Res.* **27** 301–14
- Lennie P, Krauskopf J and Sclar G 1990 Chromatic mechanisms in striate cortex of macaque *J. Neurosci.* **10** 649–69
- LeVay S, Connolly M, Houde J and Van Essen D C 1985 The complete pattern of ocular dominance stripes in the striate cortex and visual field of the macaque monkey *J. Neurosci.* **5** 486–501
- LeVay S, Stryker M P and Shatz C J 1978 Ocular dominance columns and their development in layer IV of the cat's visual cortex: a quantitative study *J. Comput. Neurol.* **179** 223–44
- LeVay S, Wiesel T N and Hubel D H 1980 The development of ocular dominance columns in normal and visually deprived monkeys *J. Comput. Neurol.* **191** 1–51
- Leventhal A G, Thompson K G, Liu D, Neuman L M and Ault S J 1993 Form and color are not segregated in monkey striate cortex *Invest. Ophthalmol. Vis. Sci. Suppl.* **34** 813
- Linsker R 1986a From basic network principles to neural architecture: emergence of spatial-opponent cells *Proc. Natl Acad. Sci. USA* **83** 7508–12
 —1986b From basic network principles to neural architecture: emergence of orientation selective cells *Proc. Natl Acad. Sci. USA* **83** 8390–4
 —1986c From basic network principles to neural architecture: emergence of orientation columns *Proc. Natl Acad. Sci. USA* **83** 8779–83
 —1988a Self-organization in a perceptual network *Computer* **21** 105–17
 —1988b Towards an organizing principle for a layered perceptual network *Advances in Neural Information Processing Systems (Denver, CO, 1987)* ed D Z Anderson (New York: AIP) pp 485–94
 —1988c Development of feature analyzing cells and their columnar organization in a layered self-adaptive network *Computer Simulation in Brain Science (Copenhagen, 1986)* ed R M J Cotterill (Cambridge: Cambridge University Press) pp 416–31
 —1989a An application of the principle of maximum information preservation to linear systems *Advances in Neural Information Processing Systems (Denver, CO, 1988)* ed D S Touretzky (San Mateo, CA: Morgan Kaufmann) pp 186–94
 —1989b How to generate ordered maps by maximizing the mutual information between input and output signals *Neural Comput.* **1** 402–11
 —1990 Perceptual neural organization: some approaches based on network models and information theory *Ann. Rev. Neurosci.* **13** 257–81
 —1992 Local synaptic learning rules suffice to maximize mutual information in a linear network *Neural Comput.* **4** 691–702
- Liu Z, Gaska J P, Jacobson L D and Pollen D A 1992 Interneuronal interaction between members of quadrature phase and anti-phase pairs in the cat's visual cortex *Vision Res.* **32** 1193–8
- Livingstone M S and Hubel D H 1984a Anatomy and physiology of a color system in the primate visual cortex *J. Neurosci.* **4** 309–56
 —1984b Specificity of intrinsic connections in primate primary visual cortex *J. Neurosci.* **4** 2830–5

- Livingstone M S, Nori S, Freeman D C and Hubel D H 1995 Stereopsis and binocularity in the squirrel monkey *Vision Res.* **35** 345–54
- Löwel S 1994 Ocular dominance column development: strabismus changes the spacing of adjacent columns in cat visual cortex *J. Neurosci.* **14** 7451–68
- Löwel S, Bischof H, Leutenecker B and Singer W 1988 Topographic relations between ocular dominance and orientation columns in the cat striate cortex *Exp. Brain Res.* **71** 33–46
- Löwel S, Freeman B and Singer W 1987 Topographic organisation of the orientation column system in large flat-mounts of the cat visual cortex: a 2-deoxyglucose study *J. Comput. Neurol.* **255** 401–15
- Löwel S and Singer W 1987 The pattern of ocular dominance columns in flat-mounts of the cat visual cortex *Exp. Brain Res.* **68** 661–6
- 1992 Selection of intrinsic horizontal connections in the visual cortex by correlated neuronal activity *Science* **255** 209–12
- Luhmann H J, Martínez Millán L and Singer W 1986 Development of horizontal intrinsic connections in cat striate cortex *Exp. Brain Res.* **63** 443–8
- Luttrell S P 1989 Self-organization: A derivation from first principles of a class of learning algorithms *Proc. 3rd IEEE Int. Joint Conf. on Neural Networks (Washington DC)* **2** 495–8
- 1990 Derivation of a class of training algorithms *IEEE Trans. Neural Networks* **1** 229–32
- MacKay D J C and Miller K D 1990a Analysis of Linsker's simulations of Hebbian rules *Neural Comput.* **2** 173–87
- 1990b Analysis of Linsker's application of Hebbian rules to linear networks *Network: Comput. Neural Sys.* **1** 257–97
- Malonek D, Tootell R B and Grinvald A 1994 Optical imaging reveals the functional architecture of neurons processing shape and motion in owl monkey area MT *Proc. R. Soc. B* **258** 109–19
- Marr D 1970 A theory for cerebral neocortex *Proc. R. Soc. B* **176** 161–234
- Mastrorade D N 1983 Correlated firing of cat retinal ganglion cells vol I. Spontaneously active inputs to X- and Y-cells *J. Neurophysiol.* **49** 303–24
- Matsubara J A, Cynader M S and Swindale N V 1987 Anatomical properties and physiological correlates of the intrinsic connections in cat area 18 *J. Neurosci.* **7** 1428–46
- McAllister A K, Lo D C and Katz L C 1995 Neurotrophins regulate dendritic growth in developing visual cortex *Neuron* **15** 791–803
- McConnell S K 1988 Development and decision-making in the mammalian cerebral cortex *Brain Res. Rev.* **13** 1–23
- McConnell S K and LeVay S 1984 Segregation of ON- and OFF-center afferents in mink visual cortex *Proc. Natl Acad. Sci. USA* **81** 1590–3
- McGuire B A, Gilbert C D, Rivlin P K and Wiesel T N 1991 Targets of horizontal connections in macaque primary visual cortex *J. Comput. Neurol.* **305** 370–92
- Meinhardt H 1982 *Models of Biological Pattern Formation* (New York: Academic)
- Meister M, Wong R O L, Baylor D A and Shatz C J 1991 Synchronous bursts of action potentials in ganglion cells of the developing mammalian retina *Science* **252** 939–43
- Miller K D 1990a Correlation-based mechanisms of neural development *Neuroscience and Connectionist Theory* ed M A Gluck and D E Rumelhart (Hillsdale, NJ: Lawrence Erlbaum) pp 267–353
- 1990b Derivation of Hebbian equations from a non-linear model *Neural Comput.* **2** 319–31
- 1992a Models of activity-dependent neural development *Seminars in the Neurosciences* **4** 61–73
- 1992b Development of orientation columns via competition between ON- and OFF-center inputs *NeuroReport* **3** 73–6
- 1994 A model for the development of simple cell receptive fields and the ordered arrangement of orientation columns through the activity dependent competition between ON- and OFF-center inputs *J. Neurosci.* **14** 409–41
- 1995 Receptive fields and maps in the visual cortex: models of ocular dominance and orientation columns *Models of Neural Networks III* ed E Domany *et al* (Berlin: Springer)
- Miller K D, Keller J B and Stryker M P 1989 Ocular dominance column development: analysis and simulation *Science* **245** 605–15
- Miller K D and MacKay D J C 1994 The role of constraints in Hebbian learning *Neural Comput.* **6** 100–126
- Miller K D and Stryker M P 1990 The development of ocular dominance columns: mechanisms and models *Connectionist Modelling and Brain Function: The Developing Interface* ed S J Hanson and C R Olson

- (Cambridge, MA: MIT Press) pp 255–305
- Mitchell D E and Timney B 1984 Postnatal development of function in the mammalian visual system *Handbook of Physiology – The Nervous System III* (Berlin: Springer) ch 12, pp 507–55
- Mitchison G 1991 Neuronal branching patterns and the economy of cortical wiring *Proc. R. Soc. B* **245** 151–8
- 1995 A type of duality between self-organizing maps and minimal wiring *Neural Comput.* **7** 25–35
- Mitchison G and Durbin R 1986 Optimal numberings of an $N \times N$ array *SIAM J. Alg. Disc. Meth.* **7** 571–81
- Miyashita M and Tanaka S 1992 A mathematical model for the self-organization of orientation columns in visual cortex *NeuroReport* **3** 69–72
- Molnár Z and Blakemore C 1995 How do thalamic axons find their way to the cortex? *Trends Neurosci.* **18** 389–97
- Montague P R, Gally J A and Edelman G M 1991 Spatial signalling in the development and function of neural connections *Cerebral Cortex* **1** 199–220
- Montague P R and Sejnowski T J 1994 The predictive brain: temporal coincidence and temporal order in synaptic learning mechanisms *Learning and Memory* **1** 1–33
- Mountcastle V B 1957 Modality and topographic properties of single neurons of cat's somatic sensory cortex *J. Neurophysiol.* **20** 408–34
- Movshon J A, Thompson I D and Tolhurst D J 1978 Spatial summation in the receptive fields of simple cells in the cat's striate cortex *J. Physiol.* **283** 53–77
- Movshon J A and Van Sluyters R C 1981 Visual neural development *Ann. Rev. Psychol.* **32** 477–522
- Mower G D, Caplan C J, Christen W G and Duffy F H 1985 Dark rearing prolongs physiological but not anatomical plasticity of the cat visual cortex *J. Comput. Neurol.* **235** 448–66
- Niebuhr E and Wörgötter F 1993 Orientation columns from first principles *Computation and Neural Systems* ed F H Eeckman and J M Bower (Dordrecht: Kluwer) ch 62, pp 409–13
- Obermayer K and Blasdel G G 1993 Geometry of orientation and ocular dominance columns in monkey striate cortex *J. Neurosci.* **13** 4114–29
- 1996 Singularities in primate orientation maps (submitted)
- Obermayer K, Blasdel G G and Schulten K 1991 A neural network model for the formation and for the spatial structure of retinotopic maps, orientation- and ocular dominance columns *Artificial Neural Networks* ed T Kohonen *et al* (Amsterdam: Elsevier) pp 505–11
- 1992a Statistical-mechanical analysis of self-organization and pattern formation during the development of visual maps *Phys. Rev. A* **45** 7568–89
- Obermayer K, Ritter H and Schulten K 1990 A principle for the formation of the spatial structure of cortical feature maps *Proc. Natl Acad. Sci. USA* **87** 8345–9
- 1992b A model for the development of the spatial structure of retinotopic maps and orientation columns *IEICE Trans. Fundamentals* **E75-A** 537–45
- O'Brien E V, Everson R and Kaplan E 1995 Luminance contrast gain, spatial and temporal frequency tuning in CO blobs and interblobs of mammalian striate cortex measured with intrinsic optical imaging *Soc. Neurosci. Abstr.* **21** 1753
- Oja E 1982 A simplified neuron model as a principal component analyzer *J. Math. Biol.* **15** 267–73
- O'Leary D D M 1989 Do cortical areas emerge from a proto-cortex? *Trends Neurosci.* **12** 400–6
- O'Leary D D M, Schlaggar B L and Tuttle R 1994 Specification of neocortical areas and thalamocortical connections *Ann. Rev. Neurosci.* **17** 419–39
- Olshausen B A and Field D J 1995 A model for the development of orientation selectivity based on early spontaneous activity *Soc. Neurosci. Abstr.* **21** 2025
- Pei X, Vidyasagar T R, Volgushev M and Creutzfeldt O D 1994 Receptive field analysis and orientation selectivity of postsynaptic potentials of simple cells in cat visual cortex *J. Neurosci.* **14** 7130–40
- Peinado A, Yuste R and Katz L C 1993 Extensive dye coupling between rat neocortical neurons during the period of circuit formation *Neuron* **10** 103–14
- Pettigrew J D 1982 Effects of deprivation on the owl's visual system *Neurosci. Lett. Suppl.* **8** S24
- Pettigrew J D and Gynther I C 1989 Cytoarchitecture of ocular dominance columns in owl visual cortex *Soc. Neurosci. Abstr.* **15** 795
- Pockett S and Slack J R 1982 Pruning of axonal trees results in increased efficacy of surviving nerve terminals *Brain Res.* **243** 350–3
- Rakic P 1976 Prenatal genesis of connections subserving ocular dominance in the macaque monkey *Nature* **261** 467–71

- Rakic P 1977 Prenatal development of the visual system in the rhesus monkey *Phil. Trans. R. Soc. B* **278** 245–60
 —1978 Neuronal migration and contact guidance in the primate telencephalon *Postgrad. Med. J. Suppl.* **1** **54** 25–37
- Rakic P, Bourgeois J-P, Eckenhoff M F, Zecevic N and Goldman-Rakic P S 1986 Concurrent overproduction of synapses in diverse regions of the primate cerebral cortex *Science* **232** 232–5
- Rauschecker J P 1991 Mechanisms of visual plasticity: Hebb synapses, NMDA receptors, and beyond *Physiol. Rev.* **71** 587–615
- Redies C, Diksic M and Rimpl H 1990 Functional organization in the ferret visual cortex: a double-label 2-deoxyglucose study *J. Neurosci.* **10** 2791–803
- Regan D and Beverley K I 1983 Visual fields described by contrast sensitivity, by acuity, and by relative sensitivity to different orientations *Invest. Ophthalmol. Vis. Sci.* **24** 754–9
- Reiter H O and Stryker M P 1988 Neural plasticity without postsynaptic action potentials: less active inputs become dominant when kitten visual cells are pharmacologically inhibited *Proc. Natl Acad. Sci. USA* **85** 3623–7
- Rockland K S and Lund J S 1983 Intrinsic laminar lattice connections in primate visual cortex *J. Comput. Neurol.* **216** 303–18
- Roe A W and Ts'o D Y 1995 Visual topography in primate V2: multiple representation across functional stripes *J. Neurosci.* **15** 3689–715
- Roe A, Ghose G M, Smith E L, Chino Y M and Ts'o D Y 1995 Alterations in striate cortical ocular dominance columns in anisometric amblyopia *Soc. Neurosci. Abstr.* **21** 1752
- Rojer A S and Schwartz E L 1990 Cat and monkey cortical columnar patterns modelled by bandpass-filtered 2D white noise *Biol. Cybern.* **62** 381–1
- Rosa M G P, Gattass R and Fiorani M 1988 Complete pattern of ocular dominance stripes in V1 of a New World monkey *Exp. Brain Res.* **72** 645–8
- Rowe M H, Benevento L A and Rezak M 1978 Some observations on the patterns of segregated geniculate inputs to the visual cortex in New World primates: an autoradiographic study *Brain Res.* **159** 371–8
- Russell D S 1995 Neurotrophins: mechanisms of action *Neuroscientist* **1** 3–6
- Sabel B A and Schneider G E 1988 The principle of 'conservation of total axonal arborization': massive compensatory sprouting in the hamster subcortical visual system after early tectal lesions *Exp. Brain Res.* **73** 505–18
- Sanes J R 1993 Topographic maps and molecular gradients *Current Opinion Neurobiol.* **3** 67–74
- Sanger T D 1989 Optimal unsupervised learning in a single-layer linear feedforward neural network *Neural Networks* **2** 459–73
- Schmidt J T and Edwards D L 1983 Activity sharpens the map during the regeneration of the retinotectal projection in goldfish *Brain Res.* **269** 29–39
- Schuman E M and Madison D V 1994 Nitric oxide and synaptic function *Ann. Rev. Neurosci.* **17** 153–83
- Schwartz E L 1980 Computational anatomy and functional architecture of striate cortex: a spatial mapping approach to perceptual coding *Vision Res.* **20** 645–69
- Sengpiel F, Troilo D, Kind P C, Graham B and Blakemore C 1996 Functional architecture of area 17 in normal and monocularly deprived marmosets (*Callithrix jacchus*) *Vis. Neurosci.* **13** 145–60
- Shannon C E and Weaver W 1949 *The Mathematical Theory of Communication* (Urbana, IL: University of Illinois Press)
- Shatz C J, Chun J J M and Luskin M B 1988 The role of the subplate in the development of the mammalian telencephalon *Cerebral Cortex, vol 7, Development and Maturation of Cerebral Cortex* ed A Peters and E G Jones (New York: Plenum) pp 35–58
- Shatz, C J, Linstrom S and Wiesel T N 1977 The distribution of afferents representing the right and left eyes in the cat's visual cortex *Brain Res.* **131** 103–16
- Shatz C J and Luskin M B 1986 Relationship between the geniculocortical afferents and their cortical target cells during development of the cat's primary visual cortex *J. Neurosci.* **6** 3655–68
- Shatz C J and Stryker M P 1978 Ocular dominance columns in layer IV of the cat's visual cortex and the effects of monocular deprivation *J. Physiol. (Lond.)* **281** 267–83
- Sherk H and Stryker M P 1976 Quantitative study of orientation selectivity in visually inexperienced kittens *J. Neurophysiol.* **39** 63–70
- Sirosh J and Miikkulainen R 1994 Cooperative self-organization of afferent and lateral connections in cortical maps *Biol. Cybern.* **71** 65–78

- Sirosh J and Miikkulainen R 1995 Cooperative self-organization of orientation maps and lateral connections in the visual cortex *Soc. Neurosci. Abstr.* **21** 1751
- Somers D C, Nelson S B and Sur M 1995 An emergent model of orientation selectivity in cat visual cortical simple cells *J. Neurosci.* **15** 5448–65
- Soodak R E 1987 The retinal ganglion cell mosaic defines orientation columns in striate cortex *Proc. Natl Acad. Sci. USA* **84** 3936–40
- Spatz W B 1979 The retino-geniculo-cortical pathway in *Callithrix*. II. The geniculo-cortical projection *Exp. Brain Res.* **36** 401–10
- 1989 Loss of ocular dominance columns with maturity in the monkey, *Callithrix jacchus* *Brain Res.* **488** 376–80
- Sperry R W 1944 Optic nerve regeneration with return of vision in anurans *J. Neurophysiol.* **7** 57–70
- Stryker M P and Harris W A 1986 Binocular impulse blockade prevents the formation of ocular dominance columns in cat visual cortex *J. Neurosci.* **6** 2117–33
- Swindale N V 1980 A model for the formation of ocular dominance stripes *Proc. R. Soc. B* **208** 243–64
- 1981a Rules for pattern formation in mammalian visual cortex *Trends Neurosci.* **4** 102–4
- 1981b Absence of ocular dominance patches in dark reared cats *Nature* **290** 332–3
- 1982a A model for the formation of orientation columns *Proc. R. Soc. B* **215** 211–30
- 1982b The development of columnar systems in the mammalian visual cortex: the role of innate and environmental factors *Trends Neurosci.* **5** 235–40
- 1985 Iso-orientation domains and their relationship with cytochrome oxidase patches *Models of the Visual Cortex* ed D Rose and V Dobson (New York: Wiley) pp 452–61
- 1988 Role of visual experience in promoting segregation of eye dominance patches in the visual cortex of the cat *J. Comput. Neurol.* **267** 472–88
- 1990 Is the cerebral cortex modular? *Trends Neurosci.* **13** 487–92
- 1991 Coverage and the design of striate cortex *Biol. Cybern.* **65** 415–24
- 1992a A model for the coordinated development of columnar systems in primate striate cortex *Biol. Cybern.* **66** 217–30
- 1992b Elastic nets, travelling salesmen and cortical maps *Current Biol.* **2** 429–31
- Swindale N V, Cynader M S and Matsubara J 1990 Cortical cartography: a two-dimensional view *Computational Neuroscience* ed E Schwartz (Cambridge, MA: MIT Press) ch 18, pp 232–341
- Swindale N V, Matsubara J A and Cynader M S 1987 Surface organization of orientation and direction selectivity in cat area 18 *J. Neurosci.* **7** 1414–27
- Tanaka S 1989 Theory of self-organization of cortical maps *Advances in Neural Information Processing System 1* ed D S Touretzky (San Mateo, CA: Morgan Kaufmann) pp 451–8
- 1990a Experience-dependent self-organization of biological neural networks *NEC Res. Develop.* **98** 1–14
- 1990b Theory of self-organization of cortical maps: mathematical framework *Neural Networks* **3** 625–40
- 1991a Theory of ocular dominance column formation *Biol. Cybern.* **64** 263–72
- 1991b Phase transition theory for abnormal ocular dominance column formation *Biol. Cybern.* **65** 91–8
- 1995 Topological analysis of point singularities in stimulus preference maps of the primary visual cortex *Proc. R. Soc. B* **261** 81–8
- 1996 Information representation and self-organization of the primary visual cortex *Natural and Artificial Parallel Computation: Proc. 5th NEC Research Symp.* ed D L Waltz (Philadelphia, PA: SIAM) ch 5, pp 93–126
- Thoenen H 1995 Neurotrophins and neuronal plasticity *Science* **270** 593–8
- Tigges J and Tigges M 1979 Ocular dominance columns in the striate cortex of chimpanzee (*Pan troglodytes*) *Brain Res.* **166** 386–90
- Tigges J, Tigges M and Perachio A A 1977 Complementary laminar terminations of afferents to area 17 originating in area 18 and in the lateral geniculate nucleus in squirrel monkey *J. Comput. Neurol.* **176** 87–100
- Todorov E, Zipser K and Zipser D 1995 Cortical maps and modules as a solution to the problem of volume minimization *Soc. Neurosci. Abstr.* **21** 1274
- Tootell R B H, Hamilton, S L, Silverman M S and Switkes E 1988a Functional anatomy of macaque striate cortex. I. Ocular dominance, binocular interactions and baseline conditions *J. Neurosci.* **8** 1500–30
- Tootell R B H, Switkes E, Silverman M S and Hamilton S L 1988b Functional anatomy of macaque striate cortex. II. Retinotopic organisation *J. Neurosci.* **8** 1531–68

- Tootell R B H, Silverman M S, Hamilton S L, De Valois R L and Switkes E 1988c Functional anatomy of macaque striate cortex. III. Color *J. Neurosci.* **8** 1569–93
- Ts'o D Y and Gilbert C D 1988 The organisation of chromatic and spatial interactions in the primate striate cortex *J. Neurosci.* **8** 1712–27
- Udin S B and Fawcett J W 1988 Formation of topographic maps *Ann. Rev. Neurosci.* **11** 289–327
- Van Essen D C, Newsome W T and Maunsell J H R 1984 The visual field representation in striate cortex of the macaque monkey: asymmetries, anisotropies, and individual variability *Vision Res.* **24** 429–48
- Volgushev M, Vidyasagar T R and Pei X 1995 Dynamics of the orientation tuning of postsynaptic potentials in the cat visual cortex *Vis. Neurosci.* **12** 621–8
- von der Malsburg Ch 1973 Self-organization of orientation sensitive cells in the striate cortex *Kybernetik* **14** 85–100
—1979 Development of ocularity domains and growth behaviour of axon terminals *Biol. Cybern.* **32** 49–62
- von der Malsburg Ch and Cowan J D 1982 Outline of a theory for the ontogenesis of iso-orientation domains in visual cortex *Biol. Cybern.* **45** 49–56
- von der Malsburg Ch and Willshaw D J 1976 A mechanism for producing continuous neural mappings: ocularity dominance stripes and ordered retino-tectal projections *Exp. Brain Res. Suppl.* **1** 463–9
—1977 How to label nerve cells so that they can interconnect in an ordered fashion *Proc. Natl Acad. Sci. USA* **74** 5176–8
- Wiesel T N and Hubel D H 1974 Ordered arrangement of orientation columns in monkeys lacking visual experience *J. Comput. Neurol.* **158** 307–18
- Willshaw D J and von der Malsburg Ch 1976 How patterned neural connections can be set up by self-organisation *Proc. R. Soc. B* **194** 431–45
—1979 A marker induction mechanism for the establishment of ordered neural mappings: its application to the retinotectal problem *Phil. Trans. R. Soc. B* **287** 203–43
- Wong R O L, Meister M and Shatz C J 1993 Transient period of correlated bursting activity during development of the mammalian retina *Neuron* **11** 923–38
- Yoshioka T, Blasdel G G, Levitt J B and Lund J S 1996 Relation between patterns of intrinsic lateral connectivity, ocular dominance, and cytochrome oxidase-reactive regions in macaque monkey striate cortex *Cerebral Cortex* (in press)
- Young D A 1984 A local activator-inhibitor model of vertebrate skin patterns *Math. Biosci.* **72** 51–8
- Yuille A L 1990 Generalized deformable models, statistical physics, and matching problems *Neural Comput.* **2** 1–24
- Yuille A L, Kolodny J A and Lee C W 1991 Dimension reduction, generalized deformable models and the development of ocularity and orientation *Harvard Laboratory Technical Report* no 91-3
- Zahs K R and Stryker M P 1988 Segregation of ON and OFF afferents to ferret visual cortex *J. Neurophysiol.* **59** 1410–29
- Zhuo M, Small S A, Kandel E R and Hawkins R D 1993 Nitric oxide and carbon monoxide produce activity dependent long-term synaptic enhancement in hippocampus *Science* **260** 1946–50